WILEY-BLACKWELL

Cladistics 36 (2020) 259–300

Cladistics

10.1111/cla.12405

Phylogenetic analysis of phenotypic characters of Tunicata supports basal Appendicularia and monophyletic Ascidiacea

Katrin Braun[a], Fanny Leubner[b] and Thomas Stach[c,*]

[a]*Vergleichende Zoologie, Institut für Biologie, Humboldt-Universität zu Berlin, Philippstrasse 13, Haus 2, 10115 Berlin, Germany;* [b]*Animal Evolution and Biodiversity, J-F-Blumenbach Institute for Zoology & Anthropology, Georg-August-University Göttingen, Untere Karspüle 2, 37073 Göttingen, Germany;* [c]*Molekulare Parasitologie, Institut für Biologie, Humboldt-Universität zu Berlin, Philippstrasse 13, Haus 14, 10115 Berlin, Germany*

Abstract

With approximately 3000 marine species, Tunicata represents the most disparate subtaxon of Chordata. Molecular phylogenetic studies support Tunicata as sister taxon to Craniota, rendering it pivotal to understanding craniate evolution. Although successively more molecular data have become available to resolve internal tunicate phylogenetic relationships, phenotypic data have not been utilized consistently. Herein these shortcomings are addressed by cladistically analyzing 117 phenotypic characters for 49 tunicate species comprising all higher tunicate taxa, and five craniate and cephalochordate outgroup species. In addition, a combined analysis of the phenotypic characters with 18S rDNA-sequence data is performed in 32 OTUs. The analysis of the combined data is congruent with published molecular analyses. Successively up-weighting phenotypic characters indicates that phenotypic data contribute disproportionally more to the resulting phylogenetic hypothesis. The strict consensus tree from the analysis of the phenotypic characters as well as the single most parsimonious tree found in the analysis of the combined dataset recover monophyletic Appendicularia as sister taxon to the remaining tunicate taxa. Thus, both datasets support the hypothesis that the last common ancestor of Tunicata was free-living and that ascidian sessility is a derived trait within Tunicata. "Thaliacea" is found to be paraphyletic with Pyrosomatida as sister taxon to monophyletic Ascidiacea and the relationship between Doliolida and Salpida is unresolved in the analysis of morphological characters; however, the analysis of the combined data reconstructs Thaliacea as monophyletic nested within paraphyletic "Ascidiacea". Therefore, both datasets differ in the interpretation of the evolution of the complex holoplanktonic life history of thaliacean taxa. According to the phenotypic data, this evolution occurred in the plankton, whereas from the combined dataset a secondary transition into the plankton from a sessile ascidian is inferred. Besides these major differences, both analyses are in accord on many phylogenetic groupings, although both phylogenetic reconstructions invoke a high degree of homoplasy. In conclusion, this study represents the first serious attempt to utilize the potential phylogenetic information present in phenotypic characters to elucidate the inter-relationships of this diverse marine taxon in a consistent cladistic framework.

Introduction

Tunicata is a taxon that comprises approximately 3000 marine invertebrate species, including the brightly bioluminescent Pyrosomatida, the translucent Salpida with their heterogenic life cycle or the Appendicularia (= Larvacea) that are capable of producing a most delicate, yet at the same time complex, extracorporal structure often called a "house" (Shenkar and Swalla, 2011; Lemaire and Piette, 2015). The best-known and most numerous tunicates, however, are the sessile, comparatively unadorned ascidians, most of which live at shallow shores attached to various hard substrata. Tunicata had been considered to be a subgroup of bivalves by early zoologists (e.g. Cuvier, 1840) and it was an unexpected surprise when the discovery of their larval stage, resembling a miniature tadpole, showed that these animals, perhaps uncharismatic at first sight, were in fact chordates (Kowalevsky, 1866). Mirroring this epiphany was the finding based on molecular phylogenetic analyses that supported Tunicata as a sister taxon to Craniota (Delsuc et al., 2006). This so-called "Olfactores hypothesis" has been criticized, because rates of sequence

*Corresponding author:
E-mail address: thomas.stach@hu-berlin.de

evolution are known to be exceptionally high in tunicates and because analyses of internal data conflict had shown that the phylogenetic information content was not as confidence-inspiring as the statistical support values suggested (Tsagkogeorga et al., 2009; Stach, 2014). Moreover, the Olfactores hypothesis is in conflict with the interpretation of numerous characters shared by Cephalochordata and Craniota, which had been interpreted as synapomorphies (Stach, 2008). Nevertheless, subsequent molecular studies supported the position of Tunicata as the sister group to vertebrates and this is currently the dominant hypothesis (Delsuc et al., 2018; Giribet, 2018; Kocot et al., 2018).

Until recently, only a couple of genes had been used to infer the molecular phylogenetic inter-relationships of tunicate subgroups (e.g. Wada, 1998; Swalla et al., 2000; Stach and Turbeville, 2002; Tsagkogeorga et al., 2009; see review in Giribet, 2018). Despite their limitations, these studies eventually converged on certain points: the planktonic Appendicularia is placed as sister taxon to the remaining Tunicata; the sessile seasquirts (i.e. "Ascidiacea") turned out to be paraphyletic with the planktonic Thaliacea being nested within this group. The molecular markers moreover supported the monophyly of several other tunicate subtaxa, such as Stolidobranchiata, Aplousobranchiata, Pyrosomatida, Salpida or Doliolida, and clarified the controversial (e.g. Kott, 1985, 1990) position of the genus *Ciona* within Phlebobranchiata, and also found some support for the placement of Diazonidae within Aplousobranchiata (Shenkar et al., 2016). Some other groups supported in traditional taxonomies remained either weakly supported or found no support in the molecular systematic studies. Phlebobranchiata, for example, was found monophyletic in some analyses but paraphyletic with respect to Aplousobranchiata in others. In most analyses, "Pyuridae", traditionally considered to be a "family" within Stolidobranchiata, was recovered to be paraphyletic with Styelidae nested within "Pyuridae." Although the number of molecular markers has increased considerably with two recently published studies that in parallel supported the phylogenies just outlined (Delsuc et al., 2018; Kocot et al., 2018), the number of species studied remains low considering the diversity found within Tunicata.

The disparity of morphologies and life-history strategies encountered in Tunicata fascinated researchers early on and numerous scrupulous taxonomic treatises and textbooks bear witness to this attention (e.g. Chamisso, 1819; Monniot and Monniot, 1972, 2001; Van Soest, 1981; Kott, 1985, 1990, 1992, 2001; Godeaux, 2003). Therefore, although meticulous descriptions of tunicate species abound, attempts to cladistically analyze the distribution of morphological characters remained few and far between. Stach and Turbeville (2002) published a cladistic study of 24 morphological characters for Tunicata at the traditional "family" level. This study resulted in little resolution, yet the authors discussed several potential character transformations compatible with the morphological evidence and their combined analysis. The most interesting finding in this study had been the possible closer relationship of Appendicularia to Aplousobranchiata, a sister-group relationship also supported in the parsimony analysis of 18S rDNA sequences, cox1-mtDNA sequences combined with morphological characters. Moreno and Rocha (2008) published the largest morphological dataset so far. Their analysis focused on the interrelationships of "genera" in the ascidian subtaxon Aplousobranchiata. Because traditional aplousobranch ascidians comprise only colonial species, the majority of characters analyzed in this study was biologically correlated with coloniality. Therefore, the finding that colonial ascidians from other ascidian groups are closer related to Aplousobranchiata—rendering (e.g.) Phlebobranchiata paraphyletic—is probably an artifact of this data matrix. In addition to these cladistic analyses, there were some attempts to phylogenetically analyze individual characters or plot them onto molecular phylogenies (e.g. Vanadium content – Hawkins et al., 1983; sperm morphology – Holland, 1992; secondary mechanoreceptor cells – Rigon et al., 2013; adult neural complex – Braun and Stach, 2019).

Clearly, morphology with its manifold levels of comparisons can contribute phylogenetic information to substantiate phylogenetic hypotheses and should not be neglected, if one seriously considers the requirement of total evidence as an important cornerstone of natural sciences. Along this line of argumentation, the present study endeavored to compile a data matrix conceptualizing 117 characters into primary homology hypotheses for 49 species, representing all higher tunicate taxa. The characters were chosen to allow for hypotheses of primary homology hypotheses across the entire diversity of tunicate taxa. Among these are characters traditionally used in tunicate taxonomy, such as characteristics of the branchial basket or the morphology of the gonads, but also characters recently compiled in the authors' own research, such as the kinds and distribution of serotonergic cells in the nervous system (see also Braun and Stach, 2016, 2018). Besides being an independent source of evidence for phylogenetic analyses, homology hypotheses of morphological characters are quintessential for any understanding of organismal evolutionary changes beyond the branching pattern of a cladogram. Therefore, the aim of the present study is to establish a broader factual basis to include morphological characters in cladistic considerations concerning tunicate and chordate evolution. In addition to presenting homology hypotheses, this work cladistically analyzes the data matrix, compares the result to molecular hypotheses

and performs a combined analysis in order to evaluate the respective contributions of the morphological and molecular partition toward the resulting phylogenetic hypothesis.

Material and methods

Collection and rearing

Collection localities for specimens examined as well as applied fixations and microscopic methods are listed in Table 1. Ascidians were collected in the lower intertidal or upper subtidal zones. Living specimens of *Oikopleura dioica* were provided from Sars International Centre for Marine Molecular Biology and cultured at Humboldt-University zu Berlin through numerous generations. Many specimens for scanning electron microscopy (SEM) came from the collection of the Museum für Naturkunde (Berlin, Germany; Table 1) and the SEM preparations are kept in the Marine Invertebrates collection.

Fixation

Before fixation, ascidians used for light microscopy were anaesthetized for approximately 1 h using menthol crystals. *Oikopleura dioica* was fixed directly without anaesthetization. The tunic of ascidians was opened before fixation in order to facilitate penetration of the fixative.

For light microscopy, animals were fixed either in Bouin's solution, an aqueous solution containing 8% formaldehyde, 5% acetic acid and 1% picric acid, or in a cold solution of Karnovsky's primary fixative (Karnovsky, 1965), consisting of 2% glutaraldehyde, 2% paraformaldehyde, 1.52% NaOH and 1.2 g D-glucose, dissolved in 2.25% sodium hydrogen phosphate buffer (pH 7.4). *Pyrosoma atlanticum* was fixed in 10% formaldehyde and stored in 70% ethanol.

For SEM, specimens were fixed either in 70% ethanol or in 4% paraformaldehyde.

Sectioning

Specimens for light microscopy were dehydrated in a graded series of ethanol and embedded in epoxy resin (Araldite; Fluka, Sigma-Aldrich, München, Germany). Specimens were serially sectioned with a thickness of 0.5–1 μm. Two specimens of *O. dioica* were serially sectioned for light microscopy (0.7 μm); another specimen of *O. dioica* was serially sectioned alternating between semithin sections (0.5 μm) and ultrathin sections (60 nm). Sectioning was performed on a Leica Ultracut S. Semithin sections were stained using 1% toluidine blue in a solution of 1% sodium tetraborate (borax).

Treatments with antibodies

Specimens were incubated in primary antibodies against tyrosinated α-tubulin (Anti-Tubulin, Tyrosine antibody produced in mouse; Sigma Aldrich, St Louis, Missouri, USA, product no. T9028) and antibodies against serotonin (5-HT (Serotonin) Rabbit; ImmunoStar, Hudson, Wisconsin, USA, product no. 20080) for at least 2.5 days at 4 °C. Incubation in secondary antibodies Cy™3 AffiniPure goat anti-mouse IgG (Jackson ImmunoResearch Laboratories, Inc., Philadelphia, Pennsylvania, USA, code 115-035-003) and Alexa Fluor® 488 goat anti-rabbit IgG (Molecular Probes, Eugene, Oregon, USA, catalogue no. A-11008) was carried out overnight at room temperature; nuclei were labelled using 4′6-Diamidino-2-Phenylindole dihydrochloride (DAPI dihydrochloride, Thermo Fisher Scientific Inc., Waltham, Massachussets, USA, catalogue no. D1306). Details can be found in Braun and Stach (2016). Every staining experiment was performed together with two different controls: one with primary antibodies omitted and the second with secondary antibodies omitted.

Light microscopy

Semithin sections stained with toluidine blue (Araldite) or Azan (paraffin) were digitally recorded (distance between sections 1–2 μm) using a Zeiss AxioCam HRc camera mounted on a Zeiss Axioscope 2 plus microscope. Complete images were optimized for contrast and light balance using Adobe Photoshop CC software. Serial sections of *Molgula manhattensis* were used for 3D reconstructions.

Scanning electron microscopy

For SEM, specimens were critical-point dried in a Balzers Union CPD 030. Dried specimens were sputter-coated with gold in a Balzers Union SCD 040 sputter coater and viewed with a LEO 1430.

Confocal Laser Scanning Microscopy

Specimens treated with antibodies against tyrosinated α-tubulin and serotonin, and 4′,6-diamidino-2-phenylindole (DAPI) were examined using a Leica TCS SPE confocal laser scanning microscope (Leica Microsystems, Heidelberg, Germany). Appropriate filter settings were applied to record stacks of confocal optical sections.

Digital 3D reconstruction

The 3D model of the anatomy of *Molgula manhattensis* was created in Amira 5.4.3 (FEI Visualization

Table 1
Information on examined specimens; adult stages were used in all species. In doliolids and salps sexual and asexual stages were analyzed

Species	Family	Order	Origin	# specimens examined	Museum accession number*	Fixations and Methods
*Oikopleura dioica*Fol, 1872	Oikopleuridae	Appendicularia	Bergen, Norway	3	-	Karnovsky, LM
Megalocercus huxleyi(Ritter, 1905)	Oikopleuridae	Appendicularia	Seychelles, Indian Ocean	1	ZMB 1608	70% ethanol, SEM
*Fritillaria borealis*Lohmann, 1896	Fritillariidae	Appendicularia	Atlantic Ocean, West Palm Beach, USA	6	-	PFA, CLSM
*Salpa fusiformis*Cuvier, 1804	Salpidae	Thaliacea	Villa Franca, Mediterranean Sea	2	ZMB 2703	70% ethanol, SEM
*Doliolum denticulatum*Quoy & Gaimard, 1834	Doliolidae	Thaliacea	Madagascar, Indian Ocean	2	ZMB 3357	70% ethanol, SEM
*Pyrosoma atlanticum*Péron, 1804	Pyrosomatidae	Thaliacea	0° 0,8506N, 160° 27,3294E	1 colony	-	Formaldehyde, SEM
Ascidiella scabra(Müller, 1776)	Ascidiidae	Phlebobranchiata	Kristineberg, Sweden	2	-	Formaldehyde, SEM
*Ascidia virginea*Müller, 1776	Ascidiidae	Phlebobranchiata	Kristineberg, Sweden	1	-	Formaldehyde, SEM
Phallusia nigra(Savigny, 1816)	Ascidiidae	Phlebobranchiata	Sinai, Gulf of Suez	1	ZMB 3277	70% ethanol, SEM
Corella parallelogramma(Müller, 1776)	Corellidae	Phlebobranchiata	Tjärnö, Sweden	1	-	Formaldehyde, SEM
Rhodosoma callense(Ehrenberg, 1828)	Corellidae	Phlebobranchiata	Gimsah Bay, Gulf of Suez	1	ZMB 778	70% ethanol, SEM
Agnezia septentrionalis(Huntsman, 1912)	Agneziidae	Phlebobranchiata	Bering Sea	1	ZMB 2913	70% ethanol, SEM
Ciona intestinalis (Linnaeus, 1767)	Cionidae	Phlebobranchiata	Kristineberg, Sweden	2	-	Formaldehyde, SEM
*Perophora viridis*Verrill, 1871	Perophoridae	Phlebobranchiata	Newport, USA	5	ZMB 2086	70% ethanol, SEM
*Molgula citrina*Alder & Hancock, 1848	Molgulidae	Stolidobranchiata	Roscoff, Atlantic Ocean	1	ZMB 2566	70% ethanol, SEM
Molgula manhattensis (De Kay, 1843)	Molgulidae	Stolidobranchiata	Texel, NetherlandsSylt, Germany	191	-	Bouin, LM, PFA, CLSM, 70% ethanol, SEM
Halocynthia roretzi (Drasche, 1884)	Pyuridae	Stolidobranchiata	Hakodate, Japan	2	ZMB 595	70% ethanol, SEM
Herdmania momus (Savigny, 1816)	Pyuridae	Stolidobranchiata	Red Sea	2	ZMB 2357	70% ethanol, SEM
Microcosmus claudicans (Savigny, 1816)	Pyuridae	Stolidobranchiata	Rovinj, Croatia	1	ZMB 1135	70% ethanol, SEM
Dendrodoa grossularia (Van Beneden, 1846)	Styelidae	Stolidobranchiata	Kristineberg, Sweden	1	-	Bouin, LM
*Styela clava*Herdman, 1881	Styelidae	Stolidobranchiata	Texel, Netherlands	8	-	PFA, CLSM
Styela plicata (Lesueur, 1823)	Styelidae	Stolidobranchiata	Messina, Italy	1	ZMB 542	70% ethanol, SEM
Botryllus schlosseri (Pallas, 1766)	Styelidae	Stolidobranchiata	Kristineberg, Sweden	1 colony	-	Formaldehyde, SEM
Symplegma brakenhielmi (Michaelsen, 1904)	Styelidae	Stolidobranchiata	Fort Pierce, USA	6	-	PFA, CLSM
Kukenthalia borealis (Gottschaldt, 1894)	Styelidae	Stolidobranchiata	Bredefjord, Greenland	1 colony	ZMB 3713	70% ethanol, SEM
*Pelonaia corrugata*Goodsir & Forbes, 1841	Styelidae	Stolidobranchiata	Helgoland, Germany	1	ZMB 1038	70% ethanol, SEM
*Diazona violacea*Savigny, 1809	Diazonidae	Aplousobranchiata	Naples, Italy	1 colony	ZMB 568	70% ethanol, SEM
Clavelina lepadiformis (Müller, 1776)	Clavelinidae	Aplousobranchiata	Roscoff, Atlantic Ocean, Helgoland, Germany	1	ZMB 1435	70% ethanol, SEM, Karnovsky, LM
Didemnum maculosum (Milne Edwards, 1841)	Didemnidae	Aplousobranchiata	Naples, Italy	1 colony	ZMB 202	70% ethanol, SEM
Diplosoma listerianum (Milne Edwards, 1841)	Didemnidae	Aplousobranchiata	Kristineberg, Sweden	1 colony	-	Formaldehyde, SEM
Lissoclinum verrilli (Van Name, 1902)	Didemnidae	Aplousobranchiata	Fort Pierce, USA	12	-	PFA, CLSM
Distaplia stylifera (Kowalevsky, 1874)	Holozoidae	Aplousobranchiata	Fort Pierce, USA	8	-	PFA, CLSM
*Sycozoa sigillinoides*Lesson, 1830	Holozoidae	Aplousobranchiata	Kerguelen, French Southern and Antarctic Lands	1 colony	ZMB 2192	70% ethanol, SEM
Eudistoma obscuratum (Van Name, 1902)	Polycitoridae	Aplousobranchiata	Fort Pierce, USA	6	-	PFA, CLSM
*Polyclinum aurantium*Milne Edwards, 1841	Polyclinidae	Aplousobranchiata	Blacksod Bay, Ireland	1 colony	ZMB 3613	70% ethanol, SEM
*Polyclinum constellatum*Savigny, 1816	Polyclinidae	Aplousobranchiata	Fort Pierce, USA	10	-	PFA, CLSM
Synoicum pulmonaria (Ellis & Solander, 1786)	Polyclinidae	Aplousobranchiata	Kristineberg, Sweden	1 colony	-	Formaldehyde, SEM
Aplidium turbinatum (Savigny, 1816)	Polyclinidae	Aplousobranchiata	Kristineberg, Sweden	1	-	Bouin, LM
Morchellium argus (Milne Edwards, 1841)	Polyclinidae	Aplousobranchiata	Roscoff, Atlantic Ocean	1 colony	ZMB 1428	70% ethanol, SEM
Branchiostoma lanceolatum (Pallas, 1774)	Branchiostomidae	Cephalochordata	Helgoland, Germany	2	-	Formaldehyde, SEM

CLSM, confocal laser scanning microscopy; LM, light microscopy; PFA, paraformaldehyde; SEM, scanning electron microscopy.
*Catalogue number of the Museum für Naturkunde (Berlin, Germany).

Sciences Group, Berlin, Germany) based on the images of the serial semithin sections. Images were aligned in AMIRA.

Phylogenetic analysis

MESQUITE v.3.10 (Maddison and Maddison, 2018) was used to compile a data matrix for 117 morphological characters for 54 taxa (see Appendix S1) and PAUP 4.0a (build 161) (Swofford, 2003) used to analyze this matrix. All characters were treated as unordered and with equal weight. Gaps were treated as missing. An initial heuristic parsimony analysis was conducted with 10, 100 and 500 replicates. The length of the most parsimonious trees found in all analyses remained stable at 297 steps. The main analysis was then conducted as an heuristic analysis with 2000 replicates, TBR branch swapping, and ≤10 trees saved at each replicate. This analysis, although analyzing a considerably larger tree space, did not result in a shorter tree and recovered 54 distinct equally parsimonious trees. The strict consensus and the majority rule consensus trees were calculated from this search. Subsequently, the dataset was analyzed a second time, reweighting characters according to their rescaled consistency index. In addition, a branch-and-bound search was performed with the strict consensus of the main analysis as constraint, searching for optimal trees not compatible with this constraint. This analysis found no further shorter trees, indicating that all most-parsimonious solutions of the dataset were recovered. Finally, the matrix also was analyzed with TNT (Goloboff et al., 2008) under the "traditional search" option (Wagner trees, 1000 random seeds, 10 000 replicates, 1000 trees saved per replicate, swapping algorithm TBR) and recovered 54 most-parsimonious trees with a length of 297 steps. The strict consensus was identical to the strict consensus of the main heuristic analysis performed in PAUP. Statistical measures of nodal support are reported as Bremer support indices, jackknife values based on 100 replicates with 50% character deletion, and bootstrap percentages based on 100 replicates using the same search strategy as for the main analysis but with 200 replicates within each bootstrap replicate. In a second step the phenotypic data (see Appendix S2) were combined with an alignment of molecular 18S rDNA-sequence data provided by Dr Frédéric Delsuc (Université de Montpellier) and the main analysis then was repeated. All characters were treated as unordered and with equal weight in an heuristic analysis under the parsimony paradigm as detailed for the morphological data above. Here, statistical support for nodes was reported as jackknife values (JK) and bootstrap (bt) percentages. Subsequently, the same analyses were performed but the weight of the phenotypic data was increased by a factor of 2, 3, 4 and 5 in order to roughly quantify the influence of the respective data on the outcome of the resulting phylogenetic hypothesis.

Results

Phenotypic data

Homology hypotheses for morphological characters were conceptualized into a data matrix for 49 tunicate species and five chordate outgroup species. The tunicate species represented 19 families from the five higher tunicate clades, traditionally afforded the rank of classes. The final character matrix included 117 characters comprising characters regularly used in tunicate, especially ascidian, systematics as well as newly acquired characters. The characters covered the entire phenotype and could be conveniently, but not unambiguously, categorized as follows: 25 general anatomical characters, 16 sexual reproduction characters, nine asexual reproduction characters, 22 branchial basket anatomy characters, 10 excretory system and digestive tract characters, four atrium characters, six characters conceptualized as serotonin-like immunoreactivity (serotonin-lir), and 25 microscopic anatomy of the nervous system characters. Of the 117 characters, 108 were coded as binary and nine as multistate characters; 113 characters were parsimony-informative, whereas four characters (character numbers 21, 42, 77 and 94) were parsimony-uninformative (autapomorphies of *Pyrosoma atlanticum* (21, 42), *Kukenthalia borealis* (77) and *Thalia democratica* (94), respectively). The complete data matrix is given as a nexus-file in Appendix S1 and a concise description for each character is found below.

Phylogenetic analysis of phenotypic characters

The extensive heuristic search conducted in PAUP with parsimony as the optimality criterion and with equal weights attributed to all characters resulted in 54 most-parsimonious trees. The tree length of these optimal trees was 297 steps, with a consistency index (CI) of 0.45, homoplasy index (HI) of 0.55 and a retention index (RI) of 0.83. The strict consensus tree (Fig. 1) is highly resolved and identical to the strict consensus of the 54 most-parsimonious trees found with TNT. Monophyly of several traditionally recognized tunicate taxa is supported in this strict consensus tree; strongly supported clades are highlighted with capital letters in this figure and feature Bremer support indices of ≥3 along with jackknife values >0.83 and bootstrap percentages >0.84. Besides the two outgroup taxa Cephalochordata (marked A in Fig. 1) and Craniota (B), these strongly supported taxa were: Tunicata (C), Ascidiacea (G), Stolidobranchiata (I), Botryllinae (J),

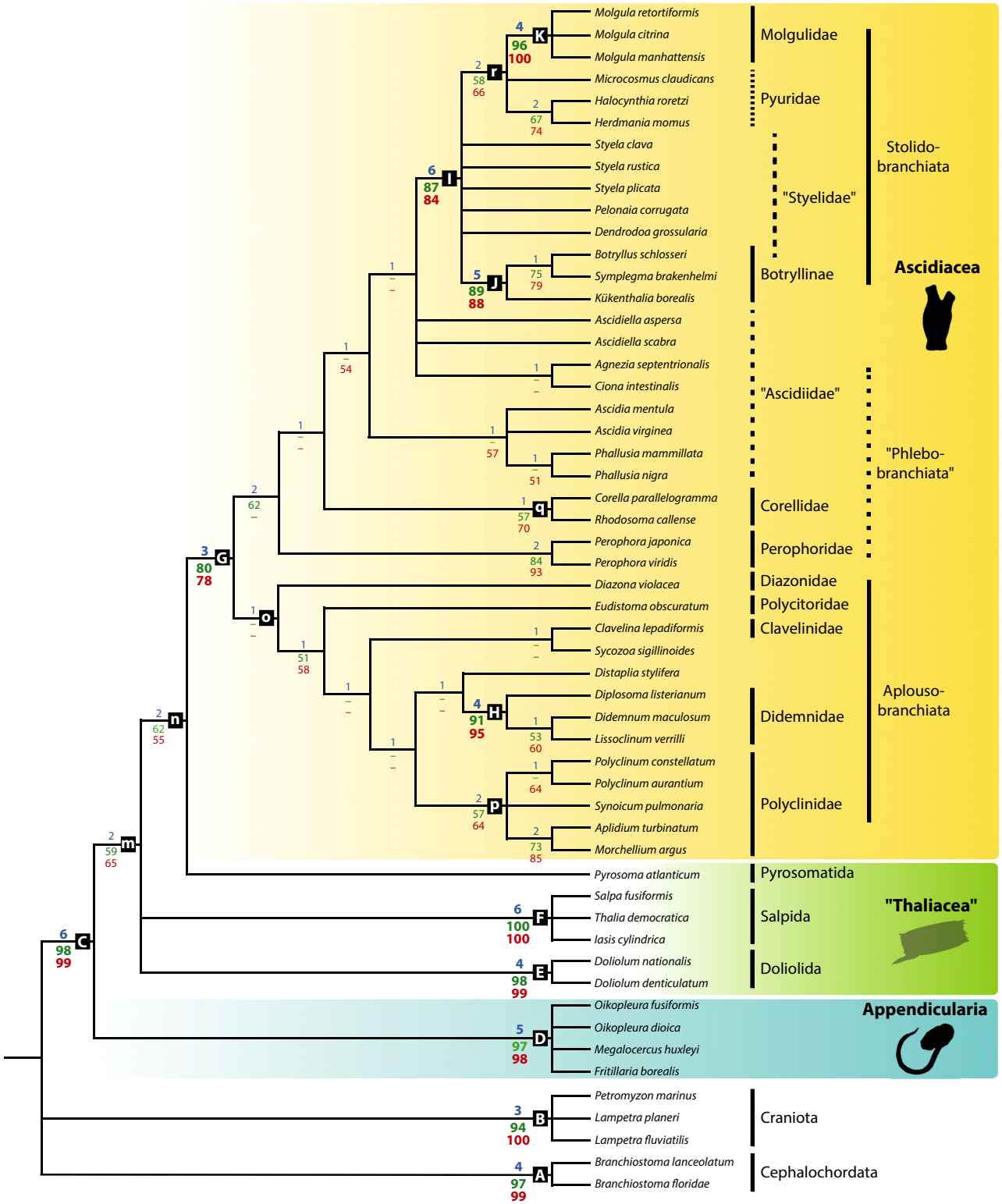

Fig. 1. Strict consensus tree of 54 equally parsimonious trees found in an heuristic analysis conducted in PAUP analyzing 117 morphological characters (113 parsimony-informative) coded for 49 tunicate species and five outgroup species. TL = 297, CI = 0.45, RI = 0.83. Numbers indicate Bremer support indices (blue), Jackknife values (green) and bootstrap percentages (red). Letters in rectangles refer to monophyla discussed in the text and listed in Table 2. Traditional taxonomic groups are indicated at the top. Quotation marks indicate traditional taxonomic groups found paraphyletic in the present analysis. Note the position of Appendicularia, the monophyly of Ascidiacea, and the paraphyly of "Thaliacea".

Didemnidae (H), Appendicularia (D), Salpida (F), Doliolida (E) and Molgulidae (K). All of these strongly supported taxa are characterized by uncontroverted apomorphies – a single one (character 57: kidney) in the case of Molgulidae and up to six (characters 14: tunic, 21: heartbeat reversal, 62: pyloric gland, 63: shape of gastrointestinal tract – U-shaped, 82: larval statocyte, 97: brain divided into cortex and neuropil) in the case of Tunicata. Clades supported with uncontroverted apomorphies, but with a Bremer support index <3 and statistical support indices <0.75 are marked with lower case letters in Fig. 1. Clades supported by uncontroverted apomorphies in the parsimony analysis are listed in Table 2 along with these apomorphic characters. Appendicularia (= Larvacea) is the sister taxon to all of the remaining tunicates in this analysis. Note that "Thaliacea," a traditionally recognized taxon, comprising approximately 80 planktonic species moving by jet propulsion, is not found as monophyletic in the present analysis. Instead the relationship between Doliolida and Salpida is unresolved, and Pyrosomatida is sister taxon to the monophyletic Ascidiacea, thereby rendering "Thaliacea" paraphyletic. The single diazonid *Diazona violacea* is the sister taxon to the remaining Aplousobranchiata.

In addition, a second analysis was conducted with reweighting of characters according to the rescaled CI from the main analysis with 2000 replicates, TBR branch swapping and ≤10 trees saved at each replicate, resulting in three most-parsimonious trees. The strict consensus was very similar to the one from the main analysis, with an increased resolution. One notable difference, for example, was the sister-group relationship between Doliolida and Salpida supported with a bootstrap value of 0.82. The tree length of these optimal trees was 110.23 steps, with CI = 0.66, HI = 0.34 and RI = 0.91 (see Fig. S1).

Combination of phenotypic data with molecular sequence data

The matrix for phenotypic data described above was used as the basis for an extended analysis in combination with molecular sequence data. To this end, the

Table 2
Monophyletic clades and respective uncontroverted apomorphies, found in the strict consensus of the analysis of the phenotypic data under the parsimony criterion (see Fig. 1) with information on the presence of the respective clades in the equally weighed combined analysis (see Fig. 2). +, taxon also supported in combined analysis; −, taxon not supported in combined analysis; nt, monophyly of taxon not tested in combined analysis (i.e. represented by a single OTU)

Traditional taxon name	Letter-label at nodes in Fig. 1	Monophyly of taxon in combined analysis	Uncontroverted apomorphy/apomorphies for respective node (numbers refer to the character numbers in the accompanying data matrix)
Cephalochordata	A	nt	25 (notochord extends from anterior to posterior tip of body), 70 (ventral origin of atrial cavity)
Craniota	B	nt	95 (adult cerebral eye with lens)
Tunicata	C	+	14 (tunic), 21 (heartbeat reversal), 62 (pyloric gland), 63 (U-shaped gastrointestinal tract),82 (larval statocyte), 97 (brain ganglion-like; i.e. divided into cortex and central neuropil)
Appendicularia	D	+	15 (tunic forms elaborate filter-feeding house), 37 (round or ovoid stigmata), 106 (caudal ganglion in adults), 116 (statocyte in adult)
Doliolida	E	+	13 (continuous muscle bands encircling body), 47 (dorsal organ absent), 115 (unpaired anterior nerve)
Salpida	F	+	37 (expanded stigmata), 110 (brain appendages)
Ascidiacea	G	–	1 (sessile adults), 38 (transverse orientation of adult stigmata)
Didemnidae	H	+	32 (pyloric epicardial budding), 77 (brood chamber in common tunic)
Stolidobranchiata	I	+	41 (internal longitudinal vessels not on papillae)
Botryllinae	J	+	34 (vascular mesenchymatic budding), 83 (larval photolith)
Molgulidae	K	+	58 (kidney)
Ascidiacea + "Thaliacea"	m	+	24 (notochord absent in adults), 68 (dorsal origin of atrial cavity), 91 (serotonin-like immunoreactivity in esophagus)
Ascidiacea + *Pyrosoma atlanticum*	n	+	66 (rectum in dorsomedian position), 89 (serotonin-like immunoreactivity in endostyle)
Aplousobranchiata (incl. *Diazona violacea*)	o	nt	3 (body division into thorax and abdomen)
Polyclinidae	p	nt	4 (body division into thorax, abdomen, and postabdomen), 33 (postabdominal strobilation)
Corellidae	q	nt	65 (gastrointestinal tract on right side of the body)
Stolidobranchiata + Ascidiidae + *Ciona* + *Agnesia*	r	–	43 (arrangement of cilia on internal longitudinal blood vessels)
Molgulidae + Pyuridae	s	–	9 (oral tentacles branched), 60 (hepatic gland)

matrix was concatenated with the aligned 18S rDNA-sequence data kindly supplied by Dr Frédéric Delsuc (Université de Montpellier) published in Tsagkogeorga et al. (2009). Although the matrix of the aligned 18S rDNA sequences possesses the highest taxon overlap of all published molecular data matrices with the phenotypic data matrix herein, taxon overlap was still <100%. The following strategy therefore was devised to combine molecular and phenotypic data: molecular data were appended to the phenotypic data when they were available for the same species. This was the case for 21 species. Molecular sequences from congeners were available for 11 more species from the phenotypic data matrix and were combined into mixed species operational taxonomic units (OTUs). The remaining 23 taxa from the phenotypic data matrix for which no congeneric sequence data were available, were completely removed before the analysis. The list of operational taxonomic units and their respective concatenation is detailed in Table 3. The combined data matrix is found in the Supporting Information (Appendix S2).

The final data matrix of phenotypic and molecular sequence data thus consisted of 32 taxa and 2122 characters. Besides the 117 phenotypic characters, up to 1005 nucleotide positions were present in a taxon, whereas the remaining characters were gapped positions. 1218 (including six phenotypic characters) of the 2122 characters were constant and 262 variable characters were parsimony-uninformative, of which 14 were phenotypic characters (see above).

Table 3
Species as operational taxonomic units (OTUs) and their respective concatenation for the analysis of combined phenotypic and molecular data

OTU (in Fig. 2)	Species used for concatenation (empty if a single species was used)
Oikopleura (fus&lab)	*Oikopleura fusiformis* & *O. labradoriensis*
Oikopleura dioica	
Megalocercus huxleyi	
Salpa (fus&thomp)	*Salpa fusiformis* & *S. thompsoni*
Thalia democratica	
Iasis cylindrica	
Doliolum nationalis	
Doliolum denticulatum	
Pyrosoma atlanticum	
Ascidia (ment&cerat)	*Ascidia mentula* & *A. ceratodes*
Ascidia (virg&ahod)	*Ascidia virginea* & *A. ahodori*
Corella (parall&infla)	*Corella parallelogramma* & *C. inflata*
Phallusia mammillata	
Phallusia nigra	
Perophora (jap&saga)	*Perophora japonica* & *P. sagamiensis*
Perophora viridis	
Ciona intestinalis	Note: may be *C. robusta*
Molgula retortiformis	
Molgula citrina	
Molgula manhattensis	
Microcosmus (claud&squa)	*Microcosmus claudicans* & *M. squamata*
Styela (cla&gib)	*Styela clava* & *S. gibsii*
Styela (rust&monte)	*Styela rustica* & *S. montereyensis*
Styela plicata	
Botryllus schlosseri	
Symplegma (brake&viri)	*Symplegma brakenhielmi* & *S. viridis*
Halocynthia roretzi	
Herdmania momus	
Pelonaia corrugata	
Clavelina (lepad&meridio)	*Clavelina lepadiformis* & *C. meridionalis*
Branchiostoma floridae	
Petromyzon marinus	

Phylogenetic analysis of phenotypic characters combined with molecular sequence data

An heuristic analysis under the parsimony paradigm was performed treating all characters as unordered and with equal weight. Two thousand replicates were analyzed starting from random trees with subsequent tree bisection and reconnection, retaining a single best tree of a tree length of ≥500 at each replicate. This search resulted in a single most-parsimonious tree with a tree length of 2390, CI = 0.56, HI = 0.44 and RI = 0.71. The strict consensus tree shown in Fig. 2 is well-resolved and is highly similar to the one published by Tsagkogeorga et al. (2009) that was based on a Bayesian analysis of the same molecular sequences, yet more taxa were included (see previous paragraph).

The strict consensus tree is highly resolved and finds strong intrinsic statistic support for the monophyly of Tunicata (JK: 1.00, bt: 1.00). Within the targeted ingroup, the Tunicata, several higher monophyletic clades are recovered: Appendicularia (JK: 1.00, bt: 1.00), Stolidobranchiata (JK: 1.00, bt: 1.00), Molgulidae (JK: 1.00, bt: 1.00), Styelidae (JK 0.96, bt: 0.96), Thaliacea (JK: 0.71, bt: 0.82), Doliolida (JK: 1.00, bt: 1.00), Salpida (JK: 1.00, bt: 1.00), Ascidiidae (JK: 1.00, bt: 1.00) and Perophoridae (JK: 1.00, bt: 1.00). Aplousobranchiata was represented by the single OTU *Clavelina (lepad&meridio)* (see Table 3) and therefore monophyly of Aplousobranchiata was not tested in this analysis. "Phlebobranchiata" is paraphyletic with respect to Thaliacea plus Aplousobranchiata, thus Thaliacea renders "Ascidiacea" also paraphyletic in this analysis. Thaliacea, now recovered monophyletic, is the sister taxon to Aplousobranchiata, which, however, was represented by a single OTU. Note the identical position of Appendicularia as the sister taxon to

the remaining tunicate taxa, as in the analysis of the phenotypic data.

In order to gauge the influence of the different data partitions, molecular data versus phenotypic data, for the outcome of the phylogenetic analysis the weight of the phenotypic data was gradually increased from zero (molecular data only) to equal (1:1) to 5:1. Because the major difference in the purely molecular and the purely phenotypic data is the monophyly of Thaliacea in the molecular analysis (paraphyletic in the phenotypic analysis) and the monophyly of Ascidiacea in the phenotypic analysis (paraphyletic in the molecular analysis), these two groups are the focus of the following paragraph.

If the weight of phenotypic data is doubled (2:1), the result is essentially the same as with the equally weighted data, which in turn is concordant with the analysis of the purely molecular data (Fig. 2). However, the bootstrap (bt) value for a monophyletic Thaliacea increases from 0.52 in the analysis of purely molecular data to 0.82 in the equal weights scheme (1:1) and then remains almost stable at 0.80 in the analysis with the weight doubled for the phenotypic data (2:1) (Fig. 3). "Ascidiacea" is still paraphyletic under this weighing scheme. At a weight of phenotypic data to molecular data of 3:1, a monophyletic Thaliacea becomes sister taxon to a monophyletic Ascidiacea. Although the sister-group relationship between these taxa is supported

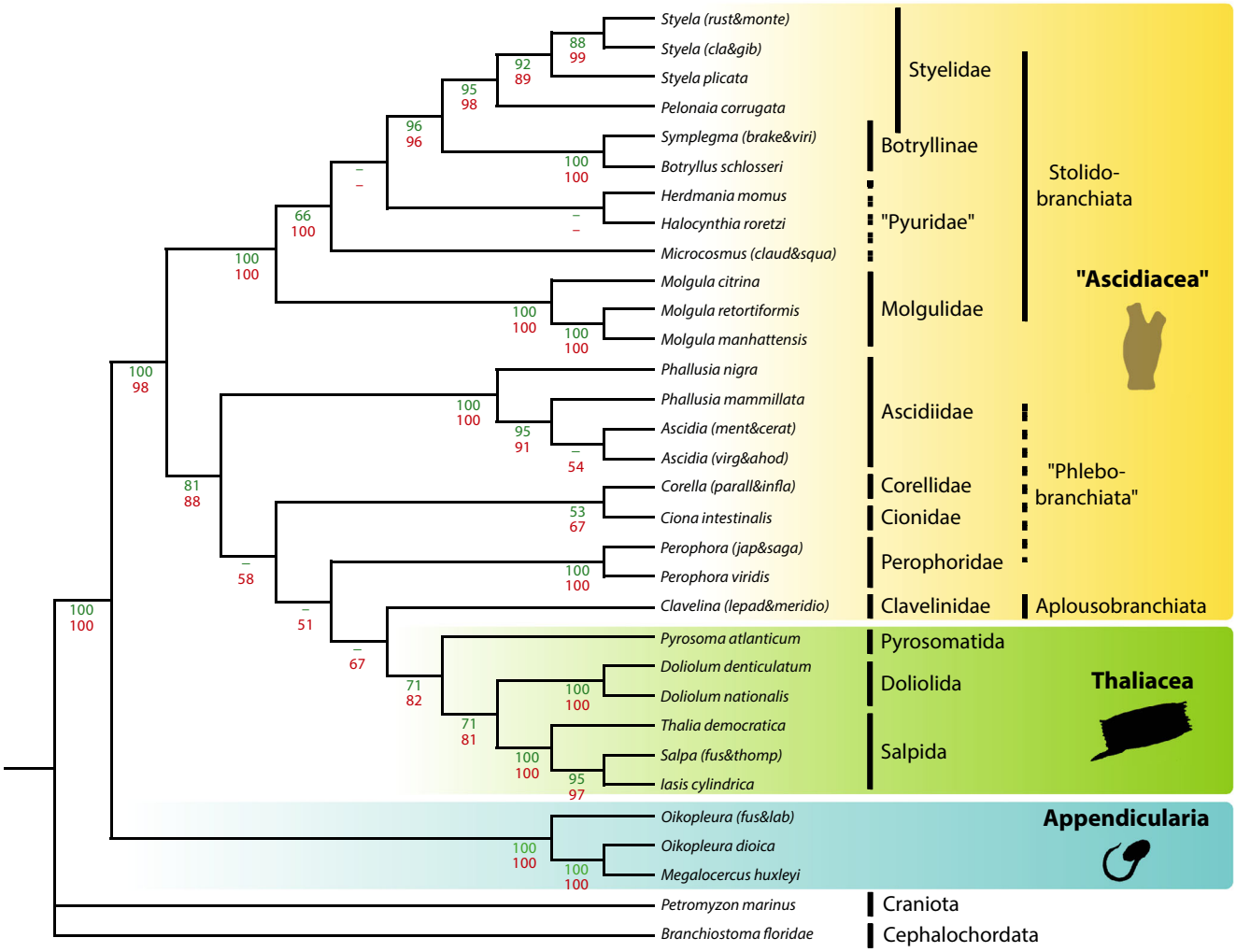

Fig. 2. Single most-parsimonious tree found in an heuristic analysis conducted in PAUP analyzing 117 morphological characters (97 parsimony informative) combined with 18S rDNA-sequence data (2005 nt-positions, 545 parsimony informative) resulting in 2122 characters for 32 tunicates (21 species and 11 OTUs consisting of two species concatenated from the same genus; see Table 3 for names of species used for concatenation and text for further details) and five outgroup species. TL = 2390, CI = 0.56, RI = 0.71. Numbers indicate jackknife values (green) and bootstrap percentages (red). Traditional taxonomic groups are indicated at the top. Quotation marks indicate traditional taxonomic groups found paraphyletic in the present analysis. Note the position of Appendicularia, the paraphyly of "Ascidiacea", and the monophyly of Thaliacea.

by bt = 1.00, Thaliacea is supported by bt = 0.51 and Ascidiacea by bt = 0.56 (Figs. S2-S6). At a weighting scheme of phenotypic data: molecular data of 4:1, Ascidiacea is monophyletic, with bt = 0.86. In this analysis "Thaliacea" is found paraphyletic as in the previous analysis. Finally, at a weighting scheme of phenotypic data to molecular data of 5:1, Ascidiacea is monophyletic, with bt = 0.92. Under this weighting scheme "Thaliacea" is again recovered as paraphyletic.

Because molecular datasets are notoriously plagued by gapped positions, the same analyses were repeated on the combined dataset including only the parsimony-informative sites. In the first round of analyses, 2005 molecular characters were analyzed together with 117 phenotypic characters (ratio = 17.14 : 1), whereas in the second round 545 parsimony-informative molecular characters and 97 parsimony-informative phenotypic characters remained (ratio = 5.62 : 1). The resulting phylogenetic hypotheses are – of course – unchanged; moreover, the observed pattern of switching from a monophyletic Thaliacea to paraphyly of thaliaceans and from a paraphyletic assemblage of ascidians to a monophyletic Ascidiacea with successively increased weight of the phenotypic characters also is the same. The only differences are slightly differing bootstrap percentages supporting the respective monophyla (see Fig. 3b,d), which, however, might be due to the idiosyncrasies of this statistical value.

List of characters

General morphology

1. Sessile adults: (0) absent; (1) present. Within tunicates, species belonging to the taxa Phlebobranchiata, Aplousobranchiata and Stolidobranchiata (ascidians) develop sessile adults after metamorphosis. Adult specimens belonging to the taxa Thaliacea and Appendicularia, as well as species belonging to the outgroup taxa are free-living, actively swimming or planktonic. Although adult cephalochordates are characterized as semi-sessile, they actively burrow in the sediment and are capable of actively changing their location via undulatory vigorous swimming (Pietschmann, 1962). Although coding this character for semaphoronts of the

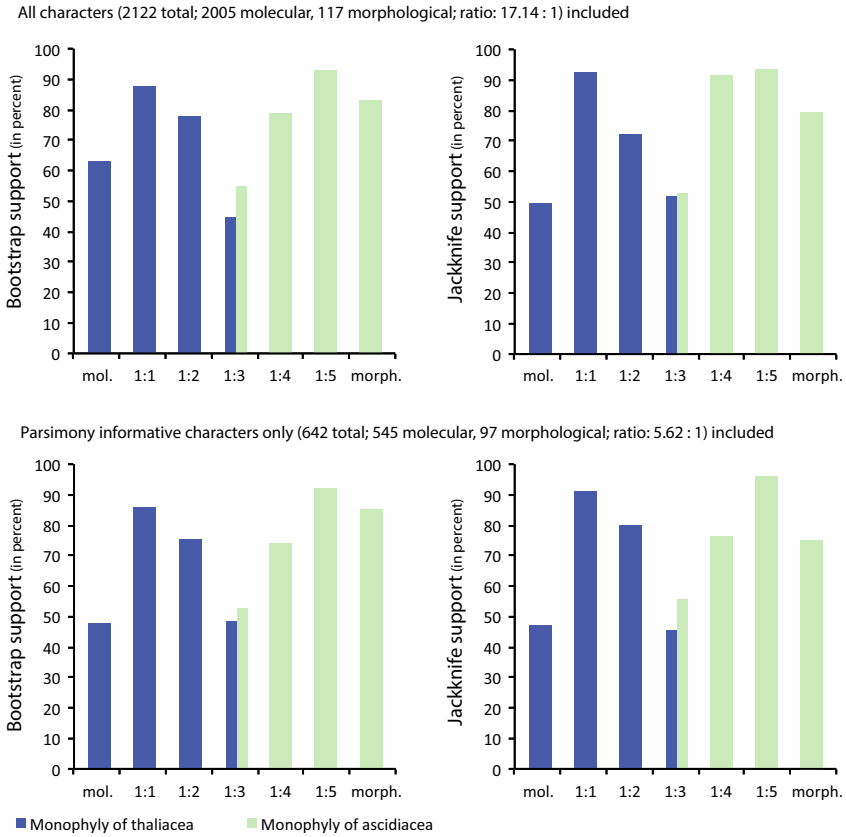

Fig. 3. Bootstrap (left) and jackknife (right) percentages supporting the monophyly of Thaliacea and the monophyly of Ascidiacea at different weighting schemes of phenotypic and molecular data. Top row: all data included: phenotypic data: $\#_{(morph)}$ = 117, number of sequence sites: $\#_{(mol)}$ = 2005; i.e. $\#_{(morph)} : \#_{(mol)} \approx 0.058 \approx 1{:}17.14$. Bottom row: parsimony-informative characters only: phenotypic data: $\#_{(morph)}$ = 97, number of sequence sites: $\#_{(mol)}$ = 545; i.e. $\#_{(morph)}: \#_{(mol)} \approx 0.18 \approx 1{:}5.62$.

respective species is straightforward, the differences between the free-living taxa (e.g. in their respective modes of locomotion) may cast doubts on the decision to assign all of them the same character state. This conceptualization tests the preposition that free-living tunicates split off early from the tunicate lineage (e.g. Seeliger, 1885 (in Neumann, 1956), Julin 1904, García-Bellido et al., 2014).

2. Undulatory locomotion in adults: (0) absent; (1) present. Coding of this character is, again, straightforward (see also Stach and Turbeville 2002). It is a dependent character of character 1 and inapplicable for species that are sessile as adults. Conceptualizing this character distinguishes between the fish-like locomotion in appendicularians together with the outgroup taxa and the jet-propulsion locomotion in the thaliacean tunicates.
3. Body division: (0) absent; (1) present. Following the classical descriptions of tunicate morphology, body division is coded as present for species with recognizably divided bodies in outer appearance and internal anatomy. This corresponds to the partition found in the anatomy of numerous ascidian species into a thorax region separate from an abdominal, and sometimes a postabdominal region, as described in virtually all classical texts on tunicate taxonomy (e.g. Van Name, 1945; Millar, 1970). Because Cionidae do not display body division in their overall morphology *Ciona intestinalis* is coded as (0).
4. Number of body parts: (0) two; (1) three. Number of body parts refers to the division of the body into thorax, abdomen, and postabdomen traditionally recognized in ascidians (e.g. Van Name, 1945; Millar, 1966). For *Distaplia stylifera*, Kott (1990) described two body parts and a posterior abdominal sac that she does not regard as a homologue of a postabdomen, which contains the heart-pericard complex and the gonads. Van Name (1945) describes three body parts, mentioning, however, that the postabdomen only contains gonads, not the heart. Kott's description is followed herein because of the absence of the heart in the abdominal sac.
5. Incurrent and excurrent siphons on opposite poles of the animal: (0) absent; (1) present. These tube-like projections of the bodies serve as entrance or exit (respectively) for water. The incurrent siphon opens into the mouth, whereas the excurrent siphon is connected to the atrium. In sessile ascidians, both siphons are directed away from the substratum, whereas in the free-living thaliacean species incurrent and excurrent siphons point towards the anterior and posterior directions, respectively.
6. Lobed incurrent siphon: (0) absent; (1) present. The incurrent siphon of many tunicate species shows more or less conspicuous lobes. Information on character distribution is found in Berrill (1950), Groepler (2016), and Van Name (1945). See also Fig. 4a–d.
7. Numbers of lobes at incurrent siphon: (0) four; (1) six; (2) eight; (3) more than eight. This character is traditionally used in identification keys to distinguish tunicate families (Van Name, 1945; Berrill, 1950; Millar, 1966, 1970; Kott, 1985, 1990, 1992, 2001; Groepler, 2016). In adult *Phallusia mammillata* the number of lobes is difficult to determine because of the irregularly bulbous and extensive external tunic, but counts result in eight or nine lobes; however, in *P. nigra* eight lobes or more than eight lobes are described for the incurrent siphon (Van Name, 1945; Rocha et al., 2012). Therefore, this character was coded as polymorphic for investigated *Phallusia* species. For *Agnezia septentrionalis* Van Name (1945) counted six or eight lobes, here we also coded this character as polymorphic. Lobes in *Dendrodoa grossularia* are inconspicuous; the opening of the incurrent siphon is tetragonal (Groepler, 2016). The tetragonal opening of the incurrent siphon is homologized with four lobes at incurrent siphons. In *D. nationalis* the oozooids possess eight lobes, whereas blastozooids possess 12 lobes (Berrill, 1950); the character was coded as polymorphic. See also Fig. 4a–d.
8. Oral tentacles: (0) absent; (1) present. Oral tentacles are elongated projections located at the transition of mouth opening and branchial basket (Huus, 1956; see also Fig. 4b,e–g). Oral tentacles are usually equipped with sensory cells (e.g. Rigon et al., 2013), although this is not known for most species. In planktonic tunicates oral tentacles are not developed, whereas they are present in all investigated ascidian species. For the outgroup species the velar tentacles are considered present in all five species homologous to oral tentacles in Tunicata.
9. Shape of oral tentacles: (0) simple, unbranched; (1) branched. Information on character distribution is found in Drasche (1884) and Berrill (1950); see also Fig. 4e–g.
10. Lobed excurrent siphon: (0) absent; (1) present. The excurrent siphon as well as the incurrent siphon in most tunicate species is lobed (see also character 6). An atrial languet,

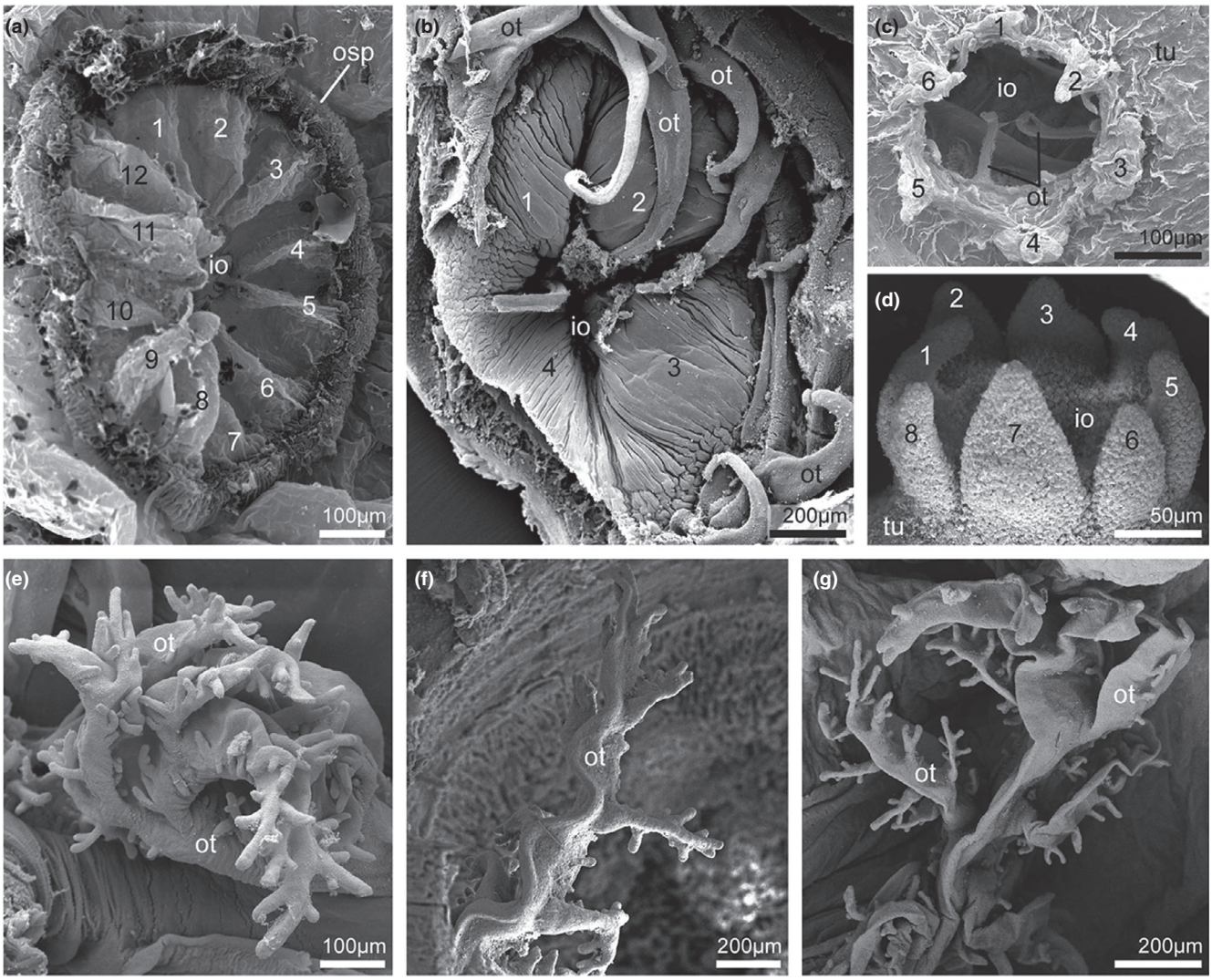

Fig. 4. Scanning electron micrographs of incurrent siphons and oral tentacles (ot). (a–d) Lobed incurrent siphons of different tunicate species. (a) The incurrent siphon of *Doliolum denticulatum* possesses 12 lobes. (b) The incurrent siphon of *Kukenthalia borealis* consists of four lobes. Oral tentacles are simple, without branching. (c) The incurrent siphon of *Diplosoma listerianum* forms six lobes, oral tentacles are simple in shape. (d) Incurrent siphons of *Morchellium argus* possess eight conspicuous lobes. (e–g) Branched oral tentacles in three different stolidobranch species. (e) In *Molgula manhattensis* oral tentacles are branched. (f) Oral tentacle of *Microcosmus claudicans*. (g) Oral tentacle of *Herdmania momus*. io: incurrent opening, osp: oral sphincter, tu: tunic.

an elongated, tongue-like projection dorsally protruding above an expanded atrial opening present in some aplousobranch species and in *Botryllus schlosseri* is considered to be homologous to a lobed excurrent siphon. Information on character distribution is found in Berrill (1950) and Van Name (1945).

11. Number of lobes at excurrent siphon: (0) two; (1) four; (2) six; (3) more than six; (4) atrial languet (i.e. one). Information on character distribution is found in Berrill (1950) and Van Name (1945).
12. Conspicuous and discrete circular muscle bands for locomotion: (0) absent; (1) present. This character is only present in Salpida and Doliolida (Ihle, 1956) and corresponds to the curious mode of movement through vigorous and individual jet propulsion in these taxa.
13. Shape of circular muscle bands: (0) discontinuous; (1) continuous. In species of Doliolida muscle bands are continuously circling the entire body, whereas in the investigated members of Salpida muscle bands are discontinuous and interrupted on the ventral sides (Ihle, 1956).
14. Tunic: (0) absent; (1) present. The tunic is an extracellular covering produced by the epidermis and containing cellulose. Tunicates are

the only animals able to produce cellulose (Lohmann, 1956; Hirose et al., 1999; Stach, 2007; Shenkar and Swalla, 2011).

15. Shape of tunic: (0) simple cover of epidermis; (1) elaborate, multi-chambered filter-feeding house. In Appendicularia the tunic additionally functions as a complex filtering system to concentrate food particles from the water column (Körner, 1952; Flood and Deibel, 1998; Sagane et al., 2010).
16. Calcareous spicules in tunic: (0) absent; (1) present. For additional protection against predators, some ascidians deposit calcareous spicules into the tunic. The tunic of species in Didemnidae is usually equipped with copious amounts of calcareous spicules; however, the didemnid *Diplosoma listerianum* possesses no spicules visible in a dissecting microscope (Berrill, 1950). In *Herdmania momus* and *Kükenthalia borealis* calcareous spicules also are present in the tunic (Van Name, 1945; Lambert and Lambert, 1987).
17. Tunic protrusions: (0) absent; (1) present. Tunic protrusions are minute protrusions of the cuticular surface of the tunic that are papillate in shape and reach up to 100 nm in height; the conceptualization of this character is as described by Hirose et al. (1992).
18. Vanadium: (0) absent; (1) present. Vanadium is a comparatively rare metal present in sea water and accumulated by tunicates, where it is found mainly in blood cells. The present analysis follows Hawkins et al. (1983) in incorporating this character.
19. Epicardium: (0) absent; (1) present. Epicardia are internal sacs lined completely by an epithelium. Ontogenetically they are derived from the posterior ventral part of the pharynx, from a paired rudiment. Extent and form in the adults may vary. Berrill (1950) homologized excretory cells and organs with epicardia. These, however, develop from vacuolized blood cells and the homology to epicardia remains uncertain. In this respect Groepler's argument (Groepler, 2016) is followed, although it is noted that Berrill's hypothesis should be investigated with modern methods (Berrill, 1950).
    Although the homology of epicardia and coelomic cavities in cephalochordates and vertebrates is not established definitively, the derivation from the archenteron and the further development (especially in vertebrates) as an epithelial lining of inner organs (including heart and intestine) support the hypothesis of homology (Romer and Parsons, 1986; Groepler, 2016). Berrill (1950) tentatively suggested this hypothesis. Therefore, the character state is coded as (1) for outgroup species. In Appendicularia, the so-called procardial sacs are not separated from the pericardium and therefore not homologous to the epicardia (own series of sections). Information on character distribution is found in Berrill (1950), and Huus (1956); see also Fig. 5a,b. For Molgulidae Huus (1956) and Berrill (1950) are followed in homologizing epicardia and kidney.
20. Shape of epicardium in adult: (0) unpaired; (1) paired, separated sacs. Information on character distribution is found in Berrill (1950) and Groepler (2016).
21. Heartbeat reversal: (0) absent; (1) present. In all tunicates the heart regularly shows a heartbeat reversal (Neumann, 1956; Kriebel, 1967; Bone et al., 1997; Fenaux, 1998).
22. Endocarp: (0) absent; (1) present. Endocarps are projections of the atrial wall into the atrial cavity. They are usually found on the parietal wall but also may be present on the visceral side. Endocarps contain a spongy tissue richly supplied with lacunae and blood cells (Kott, 1985). Endocarps are also called parietal vesicles (Berrill, 1950). *D. grossularia* possesses endocarps (Fig. 5c, contra Rocha et al., 2012). When detailed anatomical descriptions were available, but endocarps were not described, the character state was coded as 0, for example for *Pelonaia corrugata* (Millar, 1966; Rocha et al., 2012) and *K. borealis* (Van Name, 1945; Millar, 1966). Further information on character distribution is found in Berrill (1950), Kott (1985), Rocha et al. (2012) and Van Name (1945).
23. Light organs: (0) absent; (1) present. In Pyrosomatida, paired organs with conspicuously large cells that contain symbiotic bacteria with the ability to produce light, are found lateral to the mouth openings (e.g. Neumann, 1956; Mackie and Bone, 1978). Bioluminescence also is known from some salp, appendicularian and few ascidian species but without comparable organs (Hirose et al., 1996; Bone, 1998).
24. Notochord in adults: (0) absent; (1) present. A notochord is an axial skeletal stiffening rod consisting of vacuolated cells and a collagen-rich extracellular sheath. Ontogenetically the notochord derives from endoderm and, in most tunicates, the notochord is reduced after metamorphosis. However, in Appendicularia the notochord persists in the adult stage (Lohmann, 1956). In the outgroup species, the

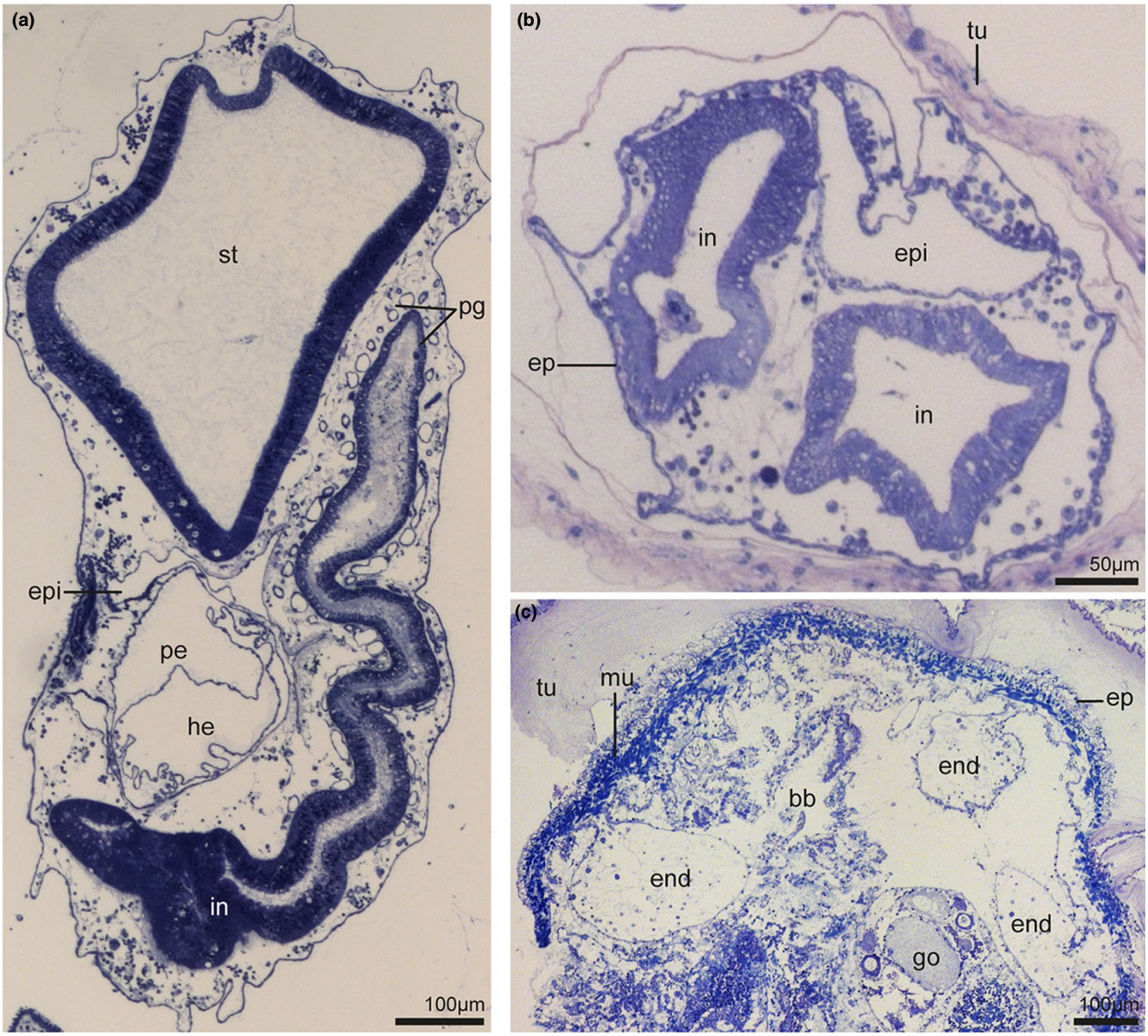

Fig. 5. Light micrographs of semithin cross sections through the abdomens of two aplousobranch species, and cross-section through one stolidobranch ascidian, stained with toluidine blue. (a) Section through *Clavelina lepadiformis*, dorsal to the top, left to the right. The epicardium (epi) is positioned in close proximity to the pericardium (pe). It is bordered by an epithelium. (b) Cross-section through *Aplidium turbinatum*, ventral to the top, right to the right. The epicardium is conspicuously large. (c) Cross-section through *Dendrodoa grossularia*, dorsal to the top, right to the right. Endocarps (end) are visible as projections from the body wall into the atrium. bb, branchial basket; ep, epidermis; go, gonad; he, heart; in, intestine; mu, musculature; pg, pyloric gland; st, stomach; tu, tunic.

cephalochordates and the agnathans, the notochord is present during the complete life cycle.

25. Length of notochord: (0) not extending to the anterior end of the body; (1) extending along the entire body to its most anterior tip. In cephalochordates the notochord extends along the whole body. In tunicates and lampreys the notochord does not extend into the anteriormost part of the body (Romer and Parsons, 1986; Ruppert, 1997a).

Asexual reproduction

26. Coloniality: (0) absent; (1) present. Colonial species develop through asexual, clonal propagation.
27. Sexually mature colonial form: (0) absent: sexually propagating chain of animals break up; (1) present: sexual forms remain entirely colonial. In members of Salpida and Doliolida the blastozooids become solitary during

later development, yet species of Pyrosomatida and the colonial ascidians stay within the colony during the entire development (Huus, 1956; Ihle, 1956).

28. Connection of zooids within colonies: (0) zooids completely embedded in a common tunic; (1) zooids connected via stolons. In *D. violacea* zooids are embedded in a common tunic that, however, does not surround the complete zooid, but is restricted to the basal part of the animals (their abdomen) whereas the apical parts of the zooids (their thorax) remain separated (Berrill, 1948). The character state for *D. violacea* is coded as 1.
29. Metagenesis: (0) absent; (1) present. Metagenesis is the obligate alteration between asexual and sexual reproductive modes in consecutive generations. Colonial species are coded as metagenesis being present, if the presence of an oozooid (i.e. an individual that does not develop gonads but reproduces only asexually) as the founder of a colony has been documented (Brien and Brien-Gavage, 1927; Deviney, 1934; Berrill, 1950; Nakauchi, 1982; Kott, 1990; Gutierrez and Brown, 2017).
30. Polymorphic generations: (0) absent; (1) present. Consecutive generations in a metagenetic life cycle can display drastically different morphologies or can be morphologically highly similar or even indistinguishable (except of course in respect to the presence of gonads; Huus, 1956; Ihle, 1956; Neumann, 1956).
31. Type of budding: (0) epicardial; (1) mesenchymatic; (2) palleal; (3) complex stolo prolifer. Different modes of budding have been discussed at length in the tunicate literature. Following different authors (Huus, 1956; Nakauchi, 1982; Groepler, 2016), four general types of budding are distinguished: epicardial (epicardia as the main source of the growing bud tissue); mesenchymatic (mesenchymatic cells are the main source of the growing bud tissue); palleal (peribranchial wall is the main source of the growing bud tissue); and budding via a complex stolo prolifer (the stolo prolifer contains at least: gonadal strand, pericardial strand, peribranchial strands, endodermal strand, neuronal strand and, of course. ectoderm). In the colonial stolidobranch ascidians *B. schlosseri* and *Symplegma brakenhielmi*, mesenchymatic and palleal budding are described (Gutierrez and Brown, 2017), and for *K. borealis* Berrill (1950, p. 175) describes palleal budding, whereas Van Name (1945, p. 234) describes stolons. Herein the character is coded as polymorphic (1 & 2) for *B. schlosseri*, *S. brakenhielmi* and *K. borealis*, as both types of budding seem to be present in the three species.
32. Type of epicardial budding: (0) strobilation; (1) pyloric (esophageal and entero-epicardial). Strobilation or transverse fission means that the thoracic region is absorbed, a series of constrictions divide the posterior part into several regions from which the buds develop. In *D. stylifera* buds already are developed in the larvae. According to Berrill (1935), the larval budding of members of *Distaplia* evolved as a heterochronic shift. The main source of tissue in the larval bud is the epicardium. In addition, that author states that larval and adult budding in *Distaplia* are essentially the same. In both cases, Berrill (1935) mentions the "constriction" of the epidermis. Investigated members of Didemnidae show an exceptional mode of budding – pyloric budding. A new thorax and abdomen are formed through epicardial budding; although the new thorax connects with the old abdomen, the new abdomen connects with the old thorax (Berrill, 1935; Sköld et al., 2011; Groepler and Stach, 2019).
33. Type of strobilation: (0) abdominal; (1) postabdominal. Members of Polyclinidae possess a tripartite body and strobilation is located in the postabdomen. In the other investigated aplousobranch species that develop buds through strobilation, budding occurs in the abdomen (Berrill, 1935; Van Name 1945).
34. Type of mesenchymatic budding: (0) septal; (1) vascular. In septal budding the septum in the stolon is the major source of cells for the development of buds (Berrill, 1935; Huus, 1956; Nakauchi, 1982; Groepler, 2016). Stolons, however, also are involved in other forms of budding (see characters 26 and 29). In vascular budding, hemocytes are the major source of tissue for the developing buds (Nakauchi, 1982; Groepler, 2016).

Branchial basket

35. Shape of branchial basket wall: (0) unfolded; (1) folded. The pharynx of primarily aquatic chordates is perforated with paired stigmata and is usually called branchial basket. In some ascidians the wall of the branchial basket is folded with clearly demarcated folds extending into the lumen of the branchial

basket. Stolidobranchiata is named after this character, yet the branchial baskets of the smaller colonial stolidobranch species and *P. corrugata* are not folded (e.g. Drasche, 1884; Van Name, 1945; Berrill, 1950). In *D. grossularia* at least one fold is present (Hartmeyer, 1923).

36. Arrangement of branchial stigmata in one side of the body: (0) one stigma; (1) three rows; (2) four rows; (3) more than four rows. The number of rows of stigmata in the branchial basket of adult individuals is considered here. Note that the orientation of rows in ascidians is perpendicular to the anterior–posterior axis and develops through stages where a row is represented by a single stigma that is then called a protostigma. Consequently, a stigma in cephalochordates and lampreys corresponds to a row of stigmata in ascidians (see also character 38), so the character state for the outgroup species was coded as 3. Information on character distribution is found in Berrill (1950), Ihle (1956), Kott (1985, 1990, 2001), Lohmann (1914) and Van Name (1945).

37. Shape of stigmata: (0) straight; (1) lunate or spiral; (2) round or ovoid; (3) expanded. Most tunicate species and outgroup species

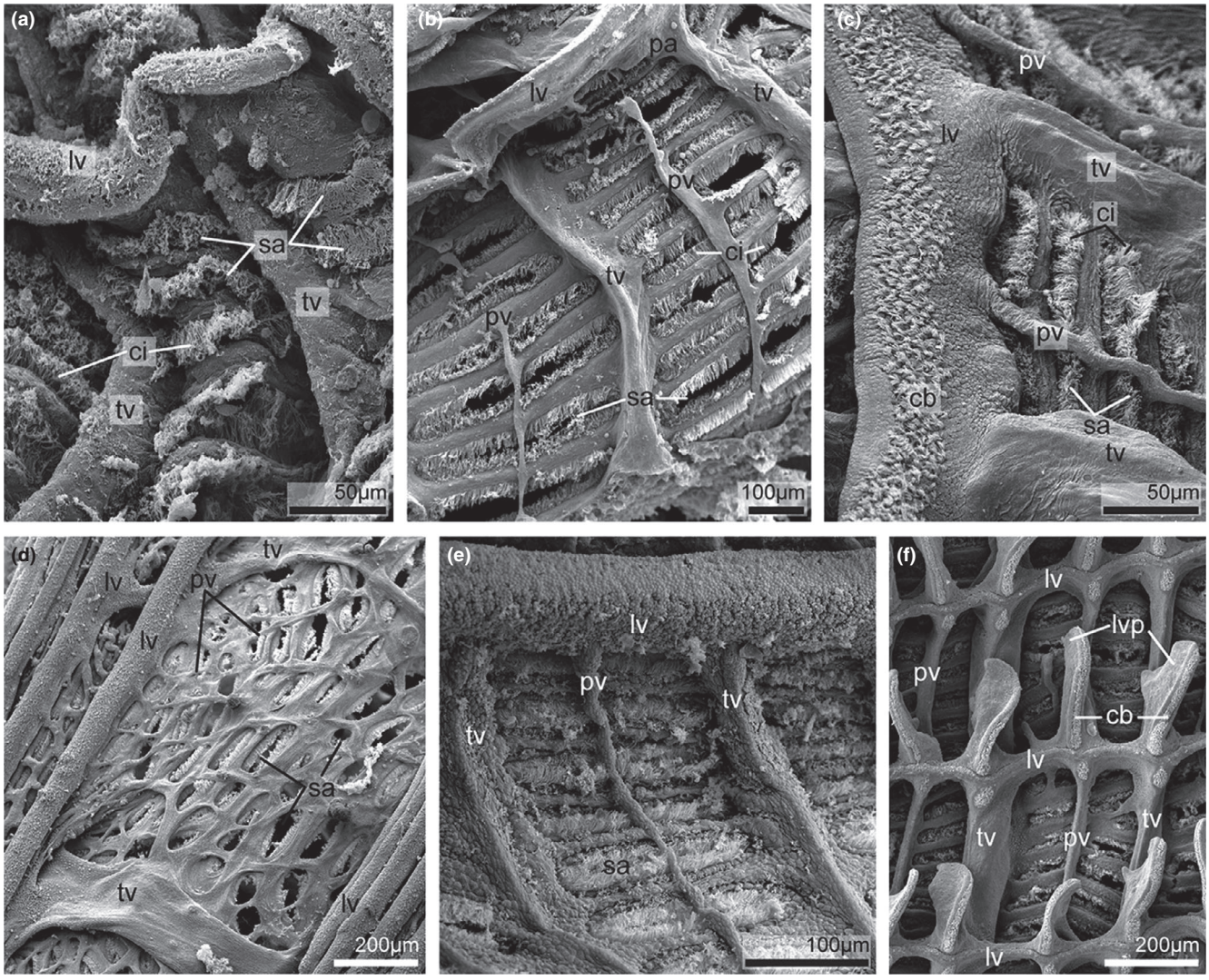

Fig. 6. Scanning electron micrographs of parastigmatic blood vessels (pv) in different ascidian species. (a) The branchial basket of *Botryllus schlosseri* lacks parastigmatic blood vessels. (b) In the branchial basket of *Kukenthalia borealis* parastigmatic blood vessels cross stigmata (sa). (c) Parastigmatic blood vessels of *Styela plicata*. Longitudinal blood vessels (lv) are equipped with ciliary bands (cb). (d) Several parastigmatic blood vessels emanate from longitudinal blood vessels, crossing the stigmata of *Molgula citrina*. (e) Parastigmatic blood vessels of *Microcosmus claudicans*. (f) In the branchial basket of *Ciona intestinalis* parastigmatic and transverse blood vessels (tv) alternate. ci, cilia; lvp, papillae on longitudinal vessel; pa, papillae supporting longitudinal blood vessel.

possess straight stigmata. Information on character distribution is found in Berrill (1950), Lohmann (1956) and Van Name (1945). In Salpida the branchial wall is almost completely missing, resulting in a single pair of largely expanded openings considered herein as the stigma and coded therefore as 3. See also Figs. 6–8, 10 and 12.

38. Orientation of stigmata in adults: (0) longitudinal (anterior to posterior); (1) transversal (ventral to dorsal). This character is only applicable for straight stigmata. The longitudinal axis of a single stigma is considered here. Although in the examined ascidian species stigmata are orientated longitudinally, in Doliolida and Pyrosomatida, and in the outgroup species, stigmata are transversal in orientation (see also comment for character 36).
39. Parastigmatic blood vessels: (0) absent; (1) present. Parastigmatic blood vessels are intermediate transverse vessels that cross the stigmata but do not interrupt them (Kott, 1985). Information on character distribution is found in Van Name (1945); see also Fig. 6.
40. Internal longitudinal blood vessels: (0) absent; (1) present. Longitudinal blood vessels are vessels that protrude visibly into the lumen of the branchial basket (Kott, 1985 (Fig. 3); Monniot and Monniot, 1972 (see Fig. 1)). The term is equivalent to the term "internal longitudinal vessels" of Van Name (1945). Longitudinal blood vessels are present in all investigated pyrosome, phlebobranch and stolidobranch species, and in *D. violacea* (Fig. 7).
41. Internal longitudinal blood vessel on papillae: (0) no; (1) yes. Longitudinal blood vessels can be raised above the level of the stigmata. In such cases, the longitudinal blood vessels are situated on papillae (Fig. 7a–f and schematic Fig. 7i 2).
42. Cilia on internal longitudinal blood vessels: (0) absent; (1) present. Cilia on the internal longitudinal blood vessels project into the lumen of the branchial basket (Fig. 7a–h).
43. Arrangement of cilia on internal longitudinal blood vessels: (0) continuous row of cilia; (1) cilia in individual tufts. In the ascidian species where cilia on internal longitudinal blood vessels are present (character 42: 1), these cilia are arranged in a continuous row. In *P. atlanticum* cilia are arranged in groups forming individual tufts (Fig. 7a–h).
44. Branchial papillae: (0) absent; (1) present. Branchial papillae project into the lumen of the branchial basket from the level of the actual gill slits. Branchial papillae can support longitudinal vessels (Kott, 1985). They are present in all members belonging to Phlebobranchiata and in *P. atlanticum* (Fig. 7a), *D. violacea* and members of the genus *Polyclinum* (Van Name, 1945; Berrill, 1950; Moreno and Rocha, 2008; Groepler, 2016).
45. Papillae at intersections of transverse and longitudinal vessels (to avoid confusion with papillae described in character 44, the term LV-papillae is used here): (0) absent; (1) present. LV-papillae bulge into the branchial basket at the intersections of transverse and longitudinal vessels thus projecting above the level of the internal longitudinal vessels, as spoon or sickle-shaped, free-standing papillae (Fig. 7c–f).
46. Cilia on junctions of longitudinal and transverse vessels: (0) absent; (1) present. Ciliated junctions of longitudinal and transverse vessels are present in all investigated phlebobranch species (Fig. 7b–f) and in *D. violacea*.
47. Dorsal organ: (0) absent; (1) present. The dorsal organ is a structure projecting along the dorsal midline into the branchial basket. Structurally it is a ciliated elevation (that may be grooved), a ciliated fold of the branchial wall or a series of ciliated tongue-like projections along the mid-dorsal line of the branchial basket that usually is curved in transverse section (Kott, 1985). The cilia facilitate the transport of the food-particle-laden mucus net. The term "dorsal organ" is preferred herein in order to indicate the correspondence of structures situated in the dorsal midline of the branchial basket, which in traditional taxonomic treaties are labelled as dorsal lamina, dorsal languets, dorsal groove etc. A dorsal organ is present in most tunicate species, except Doliolida (Deibel and Paffenhöfer, 1988). The dorsal organ in *Branchiostoma* is usually called "epipharyngeal groove" (Franz, 1927; Ruppert, 1997b). It corresponds to the dorsal ridge in lampreys (Mallat, 1979).
48. Dorsal organ consisting of languets: (0) no; (1) yes. Languets are finger- or tongue-like projections into the lumen of the branchial basket. Information on character distribution is found in Berrill (1950), Kott (1985) and Van Name (1945); see also Fig. 8.
49. Number of languets equals number of transverse vessels: (0) no; (1) yes. In most

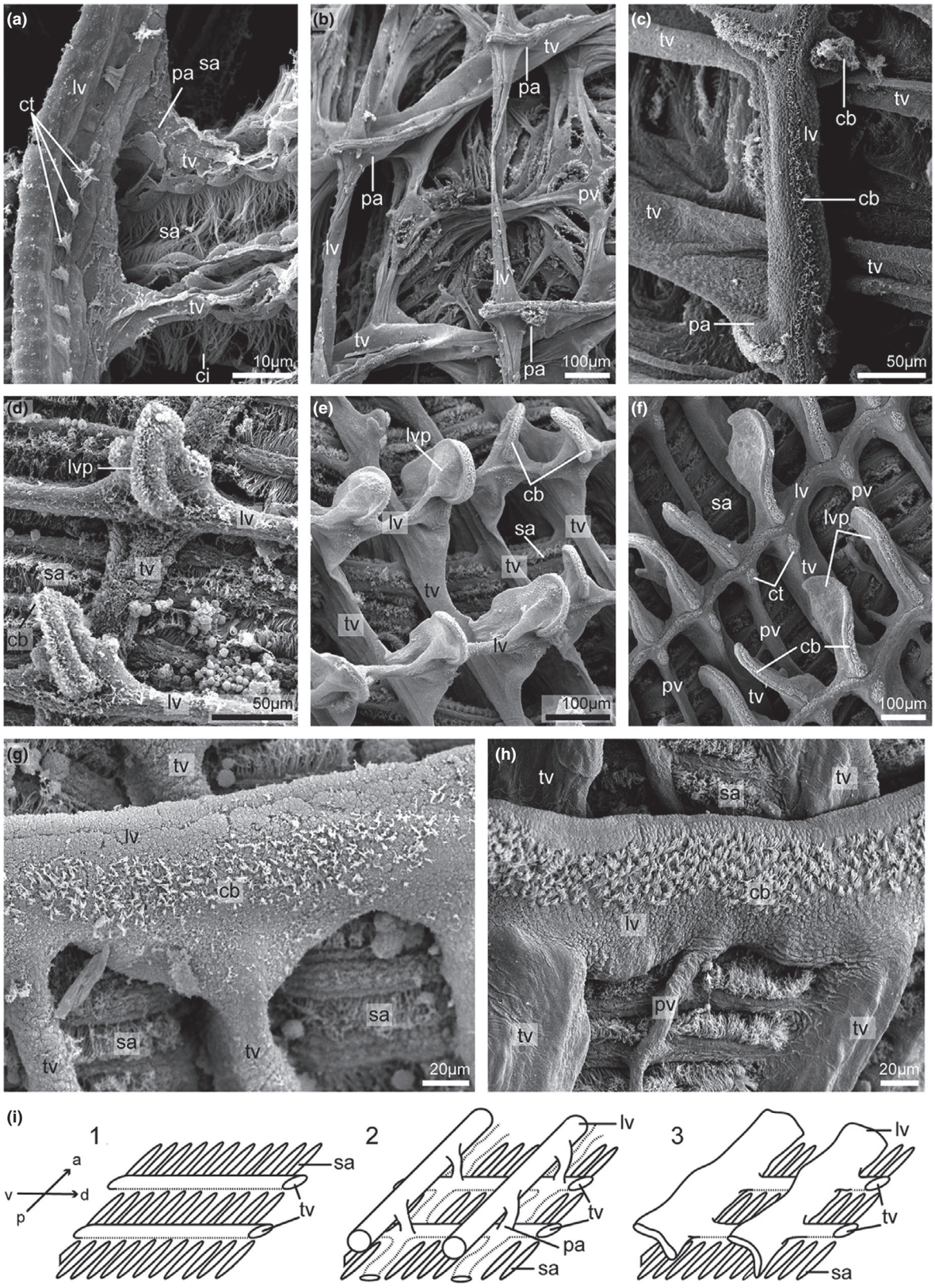
(a)
lv
pa
sa
ct
tv
sa
tv
ci
10µm
(b)
tv
pa
pa
pv
lv
lv
tv
pa
100µm
(c)
tv
tv
cb
lv
cb
tv
tv
pa
50µm
(d)
lvp
lv
sa
tv
cb
lv
50µm
(e)
lvp
cb
lv
sa
tv
tv
tv
lv
100µm
(f)
sa
lv
pv
lvp
tv
ct
pv
cb
pv
tv
100µm
(g)
tv
lv
cb
sa
sa
tv
tv
20µm
(h)
tv
sa
tv
cb
lv
pv
tv
tv
20µm
(i)
1
a
v
d
p
sa
tv
2
lv
tv
pa
sa
3
lv
tv
sa

Fig. 7. Scanning electron micrographs of longitudinal blood vessels (lv) in the branchial basket of different tunicate species. (a) Longitudinal blood vessel in the branchial basket of *Pyrosoma atlanticum*. Longitudinal blood vessels settle on papillae (pa) and bear several individual ciliary tufts (ct). (b–f) Longitudinal and transverse blood vessels of phlebobranch ascidians. Cilia settle on junctions of transverse and longitudinal vessels in form of ciliary bands or ciliary tufts. (b) In *Corella parallelogramma* longitudinal vessels also settle on papillae. (c) Longitudinal blood vessels in *Ascidiella scabra* are situated on papillae and possess ciliary bands that also proceed longitudinally (cb). (d) In *Ascidia virginea* longitudinal blood vessels that settle on papillae and possess longitudinal ciliary bands are present. (e) In the branchial basket of *Phallusia nigra* longitudinal vessels are situated on papillae. Ciliary bands run along the longitudinal vessels. (f) In *Ciona intestinalis* longitudinal blood vessels settle on papillae. Note ciliary bands running along the longitudinal vessels. At each intersection of longitudinal and transverse blood vessels (tv) an individual ciliary tuft is visible. (g) Longitudinal blood vessels of *Halocynthia roretzi* are not situated on papillae. They overlap into the cavity of the branchial basket and bear a wide ciliary band. (h) In *Styela plicata* papillae in the branchial basket are missing. A broad ciliary band runs along with the longitudinal blood vessel. (i) Schematic drawings of the arrangement of longitudinal and transverse blood vessels in tunicates. 1, solely transverse blood vessels are developed; 2, longitudinal blood vessels are present, these settle on papillae; 3, longitudinal vessels settle on transverse vessels, not on papillae. They project into the lumen of the branchial basket. ci, cilia; lvp, papillae on longitudinal blood vessel; sa, stigma.

investigated aplousobranch and phlebobranch species the number of languets of the dorsal lamina equaled the number of transverse vessels (Fig. 8b,c,f,h). In a few other species the number of transverse vessels is higher than the number of languets (Fig. 8a,g).

50. Dorsal organ with a membrane: (0) no; (1) yes. In cases where the dorsal organ membrane was coded as present, the rim of the dorsal organ is present as a thin, yet clearly continuous rim (see Fig. 8k 3&4). In *P. atlanticum*, investigated phlebobranch species and most investigated stolidobranch species a membrane is developed in the dorsal organ that projects into the lumen of the branchial basket and connects the languets (see character 48) (Fig. 8a,g-j,k).
51. Membrane in the dorsal organ smooth edged or plain: (0) no; (1) yes. See Fig. 8h–k.
52. Dorsal organ with multiple transverse ciliary bands: (0) no; (1) yes. Ciliary bands, usually continuous with ciliary bands on the transverse blood vessels, can extend onto the dorsal organ. See Fig. 8a–h. The cilia of the gill bar in Salpida are considered to be homologous to ciliary bands traversing the dorsal organ in ascidians (Fig. 9a). Mallat's description (1979) shows that this character is absent in lampreys.
53. Dorsal organ as a strongly ciliated, yet elevated groove: (0) no; (1) yes. See Fig. 9b–d.
54. Shape of peripharyngeal band: (0) flat ciliated epithelium; (1) ciliated groove. The peripharyngeal band (synonym: pericoronal band (Burighel et al., 2003) limits the branchial basket to the anterior and is a conspicuous ciliated band. The shape varies among tunicates. In some species it is present as a groove (Fig. 10a,b), whereas in others it is flat (Fig. 10c,d). The peripharyngeal band corresponds to the pseudobranchial groove in Petromyzontidae.
55. Peripharyngeal band with conspicuous dorsal curvature: (0) no; (1) yes. The peripharyngeal band extends from the anterior end of the ventral endostyle to the dorsal midline just behind the dorsal tubercle. In some species the course of the peripharyngeal band describes a sharp bend in its dorsal third (Figs 10c, 13e and 14c).
56. Papillae in prebranchial area: (0) absent; (1) present. The prebranchial area is the area between the ring of oral tentacles and the peripharyngeal bands. Papillae are short projections in this area. Information on character distribution is found in Millar (1966; p. 60), and Gill et al. (2003); see also Fig. 10a.

Excretory and digestive structures

57. Distinct excretory structure: (0) absent; (1) present (see also character 58). Distinct excretory structures seem to be missing in most tunicate species. In Doliolida, Godeaux et al. (1998) speculate that the pyloric gland might be an excretory organ. The pyloric gland is coded as homologous across Tunicata with a different (main) function and for Doliolida this character state is coded as 0.
58. Type of excretory structure: (0) renal sac (synonym: kidney; Van Name, 1945; Kott, 1985); (1) excretory vesicles or nephrocytes. The renal sac or kidney is a kidney-shaped organ on the right side of the body in molgulids. It is compact, sac-like and accumulates excretory products. In all other tunicate species that possess excretory structures, these are developed as excretory vesicles (also called renal vesicles) or nephrocytes. Excretory vesicles are small structures that accumulate crystalline waste products and cover the gut loop and gonads of some ascidians. Nephrocytes are cells that contain

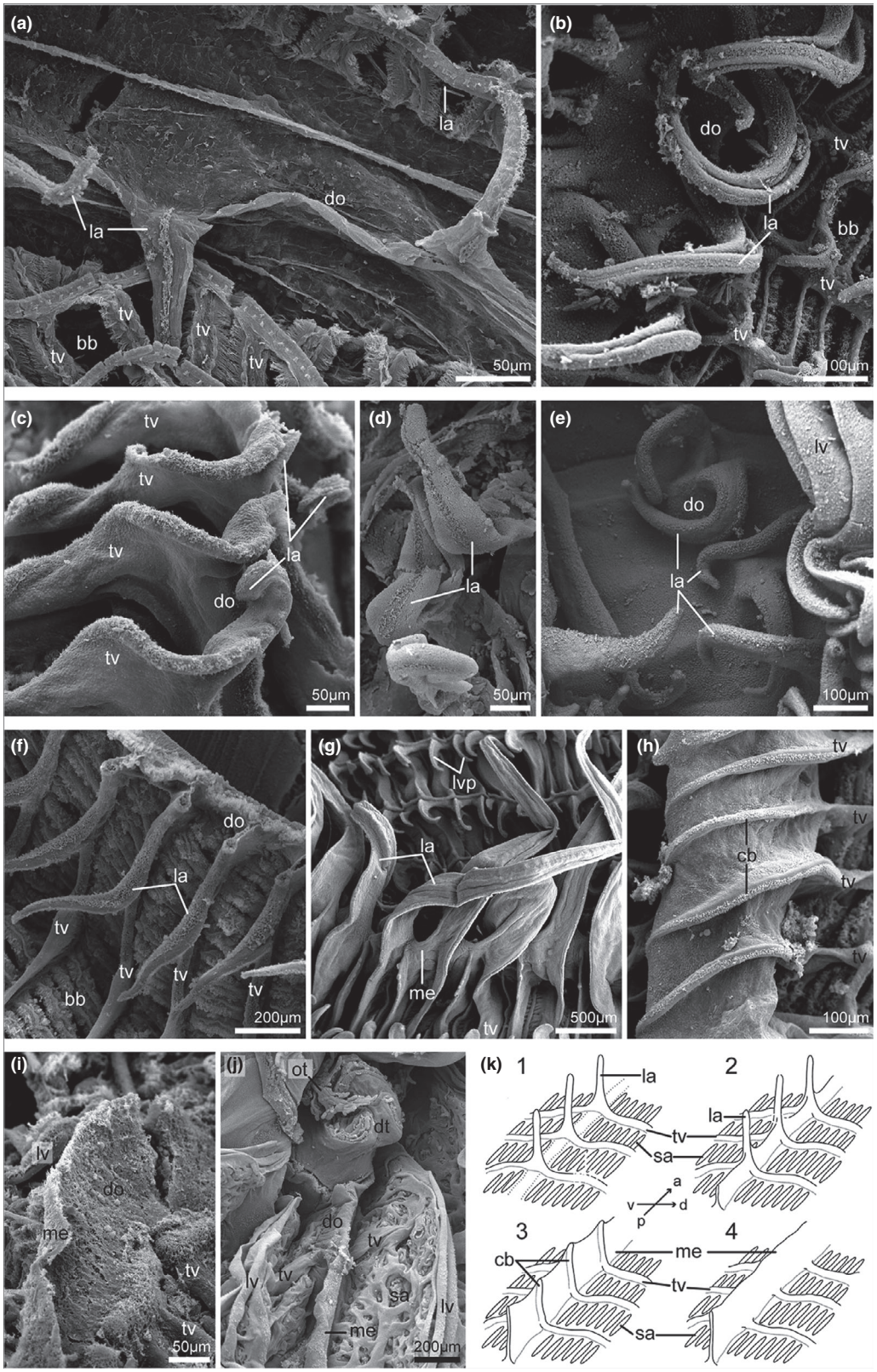
(a)
la
do
la
tv
bb
tv
tv
tv
tv
50µm
(b)
do
tv
la
bb
tv
tv
100µm
(c)
tv
tv
tv
la
do
tv
50µm
(d)
la
50µm
(e)
lv
do
la
100µm
(f)
do
la
tv
tv
tv
tv
bb
200µm
(g)
lvp
la
me
tv
500µm
(h)
tv
tv
cb
tv
tv
100µm
(i)
lv
do
me
tv
tv
50µm
(j)
ot
dt
do
tv
lv
tv
sa
lv
me
200µm
(k)
1
la
tv
sa
2
la
a
v
d
p
3
cb
4
me
tv
sa

Fig. 8. Scanning electron micrographs of the dorsal organs (do) in the branchial basket (bb) of diverse tunicate species. (a) Dorsal organ with languets (la) in the branchial basket of *Pyrosoma atlanticum*. The number of transverse blood vessels (tv) is higher than the number of languets. (b) In *Rhodosoma callense* the dorsal organ is equipped with languets, numbers of languets and transverse blood vessels equal. (c) Languets of the dorsal organ in *Clavelina lepadiformis* are transversally broadened. Numbers of languets correspond to numbers of transverse blood vessels. (d) In *Herdmania momus* languets settle on the dorsal organ. The number of transverse blood vessels is higher than the number of languets. (e) In *Halocynthia roretzi* languets at the dorsal organ are present but the number of languets is not identical to the number of transverse blood vessels. (f) Dorsal organ with languets in *Sycozoa sigillinoides*. Numbers of transverse blood vessels and languets are equal. (g) In *Ciona intestinalis* every second transverse blood vessels runs into a languet of the dorsal organ, others end blindly. At the base of the languets a membrane (me) is developed connecting the languets. (h) The membrane of the dorsal organ in *Phallusia nigra* completely covers the languets. They are visible as protruding ciliary bands (cb). The number of languets equals the number of transverse blood vessels. (i) In *Botryllus schlosseri* the dorsal organ is visible as a smoothly edged membrane without individual languets. (j) The dorsal organ in *Molgula manhattensis* forms a plain membrane without detectable languets. (k) Schematic drawings of the different forms of the dorsal organ in tunicates. 1, transverse blood vessels form languets that are not connected by a membrane at their base; 2, a longitudinal membrane connects languets; 3, a longitudinal membrane completely covers languets. Languets are detectable as ciliary protrusions; 4, the dorsal organ is smoothly edged or plain without ciliary protrusions. Languets are not present. dt, dorsal tubercle; lv, longitudinal blood vessel; ot, oral tentacle; lvp, papillae on longitudinal blood vessel; sa, stigmata.

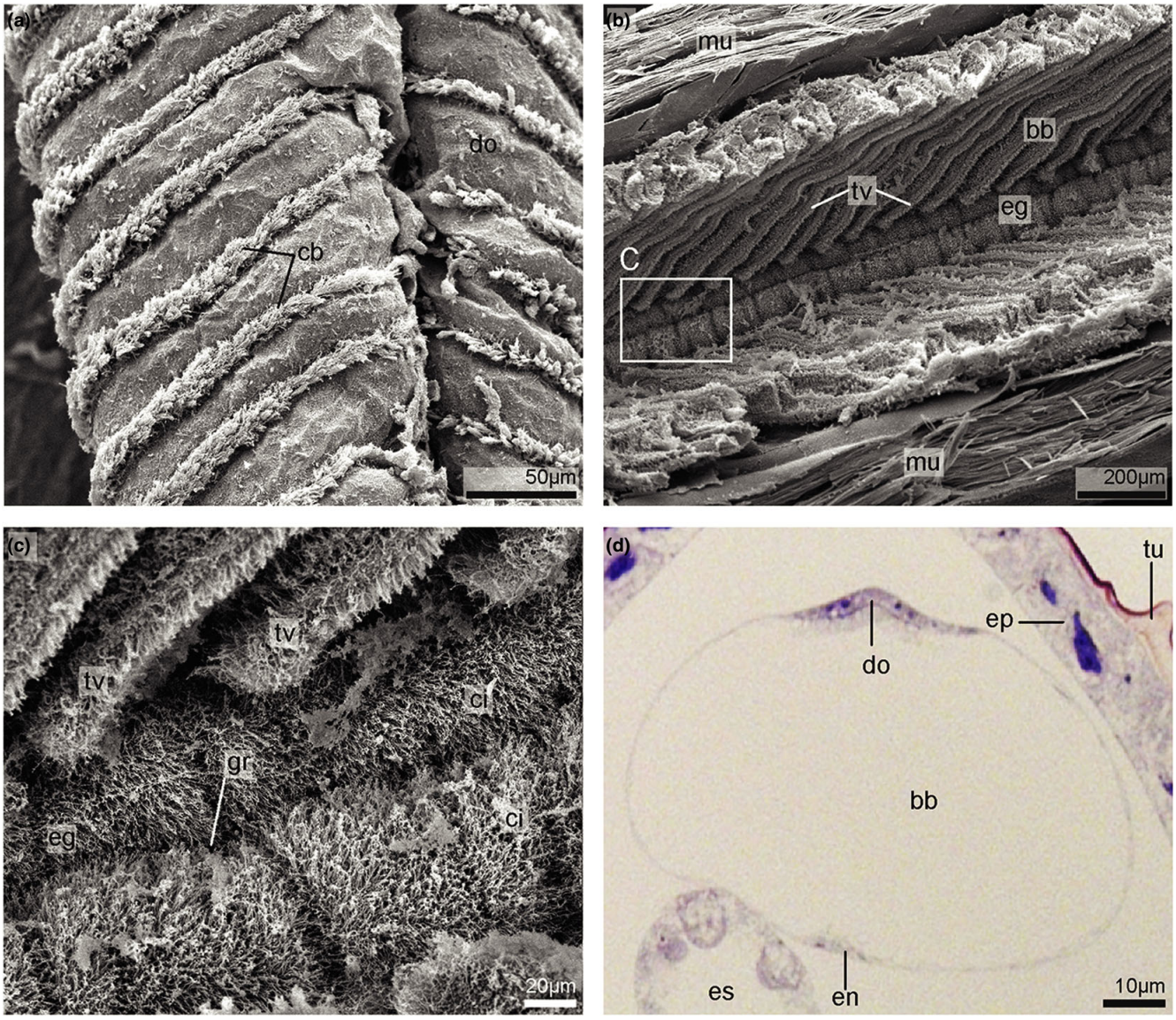

Fig. 9. Scanning electron micrographs of the dorsal organs (do) and cilia (ci) in two different tunicate species and the cephalochordate species *Branchiostoma lanceolatum*. (a) Dorsal organ with evenly distributed ciliary bands (cb) in *Salpa fusiformis*. (b, c) In *Branchiostoma lanceolatum* the dorsal organ is called epipharyngeal groove (eg). Two ciliated membranes border the ciliated groove (gr). Area marked with a white rectangle is shown in higher magnification in C. (d) Light micrograph of a semithin cross-section through *Oikopleura dioica* stained with toluidine blue, dorsal to the top, right to the right. The dorsal organ is visible as a ciliated groove. bb, branchial basket; en, endostyle; ep, epidermis; es, oesophagus; mu, musculature; tu, tunic; tv, transverse blood vessel.

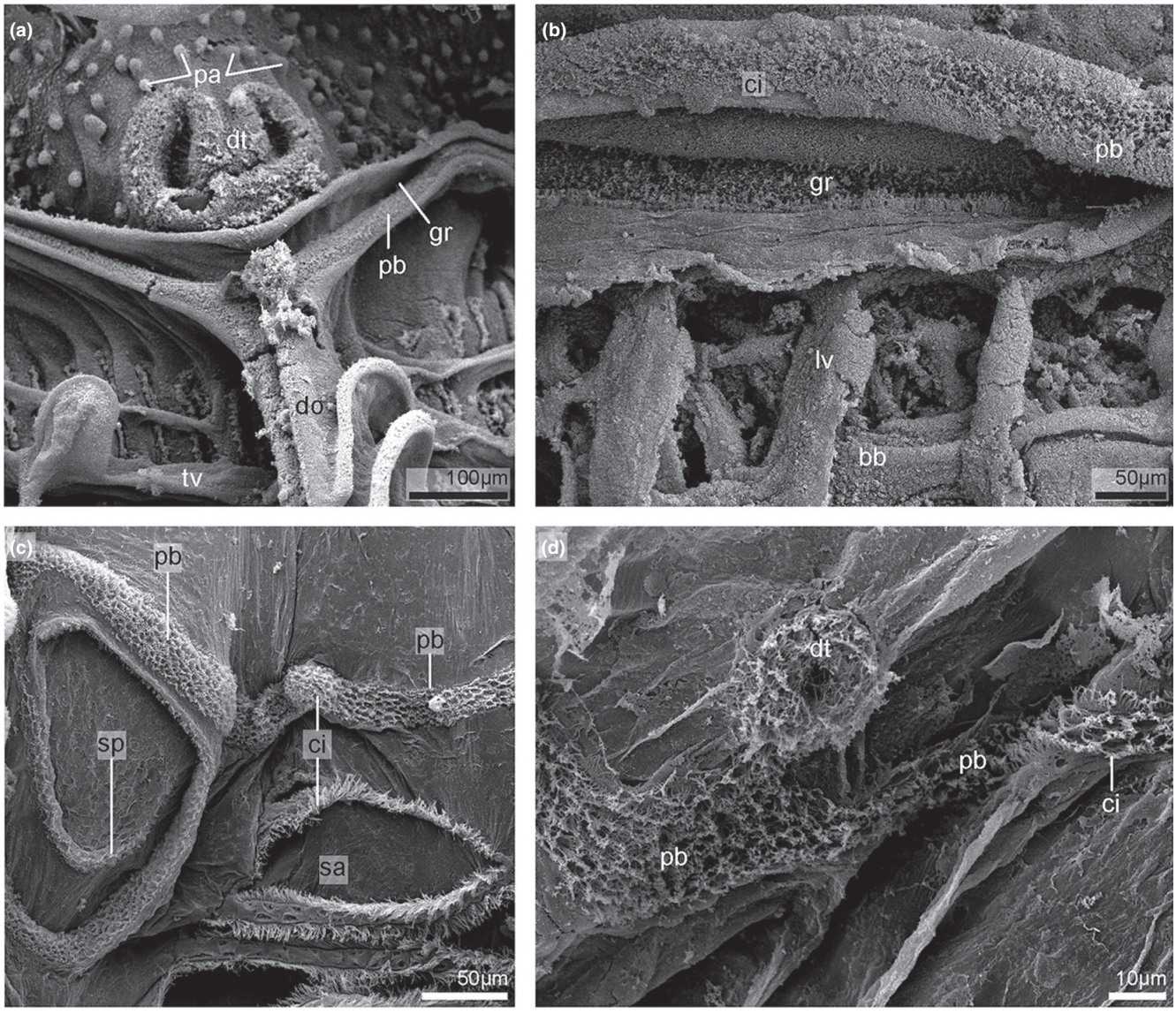

Fig. 10. Scanning electron micrographs of the peripharyngeal band (pb) and prebranchial area of four different tunicate species. (a) In *Phallusia nigra* several papillae (pa) are situated in the prebranchial area. The peripharyngeal band is developed as a ciliated groove (gr). The opening of the dorsal tubercle (dt) is U-shaped. (b) The peripharyngeal band in *Herdmania momus* is visible as ciliated groove. (c) The peripharyngeal band in *Doliolum nationalis* is a flat ciliated epithelium that has a conspicuous curvature on its dorsal side, the dorsal spiral (sp). (d) *Pyrosoma atlanticum* possesses a flat ciliated peripharyngeal band. The opening of the dorsal tubercle is a simple ciliated funnel. bb, branchial basket; ci, cilia; do, dorsal organ; lv, longitudinal blood vessel; sa, stigma; tv, transverse blood vessel.

vacuoles that store excretory crystals and that occur throughout the hemocoel but in many cases are especially numerous around the intestinal tract. The filtration kidneys in Cephalochordata and Petromyzontidae are not considered to be homologous to kidneys or nephrocytes in tunicates, and the character state is coded as "not applicable" in the outgroup species.

59. Stomach: (0) smooth; (1) folded or irregularly plicated. This character considers glandular swellings or folds that can be apparent on the stomach wall. The stomach in Salpida is not clearly demarcated from the remainder of the intestine. There are, however, a number of caeca that are traditionally considered to open into the area corresponding to the stomach in other tunicates (Ihle, 1956). The exact number of these caeca differs among species and also between generations, yet the corresponding area in salps is therefore sculpted and accordingly

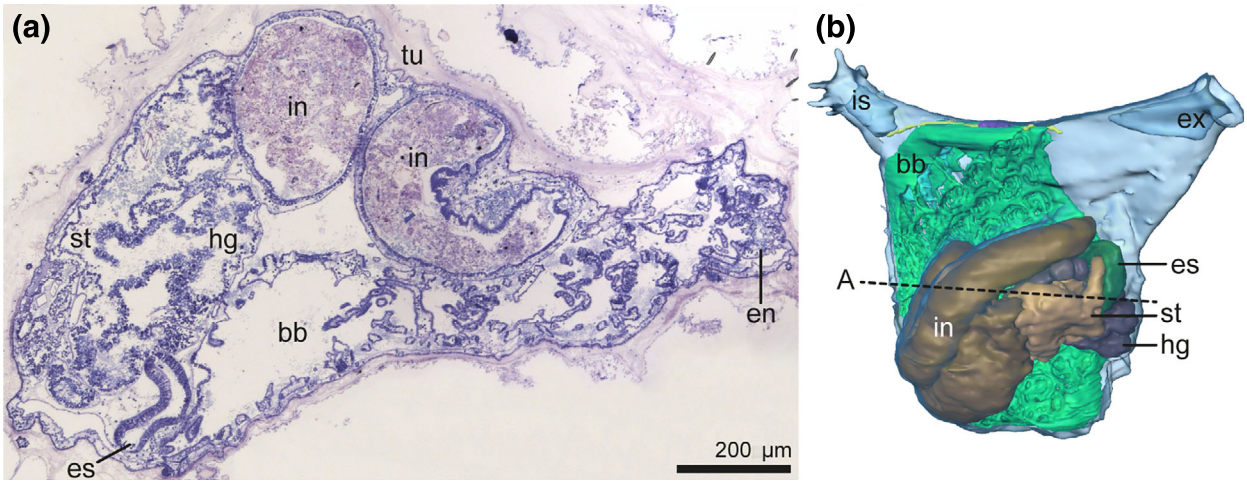

Fig. 11. Hepatic gland (hg) in *Molgula manhattensis*. (a) Light micrograph of a semithin cross-section through the branchial basket and digestive tract stained with toluidine blue, ventral to the right, left to the top. Several outgrowths on the ventral side of the stomach (st) are visible that constitute the hepatic gland. (b) 3D reconstruction of the internal anatomy, view from left side, anterior to the top. The section plane of (a) is indicated by a dotted back line. The hepatic gland is shown in dark purple and visible as several outgrowths of the stomach. bb, branchial basket; en, endostyle; es, oesophagus; ex, excurrent siphon; in, intestine; is, incurrent siphon; tu, tunic.

coded as 1. Fenaux (1998) depicts a specimen of the appendicularian *Megalocercus abyssorum* Chun, 1887 as representative for the genus and describes the stomach in the general diagnosis of the genus as being without any folds.

60. Hepatic gland: (0) absent; (1) present. A hepatic gland (Van Name, 1945) or liver (Kott, 1985) or digestive gland (Collin et al., 2016) consists of irregular outgrowths on the ventral side of the stomach. In cross-sections of the stomach, these outgrowths appear branched or more complex compared to the simple regular folds in some other species (Fig. 11). Hepatic glands are developed in some stolidobranch ascidian species (Huus, 1956). The "hepatic gland" is homologized with the "stomach caecum" (see character 61) yet it is regarded as a more complex, more obviously glandular form of this organ; therefore, this character is not applicable for species without a stomach caecum.

61. Stomach caecum: (0) absent; (1) present. A stomach caecum is a simple, blindly ending diverticulum protruding from the stomach into the gut loop (Kott, 1985). The hepatic gland of Molgulidae and Pyuridae is homologized with the stomach caecum. Accordingly, stomach caeca are scored as present in Salpida (Ihle, 1956), and most Stolidobranchiata. Some authors refer to the stomach caecum as "pyloric caecum" or "hepatic caecum" (Kott, 1985).

62. Pyloric gland: (0) absent; (1) present. The pyloric gland consists of tubules that encircle the ascending limb of the gut loop. The tubules merge into a single duct, which opens into the distal end of the stomach (Kott, 1985). The pyloric gland is developed in all investigated tunicate species. In the outgroup species it is not present (Huus, 1956). Synonym: gastrointestinal gland (Kott, 1985).

63. Shape of gastrointestinal tract: (0) straight; (1) U-shaped. In most tunicate species the gastrointestinal tract is curved or U-shaped concordant with a close proximity of the incurrent and excurrent siphons. Notably, in the planktonic thaliacean species the gastrointestinal tract is U-shaped, whereas incurrent and excurrent siphons are at opposite ends of the animals. In the investigated outgroup species the gastrointestinal tract is straight.

64. Position of gastrointestinal tract in relation to branchial basket: (0) mostly posterior; (1) lateral.

65. Position of lateral gastrointestinal tract: (0) on left side; (1) on right side. Although in most ascidians with lateral gastrointestinal tracts the latter are situated on the left side of the body, gastrointestinal tracts are situated on the right side of the body in members of Corellidae.

66. Position of rectum in species with a mostly posterior gastrointestinal tracts

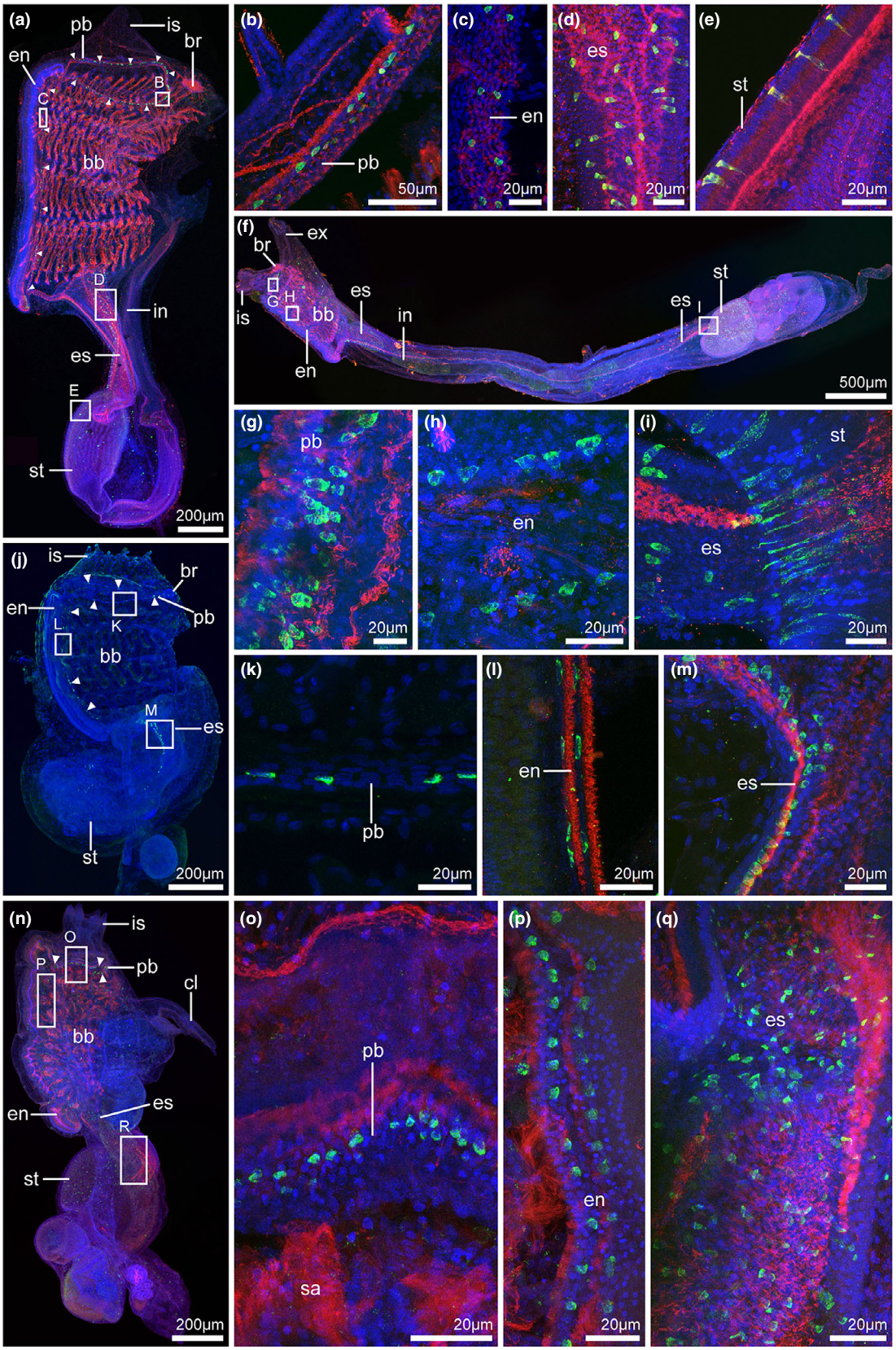
(a)
pb
is
br
en
B
C
bb
D
in
es
E
st
200µm
(b)
pb
50µm
(c)
en
20µm
(d)
es
20µm
(e)
st
20µm
(f)
ex
br
G H
is
bb
es
in
en
es
I
st
500µm
(g)
pb
20µm
(h)
en
20µm
(i)
st
es
20µm
(j)
is
br
en
pb
L
K
bb
M
es
st
200µm
(k)
pb
20µm
(l)
en
20µm
(m)
es
20µm
(n)
is
O
P
pb
cl
bb
en
es
R
st
200µm
(o)
pb
sa
20µm
(p)
en
20µm
(q)
es
20µm

Fig. 12. Z-projections of confocal laser scanning micrographs of immunohistochemical stainings with antibodies against serotonin (green) and tyrosinated-α-tubulin (red), and with DAPI and Hoechst (blue) in four different aplousobranch species. (a–e) Localization of serotonin-like immunoreactivity (serotonin-lir) in *Distaplia stylifera*, anterior to the top, dorsal to the right. Areas with immunopositive cells are marked with white rectangles, higher magnifications of these areas shown in (b–e). (a) Lateral view of an entire animal. (b) Higher magnification of the peripharyngeal band (pb). (c) Detail of serotonin-lir in the endostyle (en). (d) Serotonin-lir cells are present as more or less spherical cells and bottle-shaped cells in the esophagus (es). (e) Elongated serotonin-lir cells are situated in the epithelium of the stomach (st). (f–i) Serotonin-lir in *Eudistoma obscuratum*, dorsal to the top, anterior to the left. (f) Lateral view on a complete zooid. White rectangles mark areas that are shown in higher magnification in (g–i). (g) Serotonin-lir in the peripharyngeal band. (h) Localization of serotonin-lir in the endostyle. (i) Transition zone of esophagus and stomach is characterized by diverse elongated serotonin-lir cells. (j–m) Distribution of serotonin-lir cells in *Lissoclinum verrilli*, view from left side, anterior to the top. Regions marked with white rectangles are shown in higher magnification in (k–m). (k) Detail of the peripharyngeal band. (l) Higher magnification of the endostyle. (m) In the esophagus few rows of serotonin-lir cells are situated. (n–r) Serotonin-lir in *Polyclinum constellatum*, view from left side, anterior to the top, dorsal to the right. White rectangles indicate regions of which higher magnifications are shown in (o–r). (o) Serotonin-lir cells in the peripharyngeal band. (p) In the endostyle two parallel rows of serotonin-lir cells are visible. (q) Detail of serotonin-lir in the esophagus. bb, branchial basket; br, brain; cl, atrial languet; ex, excurrent siphon; in, intestine; is, incurrent siphon.

(character 64: 0): (0) dorsomedian; (1) ventromedian.

Atrium

67. Atrium: (0) absent; (1) present. The atrium is the enclosed room opening into the excurrent siphon. Where present, the atrium takes up water that passed through the gill slits of the branchial basket. Gonoducts as well as the anus open into the atrium. An atrium is present in most tunicate species and in cephalochordates (Huus, 1956). In Appendicularia, gill slits open directly to the exterior and an atrium is absent. In ammocoete larvae, gills open individually to the exterior (despite the occurrence in cross-sections - see Goodrich (1909) who depicts a longitudinal section); the same situation is observed for adult specimens. Therefore, this character state is coded as 0 for Petromyzontidae.
68. Origin of atrium: (0) ventral; (1) dorsal. The atrium in tunicate species develops (in most cases) as a dorsal invagination of the ectoderm, whereas in cephalochordates two ventral folds extend and fuse to form the atrium (Franz, 1927; Huus, 1956; Stokes and Holland, 1995).
69. Shape of ontogenetic rudiment of atrial opening: (0) paired; (1) unpaired. In most ascidian species, paired rudiments of the atrial cavities fuse during ontogeny on the dorsal side. In Salpida, Stolidobranchiata and Cephalochordata the ontogenetic rudiment of the atrial opening is unpaired. Information on character distribution is found in Huus (1956) and Ihle (1956).
70. Position of unpaired rudiment of atrial opening: (0) ventral; (1) dorsal. Rudiments of the atrial opening in tunicates with unpaired rudiments are present on the dorsal side, whereas in Cephalochordates these rudiments are located on the ventral side (Huus, 1956; Ihle, 1956; Stokes and Holland, 1995).

Sexual reproduction

71. Hermaphroditism: (0) absent; (1) present. With the exception of *O. dioica* and *Sycozoa sigillinoides* most examined tunicate species are hermaphroditic. Cephalochordata and Petromyzontidae are dioecious.
72. Type (position) of gonads: (0) enterogon; (1) pleurogon. This character is traditionally used in ascidian taxonomy. "Enterogon" gonads are positioned on the visceral side in proximity to the intestinal tract as, for example, in Phlebobranchiata and Aplousobranchiata. The position of gonads in Thaliacea and Appendicularia is homologized with the enterogon type. Lampreys are coded as enterogon (0) here, because lamprey gonads are unpaired and closely associated with the intestine (Ihle, 1971). In species coded as 1, pleurogon gonads are located on the parietal side as in stolidobranch ascidians. In *Branchiostoma* gonads are positioned on the parietal side of the pharyngeal region (see, e.g., Franz, 1927), and accordingly are coded 1 here.
73. Position of gonads in relation to branchial basket: (0) lateral; (1) posterior. In Appendicularia, Thaliacea, *C. intestinalis*, Aplousobranchiata and Petromyzontidae, gonads are positioned posterior to the branchial basket, yet they are positioned lateral to the branchial basket in most Phlebobranchiata, Stolidobranchiata and Cephalochordata.
74. Occurrence of gonads: (0) unpaired; (1) paired. In most tunicate species and in lampreys gonads are unpaired. Information on character distribution is found in Berrill

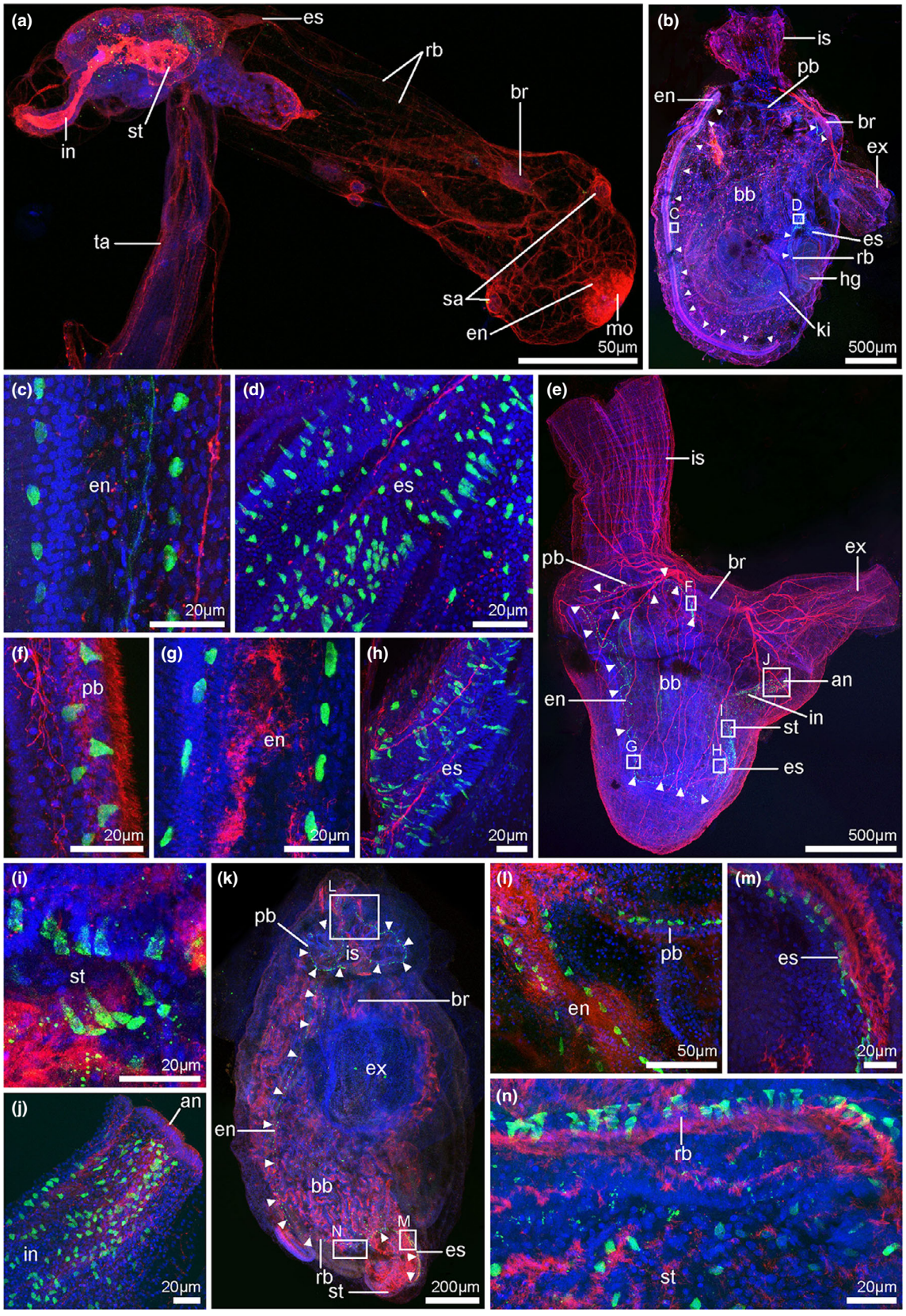
(a)
es
rb
br
st
in
ta
sa
en
mo
50µm
(b)
is
pb
en
br
ex
bb
C
D
es
rb
hg
ki
500µm
(c)
en
20µm
(d)
es
20µm
(e)
is
pb
br
ex
F
bb
J
an
en
I
in
st
G
H
es
500µm
(f)
pb
20µm
(g)
en
20µm
(h)
es
20µm
(i)
st
20µm
(j)
an
in
20µm
(k)
L
pb
is
br
ex
en
bb
N
M
es
rb
st
200µm
(l)
pb
en
50µm
(m)
es
20µm
(n)
rb
st
20µm

Fig. 13. Z-projections of confocal laser scanning micrographs of immunohistochemical stainings with antibodies against serotonin (green) and tyrosinated-α-tubulin (red), and with DAPI and Hoechst (blue) in four different tunicate species. (a) In the appendicularian *Fritillaria borealis* serotonin-lir is not detectable. (b–n) Serotonin-like immunoreactivity in three different stolidobranch ascidian species. (b–d) Localization of serotonin-lir cells in *Molgula manhattensis*, anterior to the top, dorsal to the right. Areas with positively labelled cells are marked with white rectangles, higher magnifications of these areas shown in (c, d). (b) Lateral view on one complete individual. Exclusively in the dorsal part of the peripharyngeal band (pb) serotonin-lir cells are detectable. (c) Higher magnification of serotonin-lir cells in the endostyle (en). (d) Detail of serotonin-lir in the esophagus (es). Approximately spherical and elongated serotonin-lir cells are visible. (e–j) Serotonin-lir in *Styela clava*, dorsal to the right, anterior to the top. (e) Lateral view on an entire animal. Note that the peripharyngeal band continuously possesses serotonin-lir cells and on the dorsal side the peripharyngeal band conspicuously curves (character 55). White rectangles mark areas that are shown in higher magnification in (f–j). (f–j) Details of the localization of serotonin-lir cells in the peripharyngeal band (f), the endostyle (g), the esophagus (h), the stomach (st, i) and the intestine (in, j). (k–n) Distribution of serotonin-lir cells in *Symplegma brakenhielmi*, anterior view, ventral to the left. Regions marked with white rectangles are shown in higher magnification in l–n. (l) Serotonin-lir at the transition of peripharyngeal band and endostyle. (m) Detail of serotonin-lir cells in the oesophagus. (n) Elongated serotonin-lir cells are located in the retropharyngeal band (rb). In the stomach approximately spherical serotonin-lir cells are detectable. an, anus; bb, branchial basket; br, brain; ex, excurrent siphon; hg, hepatic gland; is, incurrent siphon; ki, kidney; mo, mouth; sa, stigma; ta, tail.

(1950), Drasche (1884), Rocha et al. (2012), and Van Name (1945).

75. Site of fertilization: (0) external; (1) internal. Tunicate species with internal fertilization also brood their developing embryos (see also character 76). Information on character distribution is found in Berrill (1950), Groepler (2016), Mukai et al. (1983), Rocha et al. (2012) and Van Name (1945).
76. Site of brooding: (0) atrial (= peribranchial) cavity; (1) brood chambers. Species with internal fertilization either brood the embryos in the unaltered atrial cavity or in specialized pouches, so-called brood or incubation chambers. Information on character distribution is found in Berrill (1950), Groepler (2016), Kott (1990, 1992), Manni et al. (2007) and Van Name (1945).
77. Site of brood chamber: (0) outgrowth of atrial cavity; (1) common tunic. Information on character distribution is found in Van Name (1945) and Kott (1990, 1992, 2001).
78. Location of atrial brood chamber: (0) left side; (1) dorsal side. Brood chambers that are outgrowths of the atrial wall are either positioned on the left side of the body (in *K. borealis*) or on the dorsal side of the body (in *D. stylifera* and *S. sigillinoides*) (Van Name, 1945).
79. Chordate-type larva: (0) absent; (1) present. The chordate-type larva features a trunk and a locomotory tail, with a dorsal brain situated in the trunk above the endodermal and mesodermal tissues. The brain is connected to a posteriorly extending dorsal neural tube that runs through the length of the tail. In this tail a notochord, flanked by muscle cells, and endodermal tissue is present. The tail propels the larva through undulatory movements. Salpida, Pyrosomatida, *Molgula retortiformis* and *P. corrugata* do not develop through a tailed larval stage. In all other investigated species a chordate-type larva is present (Van Name, 1945; Millar, 1954; Ihle, 1956).
80. Orientation of larval tail in relation to larval trunk: (0) vertical; (1) horizontal. In vertical-orientated larval tails, the fluke is oriented along the dorsoventral axis of the body as in most fishes. The power is generated by lateral undulatory movements. In the horizontal orientation the fluke is orientated laterally, as in whales and dolphins. The forward thrust is generated via dorsoventral undulations. Information on character distribution is found in Huus (1956).
81. Larval eye: (0) absent; (1) present. A larval eye is a photoreceptor consisting of at least two cells present in the chordate-type larva. In most ascidian species the larval eye consists of pigment cells, receptor cells and lens cells, and is situated in the sensory vesicle. Information on character distribution is found in Berrill (1950), Groepler (2016), Huus (1956), Kott (1990, 1992), Lacalli (1996), Lamb et al. (2007), Millar (1971) and Van Name (1945).
82. Larval statocyte: (0) absent; (1) present. Statocytes are sensory cells situated in the larval sensory vesicle. Statocytes contain a dark, pigmented otolith (or statolith) and are involved in gravitropic perception. They are present in larvae of Appendicularia, Doliolida, Phlebobranchiata, Stolidobranchiata and Aplousobranchiata (Huus, 1956; Millar, 1971; Burighel and Cloney, 1997).
83. Larval photolith: (0) absent; (1) present. The photolith combines the light-sensitive larval eye and the gravity-receptive statocyte in a single organ. Photoliths are only described for examined colonial styelids (Garstang, 1928; Berrill, 1950; Sorrentino et al., 2000).

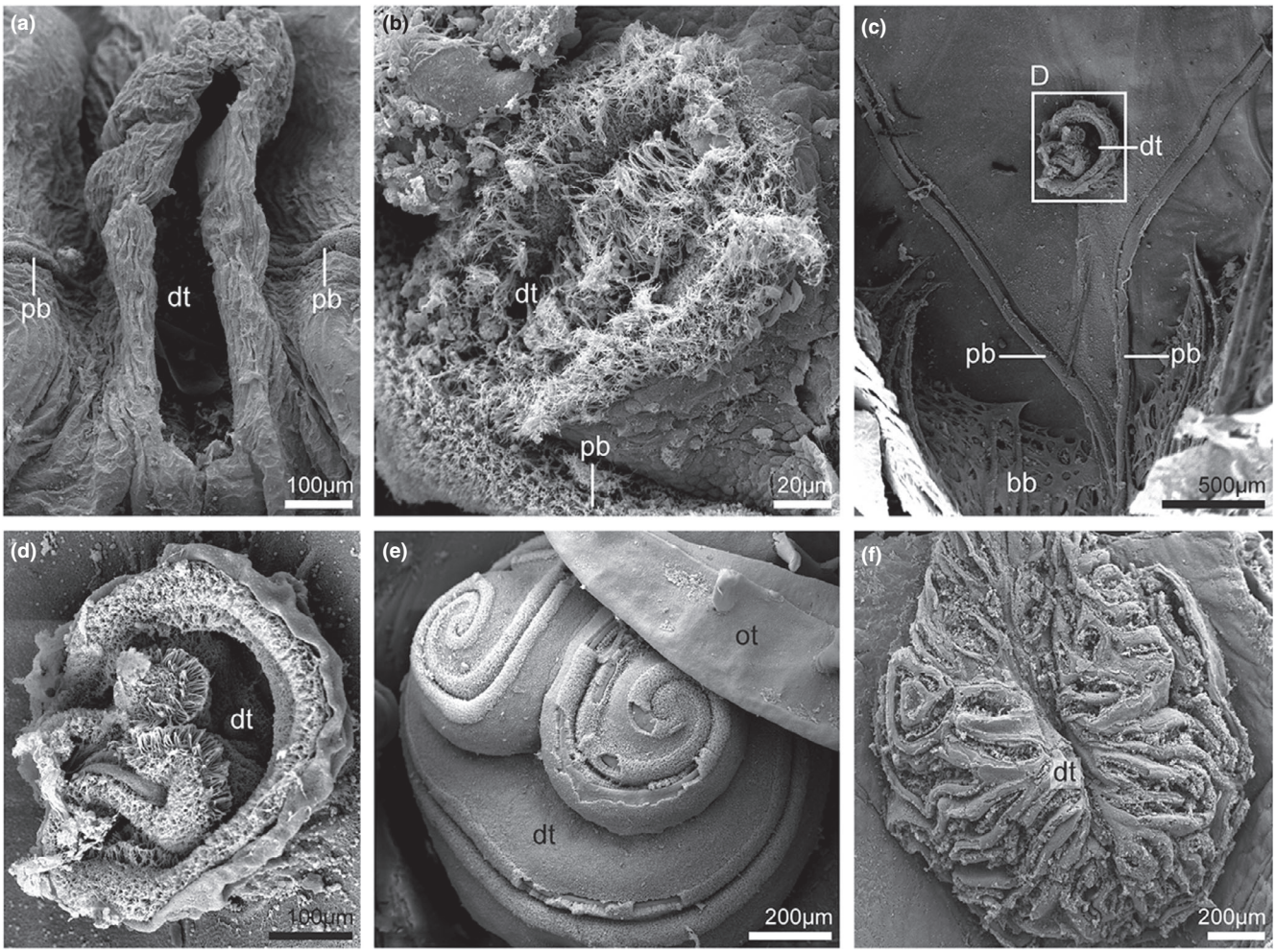

Fig. 14. Scanning electron micrographs of the dorsal tubercle (dt) in five different tunicate species. (a) In *Salpa fusiformis* the dorsal tubercle is shaped as a simple ciliated funnel. (b) The dorsal tubercle of *Diazona violacea* is U-shaped. (c, d) In *Molgula citrina* the dorsal tubercle is C-shaped. The peripharyngeal band (pb) possesses a conspicuous dorsal curvature (character 55). The opening of the dorsal tubercle is pedestal-like and elevated in excess of the wall of the branchial basket (bb). (e) *Halocynthia roretzi* possesses a pedestal-like elevated dorsal tubercle with an involute ciliated opening. (f) In *Herdmania momus* the dorsal tubercle is pedestal-like, elevated and possesses several ciliated openings into the branchial basket. ot, oral tentacle.

84. Larval ampullae: (0) absent; (1) present. Ampullae are epidermal outgrowths that usually form a ring surrounding the anterior trunk region. Ampullae are present in most examined stolidobranch larvae, in Didemnidae and Polyclinidae (Van Name, 1945; Berrill, 1950; Kott, 1985, 1990, 1992, 2001).
85. Larval adhesive papillae (more than one): (0) absent; (1) present. Larval adhesive papillae are epidermal thickenings present in most tunicate larvae at the anterior trunk region to facilitate the attachment to the substrate before metamorphosis. Besides secretion of adhesives, the larval adhesive papillae contain sensory cells. Adhesive papillae are absent in Appendicularia, Doliolida, Molgulidae,- and larvae of the outgroup species (Huus, 1956).
86. Orientation of larval papillae: (0) triradial; (1) sagittal. Usually, three adhesive papillae are present in ascidian tadpole larvae. These are either positioned anteriorly at three corners of a triangle: two dorsolaterally and one medioventrally. This arrangement is called triradial. Alternatively, all papillae are positioned in a single vertical plane, midsagittally. Information on character distribution is found in Berrill (1950), Grave (1926), Groepler (2016), Huus (1956),- and Van Name (1945).

Serotonin-like immunoreactivity (serotonin-lir)

87. Serotonin-lir in the brain of adult specimens: (0) absent; (1) present. Serotonin-lir in the brain has been detected only in investigated outgroup species (Baumgarten et al., 1973; Sakharov and Salimova, 1980; Holland and Holland, 1993; Candiani et al., 2001; Barreiro-Iglesias et al., 2009), Salpida, Doliolida (Braun and Stach, 2018) and *O. fusiformis* (Stach, 2005), but could not be detected in other tunicate species examined.
88. Serotonin-lir in the peripharyngeal band: (0) absent; (1) present. Serotonin-lir in the peripharyngeal band is described for all Thaliacea, all examined ascidian species, and lampreys (Sakharov and Salimova, 1982; Barreiro-Iglesias et al., 2009; Braun and Stach, 2016, 2018; Fig. 12a,b,g,k,o; Fig. 13b,f,l).
89. Serotonin-lir in the endostyle: (0) absent; (1) present. The endostyle is a conspicuous, trough along the ventral midline of the branchial basket. It contains glandular cells, ciliated cells and produces mucus involved in feeding. In Pyrosomatida and ascidians serotonin-lir cells are located in the endostyle (Braun and Stach, 2016, 2018; Fig. 12c,h,l,p; Fig. 13c,g,l).
90. Serotonin-lir in the retropharyngeal band: (0) absent; (1) present. The retropharyngeal band limits the branchial basket to the posterior and is a conspicuous ciliated band. Information on character distribution is found in Braun and Stach (2016, 2018); see also Fig. 13b,e,n.
91. Serotonin-lir in the oesophagus: (0) absent; (1) present. The oesophagus is the part of the intestinal tract that connects the branchial basket with the stomach. Serotonin-lir cells are present in the esophagus of Thaliacea and ascidians (Braun and Stach, 2016, 2018; Figs 12d,i,m,r and 13d,h,m).
92. Serotonin-lir in the gastrointestinal tract: (0) absent; (1) present. The gastrointestinal tract is the part of the intestinal tract posterior to the esophagus. Serotonin-lir cells are located in the gastrointestinal tract of *T. democratica*, ascidians, and species belonging to the outgroup (Sakharov and Salimova, 1980; Candiani et al., 2001; Barreiro-Iglesias et al., 2009; Braun and Stach, 2016, 2018; Figs 12e,f,i,j,n and 13a,b,e,i-k,n).

Nervous system

93. Adult cerebral eye(s): (0) absent; (1) present. Cerebral eyes are photoreceptors consisting of at least two cells (Richter et al., 2010) and are closely associated with the brain; thus, cerebral eyes are organs continuous at the tissue level with the brain enclosed in the same extracellular matrix (Cohen, 1963; Lacalli et al., 1994; Lacalli and Holland, 1998; Braun and Stach, 2017).
94. Type of photoreceptor cells in adult cerebral eyes: (0) rhabdomeric; (1) ciliary. In rhabdomeric photoreceptor cells the membrane storing the light-sensitive photopigments originates in the apical cell membrane and therefore forms microvilli. In ciliary photoreceptor cells this membrane originates from a ciliary membrane (e.g. Eakin, 1979; Salvini-Plawen, 1982). Photoreceptor cells in *T. democratica* are rhabdomeric (Braun and Stach, 2017). In cerebral eyes of Cephalochordata and Petromyzontidae photoreceptor cells are described as ciliary (Cohen, 1963; Lacalli, 1996).
95. Lens in adult cerebral eye: (0) absent; (1) present. Lenses are transparent structures that refract light (Jonasova and Kozmik, 2008). Lenses in adult cerebral eyes are present in members of Petromyzontidae (Slingsby et al., 2013).
96. Shape of adult brain: (0) ovoid, pear-shaped; (1) elongated. We considered brains with a relation of length to breadth of at least 1.5 as elongated, and brains with length/breadth of approximately 1 as ovoid. Information on character distribution is found in Braun and Stach (2019), Nieuwenhuys (1977) and Wicht and Lacalli (2005).
97. Brain divided into cortex and neuropil: (0) no; (1) yes. In all examined tunicate species, the brain is divided into a superficial layer where somata of neurons are concentrated and a central neuropil that almost exclusively contains nerve fibres. In the outgroup species the brain is not divided into cortex and neuropil (Nieuwenhuys, 1977; Wicht and Lacalli, 2005; Braun and Stach, 2019).
98. Neural gland: (0) absent; (1) present. The neural gland is a glandular structure closely associated with the brain in tunicates; together they form the neural complex (see, e.g., Huus, 1956; Burighel and Cloney, 1997). A neural gland is present in nearly all investigated species, except thaliacean species (Braun and Stach, 2019). Based on the similar position of Hatschek's pit and groove as well as the presence of gonadotropin hormones and the indication that gonadotropin-releasing hormones are found in neural fibres

close to Hatschek's pit, Hatschek's pit are coded in Cephalochordata as homologous to the neural gland and dorsal tubercle in tunicates (Stach, 1996; Gorbman, 1999; Roch et al., 2014). For Petromyzontidae the neural gland is homologized with the adenohypophysis, based on similarities of development, position and function (Romer and Parsons, 1986; Gorbman, 1995, 1999; Kah et al., 2007).

99. Position of neural gland compared to brain: (0) not ventral; (1) ventral. Information on character distribution is largely from Braun and Stach (2019). Hatschek's pit in Cephalochordates and the adenohypophysis in Petromyzontidae also are positioned on the ventral side of the brain (see character 98). Terakado (2010) described a ventral position of the neural gland in *Halocynthia roretzi*. A dissection of animals of this species revealed that the neural gland is positioned dorsal from the brain slightly shifted to the right so the position is coded as 0 for the species.
100. Position of the not ventrally positioned neural gland (see character 99): (0) dorsomedian; (1) right. In cases, where the neural gland is not ventrally situated, it may be positioned centrally dorsal of the brain (dorsomedian) or on the right side of the brain. Information on character distribution is found in Braun and Stach (2019).
101. Dorsal tubercle in adults: (0) absent; (1) present. The neural gland is connected to the anterior part of the pharynx via a tube. The opening of this tube is called dorsal tubercle. The dorsal tubercle also can be present when the neural gland is absent (Salpida, see character 98; Braun and Stach, 2019). Hatschek's pit in Cephalochordata is homologized with the neural gland in tunicates (see character 99) and the ciliated opening of Hatschek's pit with the dorsal tubercle in tunicates. Therefore, all investigated species possess a dorsal tubercle, except for Petromyzontidae, where a homologous structure is missing in adults.
102. Shape of dorsal tubercle: (0) simple; (1) more complex. The dorsal tubercle in some species is a simple ciliated funnel (Fig. 14a); in others it is of a more complex shape, usually a U-, C- or heart-shaped structure (Fig. 14b–f). Information on character distribution is found in Braun and Stach (2019).
103. Opening of the dorsal tubercle pedestal-like elevated: (0) no; (1) yes. The opening of the dorsal tubercle can be in the same plane as the wall of the branchial basket or can be elevated pedestal-like above this plane extending into the lumen of the branchial basket (Fig. 14c–f).
104. Dorsal strand: (0) absent; (1) present. The dorsal strand is an extension of the neural gland extending along the roof of the branchial basket to the posterior. It is a tube-like structure, with an epithelial layer surrounding a narrow central lumen (Burighel and Cloney, 1997). Information on character distribution is found in Braun and Stach (2019).
105. Dorsal strand ends in close proximity to the brain: (0) no; (1) yes. In some species the dorsal strand extends all the way to the gonads, in others it ends blindly close to the brain. Information on character distribution is found in Braun and Stach (2019).
106. Caudal ganglion in adults: (0) absent; (1) present. The caudal ganglion is a concentration of nerve cell bodies in the locomotory tail, resulting in a local swelling of the neural tube in the anterior part of the locomotory tail. In adults it is present only in Appendicularia (Lohmann, 1956).
107. Ventral visceral nerve: (0) absent; (1) present. Ventral visceral nerves are nerves that project from the midline of the brain from its ventral side posteriorly (Manni and Pennati, 2016). Information on character distribution is found in Braun and Stach (2019).
108. Number of ventral visceral nerves (see character 107): (0) 1; (1) 2; (2) 4. In most tunicate species the ventral nerve is developed as a single unpaired nerve, but in *B. schlosseri* and *P. constellatum* a pair of ventral visceral nerves is present. Specimens of *D. stylifera* even possess four ventral visceral nerves (Braun and Stach, 2019).
109. Dorsal strand plexus: (0) absent; (1) present. In association with the dorsal strand the ventral visceral nerve can form a richly anastomosing plexus. It is then termed dorsal strand plexus (see Mackie, 1995; Braun and Stach, 2019). The dorsal strand plexus contains neurons in all stages of differentiation, therefore being a possible region where neurogenesis takes place in adults (Mackie, 1995).
110. Brain appendages: (0) absent; (1) present. Brain appendages are blindly ending outgrowths of the brain cortex that are usually bilaterally symmetrical on the ventral side of the brain (Braun and Stach, 2017). These

appendages are present only in examined specimens belonging to Salpida (Braun and Stach, 2017, 2019).

111. Number of anterior nerves per side: (0) one; (1) two; (2) three; (3) four; (4) six. Anterior nerves exit the brain on the anterior side and mainly extend anteriorly toward the muscles of the oral sphincter, the oral tentacles and the peripharyngeal band. They are present in all tunicate species. The homology to anterior nerves in outgroup species is ambiguous, so the character state for these species is coded as "?" In Salpida this character is coded as polymorphic, because of the different character states in the brains and nerves of the blastozooid and oozooid stage (Braun and Stach, 2019).
112. Number of posterior nerves per side: (0) one; (1) two; (2) three; (3) four. Posterior nerves branch off the brain on the posterior side and mainly extend toward the muscles of the excurrent siphon and lateral body wall. They are present in all tunicate species. The homology to posterior nerves in outgroup species is ambiguous, so the character state for these species is coded as "?" In Salpida this character is coded as polymorphic, because of the different character states in the brains and nerves of the blastozooid and oozooid stage (Braun and Stach, 2019).
113. Lateral nerves: (0) absent (1) present. Lateral nerves leave the brain laterally and project toward the branchial basket, digestive tract, and the lateral muscles of the body wall (Braun and Stach, 2019).
114. Number of lateral nerves per side: (0) one; (1) two; (2) three; (3) four; (4) six; (5) more than six. The homology to lateral nerves of outgroup species is ambiguous, so the character state for these species is coded as "?" In Salpida this character is coded as polymorphic, because of the different character states in the brains and nerves of the blastozooid and oozooid stage (Braun and Stach, 2019).
115. Unpaired anterior nerve projecting toward dorsal tubercle: (0) absent; (1) present. An exceptional unpaired anterior nerve that projects toward the dorsal tubercle is only present in species of Doliolida (Neumann, 1956; Braun and Stach, 2019).
116. Statocyte in adult brain: (0) absent; (1) present. Statocytes are sensory cells situated in the sensory vesicle in the brain. A brain that is equipped with a statocyte is present in species of Appendicularia (Lohmann, 1956).
117. Conspicuous fibre tracts in adult brains: (0) absent; (1) present. Here conspicuous fiber tracts detectable with the help of immunohistological stainings are considered, as investigated in the studies of Braun and Stach (2017, 2019). Information on Cephalochordata and Petromyzontidae can be found in Barreiro-Iglesias et al. (2009), Lacalli (1996) and Nieuwenhuys (1977).

Discussion

The phylogenetic position of ascidians assured the group a place "back in the limelight" (Pourquié, 2001), just like more than a hundred years earlier, when the affinities between ascidians, cephalochordates and craniates were discovered by the young Russian zoologist Alexander Kowalevsky in St Petersburg (Kowalevsky, 1866). The renewed interest at the onset of the 21st Century, similar to the interest generated by Kowalevsky, was fuelled by studies of the larval stages of ascidians that, more obviously than studies of the adults, revealed correspondences to the more fish-like chordates. Ascidians, however, although constituting the majority of Tunicata, represent only a fraction of the life-history strategies found within Tunicata. Moreover, molecular phylogenetic analyses consistently found "Ascidiacea" as not monophyletic and cladistic analyses of phenotypic data of Tunicata are almost completely lacking.

Molecular analyses over the last decades have included an increasing number of taxa (Swalla et al., 2000; Stach and Turbeville, 2002; Delsuc et al., 2006; Tsagkogeorga et al., 2009; Govindarajan et al., 2011), concentrated on the usage of slowly evolving genes (Tsagkogeorga et al., 2010) or applied "phylogenomic" methods (Delsuc et al., 2018; Kocot et al., 2018) to resolve phylogenetic inter-relationships between higher tunicate taxa (see review in Giribet, 2018). Although these studies seemingly approach a more stable framework regarding some contentious points of tunicate phylogeny, it has been pointed out that phylogenetic analysis of tunicate DNA sequences is difficult due to generally increased mutation rates (Tsagkogeorga et al., 2010) and that phylogenetic information might not be as solid as suggested by statistical support values in published phylogenies (Stach, 2014). Phenotypic data analyzed according to a consistent phylogenetic method can be seen as a way of scrutinizing molecular phylogenies as an additional source of phylogenetic information (Wägele, 2001). Phenotypic data are necessary to suggest hypotheses of character

transformation and the reconstruction of ground patterns (Hennig, 1982). Moreover, phenotypic data cannot be dismissed according to a foundational principle of science, the requirement of total evidence (Kluge, 1998; Fitzhugh, 2006).

Moreno and Rocha (2008) published the first detailed analysis of phenotypic data (47 characters in 41 genera as terminal taxa), traditionally considered in tunicate taxonomy for a higher taxonomic group of Tunicata, Aplousobranchiata. In their study they focused on characters already published in the literature, emphasizing characters associated with coloniality. This had the unfortunate effect that colonial taxa from Phlebobranchiata clustered as sister taxa to the colonial Aplousobranchiata. Colonial Stolidobranchiata, however, were not included in the analysis, rendering Phlebobranchiata polyphyletic, without testing the influence of characters associated with coloniality. Another study utilizing phenotypic data in a cladistic analysis was published by Stach and Turbeville (2002) and analyzed merely 24 characters for 19 higher tunicate taxa (traditionally given the rank of "family"). This study found the higher taxa Tunicata, Thaliacea, Phlebobranchiata, Aplousobranchiata and Stolidobranchiata to be monophyletic, but otherwise showed no resolution among these taxa. A third study of phenotypic data investigated the phylogenetic signal in characters relating to secondary mechanoreceptor cells in Tunicata (Rigon et al., 2013). That analysis recovered major ascidian taxa as monophyletic taxa (Phlebobranchiata, Aplousobranchiata, Stolidobranchiata) but found no support for Thaliacea or "Ascidiacea". "Ascidiacea" was recovered as polyphyletic due to thaliacean taxa as well as appendicularians being nested among ascidians. Interestingly, the appendicularian *Oikopleura dioica* was sister taxon to the two aplousobranch ascidian species in Rigon et al.'s study. Older treatments of detailed tunicate taxonomy did not apply cladistic rigor and often the taxonomic groupings or evolutionary interpretations are not easy to deduce (see below).

The current analysis of 117 phenotypic characters in a consistent cladistic approach therefore can serve as an independent source of evidence not only for analyses based on molecular data, but also for taxonomic groupings not based on cladistic argumentation. The strict consensus tree of the parsimony analysis of the equally weighted character matrix is highly resolved and suggests several groupings in accordance with previous hypotheses but also some unexpected sister-group relationships. The hypotheses will be addressed briefly here and discussed in more detail separately below. Tunicata is monophyletic with a high Bremer support as well as with high statistical support. On the higher taxonomic levels within Tunicata, the position of Appendicularia as the sister taxon to the remaining Tunicata has been found in several molecular phylogenetic analyses before (e.g. Wada, 1998; Swalla et al., 2000; Delsuc et al., 2018; Kocot et al., 2018) and has been discussed based on morphological data as well (Ax, 2001; Wada, 1998; see detailed discussion below). The support for this positioning of Appendicularia is low. Unexpectedly, Thaliacea, which is a well-supported monophyletic taxon as suggested by molecular data (e.g. Stach and Turbeville, 2002; Govindarajan et al., 2011; Delsuc et al., 2018; Kocot et al., 2018) but also according to morphological considerations (Brien, 1948; Ax, 2001; Stach and Turbeville, 2002), has not been found to be monophyletic in the more extensive analysis of phenotypic characters herein. Instead it forms a paraphyletic group with the relationship between Salpida and Doliolida unresolved, and the pyrosome *Pyrosoma atlanticum* forming the sister taxon to monophyletic Ascidiacea. None of the nodes separating the respective thaliacean taxa from Ascidiacea is strongly supported. Ascidiacea, however, which has been regarded by most modern studies as an obsolete taxon name for a paraphyletic group united by symplesiomorphic sessility of adults (Wada, 1998; Tsagkogeorga et al., 2009; Govindarajan et al., 2011; Delsuc et al., 2018; Kocot et al., 2018), is strongly supported, with high Bremer support index and statistical measures as a monophyletic taxon in the present analysis. At an intermediate level Stolidobranchiata is found to be monophyletic with strong support. Aplousobranchiata, although monophyletic, is only weakly supported. "Phlebobranchiata", however, is paraphyletic in respect to Stolidobranchiata. Also, *Diazona violacea,* which traditionally has been included within "Phlebobranchiata" (e.g. Millar, 1970), clustered as the sister taxon to Aplousobranchiata supporting a hypothesis proposed recently based on mitochondrial protein coding genes (Shenkar et al., 2016; see discussion below). At a lower taxonomic level, "Ascidiidae" is paraphyletic with respect to Stolidobranchiata. Within Stolidobranchiata, a monophylum consisting of Pyuridae and Molgulidae is nested within "Styelidae" rendering "Styelidae" paraphyletic. Within Aplousobranchiata, Polyclinidae and Didemnidae are both monophyletic and form a monophyletic sister group contrary to previous studies (Moreno and Rocha, 2008; Tsagkogeorga et al., 2009). In their study, focusing on the phylogenetic relationships of aplousobranch taxa, Moreno and Rocha (2008) found Polyclinidae paraphyletic and Didemnidae nested within paraphyletic "Holozoidae". "Holozoidae" also is recovered as not monophyletic in the present analysis. The monophyly of Clavelinidae or Polycitoridae were not tested.

Monophyly of Ascidiacea

Traditionally, Ascidiacea is one of three major taxa within Tunicata, often given the rank "Class" (e.g.

Van Name, 1945; Millar, 1966; Lützen, 1967; Kott, 1985; Shenkar and Swalla, 2011): "The class Ascidiacea comprises those tunicates which have sessile adults." (Millar, 1966, p. 5).

The monophyly of Ascidiacea was challenged by several molecular phylogenies, positioning Thaliacea within Ascidiacea (e.g. Stach and Turbeville, 2002; Tsagkogeorga et al., 2009; Govindarajan et al., 2011). Delsuc et al. (2018) and Kocot et al. (2018) even suggest abandoning the name "Ascidiacea". However, the phenotypic data from the present study support a monophyly of Ascidiacea with three unambiguous apomorphies: sessile adults (character 1), oral tentacles (8), and longitudinal orientation of stigmata in adults (38). Although sessility clearly evolved several times independently, if one considers all animal taxa, there is no reason to suggest that sessility within Tunicata evolved more than once. In fact, even in the hypotheses based mainly on molecular data, where Thaliacea (e.g. Govindarajan et al., 2011; Kocot et al., 2018) or Thaliacea and Appendicularia (Stach and Turbeville, 2002; Zeng and Swalla, 2005; Zeng et al., 2006) rendered "Ascidiacea" paraphyletic, authors usually assumed that the characteristic ascidian biphasic life history with a tadpole-like larva and a sessile adult stage evolved once at the base of Tunicata and was subsequently lost in the stem lineage of Appendicularia and Thaliacea, respectively. The presence of oral tentacles as an apomorphic character that evolved in the stem lineage of a monophyletic Ascidiacea also is not without problems. The velar tentacles of cephalochordates and agnathan craniates are similarly placed, equipped with sensory cells (Rigon et al., 2013) and herein they are considered homologous to the oral tentacles of ascidians. Therefore, this character is an autapomorphy for a potentially monophyletic Ascidiacea, but it is homoplastic in comparison to the chordate outgroup taxa considered in the present analysis. Also, the orientation of the stigmata in adults is liable to evolutionary change as can be seen by the transverse arrangement of the longitudinal stigmata in the pyurid ascidian *Boltenia* spp. or by the spiral stigmata found in corellid ascidians. Interestingly, the combination of these three characters in the matrix herein has sufficient informational weight to render Ascidiacea monophyletic in a weighting scheme of 3:1 in favour of the morphological data in a combined matrix, where the molecular positions outnumber the morphological characters by roughly a factor of 17:1 (6:1, if only parsimony-informative characters are considered). In conclusion, considerable support was found for a monophyletic Ascidiacea in the purely phenotypic characters, but because each of the apomorphic characters is liable to homoplasy, it is suspected that additional evidence is needed to settle this question. Nevertheless, abandoning the name Ascidiacea at the current state of phylogenetic knowledge seems premature.

Within Ascidiacea the phenotypic data herein do not support the monophyly of Enterogona, which is considered a higher taxon comprised of monophyletic Phlebobranchiata and monophyletic Aplousobranchiata (e.g. Perrier, 1898; Plough, 1978; Kott, 1985). Instead, in the present analysis Stolidobranchiata groups within Phlebobranchiata, thereby rendering both "Phlebobranchiata" and "Enterogona" paraphyletic. Nonetheless, Stolidobranchiata and Aplousobranchiata were recovered monophyletic in the present analysis, as has been supported in most molecular phylogenetic analyses (e.g. Tsagkogeorga et al., 2009; Delsuc et al., 2018; Kocot et al., 2018).

One of the main model organisms for research on molecular aspects of chordate development (see, e.g., Lemaire, 2011), the ascidian *Ciona intestinalis*, has traditionally been included in the taxon Phlebobranchiata (e.g. Millar, 1966; Plough, 1978). This assessment was based on shared morphological similarities, mainly in the branchial basket, such as the presence of papillae on the internal longitudinal blood vessels projecting into the branchial sac. The affinity of Cionidae to Phlebobranchiata also is recovered in molecular phylogenetic analyses (Stach and Turbeville, 2002; Tsagkogeorga et al., 2009; Delsuc et al., 2018; Kocot et al., 2018). Kott (1990), on the other hand, pointed out that other morphological characteristics, such as the role of the epicardia in wound repair, could be seen as evidence for a closer relationship of Cionidae to the colonial aplousobranchs. The present phenotypic analysis does not support a closer relationship of Cionidae to Aplousobranchiata; rather, it recovers Phlebobranchiata paraphyletic with the traditional phlebobranch taxa Perophoridae and Diazonidae more closely related to Aplousobranchiata than is Cionidae. Like aplousobranch taxa, species in Perophoridae and Diazonidae are colonial and it should be noted that there is recent molecular evidence that Diazonidae belong to Aplousobranchiata (Shenkar et al., 2016) contrary to the traditional taxonomic inclusion of Diazonidae in Phlebobranchiata (e.g. Van Name, 1945; Lützen, 1967; Millar, 1970). The present study grouped Diazonidae as a sister taxon to a monophyletic Aplousobranchiata although the statistical support is low. In this analysis, morphological arguments to support a sister-group relationship between Diazonidae and Aplousobranchiata as apomorphic characters are the division of the body (3) and coloniality due to asexual epicardial budding (31).

Position of "Thaliacea"

One of the most surprising outcomes of the present study is the paraphyly of "Thaliacea". The monophyly

of Thaliacea is traditionally thought to be strongly supported (e.g. Govindarajan et al., 2011; see also review in Piette and Lemaire, 2015). A number of life-history traits and phenotypic characters are usually interpreted as synapomorphies of thaliacean species. These characters are, for example, the obligate alteration between sexual and asexual reproduction in consecutive generations (Neumann, 1956). In Doliolida and Salpida this metagenetic life cycle is accompanied with a distinct polymorphy of the successive generations. In addition, the position of the excurrent and incurrent openings at opposite ends of the animals is a common character to all thaliaceans (reviewed in Bone, 1998). This latter trait is especially convincing as a synapomorphy, as the intestine at the same time is U-shaped. A U-shaped gut is quite common in sessile animals, but rarely found in planktonic animals (Williams, 1996; Cohen et al., 2003). Therefore, the combination of a U-shaped gut with incurrent and excurrent siphons at opposite ends of the body together with a holoplanktonic lifestyle had been taken as evidence that the planktonic Thaliacea were derived from sessile ascidian-like ancestors (Stach and Turbeville, 2002; but see below). The present analysis turns this evolutionary interpretation upside down: according to this, the ancestral life-history strategy in Tunicata was planktonic and the sessility of Ascidiacea was a later phenomenon evolved within Tunicata. Interestingly, it might be pointed out here, that palaeontologists interpret fossils from the early Cambrian relegated to the taxon Vetulicolia as early planktonic chordates with some as yet unclear affinity to present day thaliaceans (García-Bellido et al., 2014; Gee, 2001; Lacalli, 2002; Li et al., 2018). The present analysis of morphological data can therefore be seen as being in agreement with the early appearance of vetulicolans in the fossil record and their tentative interpretation as planktonic chordates. Note, however, that the paraphyletic positions of Pyrosomatida as sister taxon to Ascidiacea has weak statistical support and that the relationship of Doliolida and Salpida is unresolved. Although Salpida and Doliolida with high statistical support constitute monophyletic groups the monophyly of Pyrosomatidae was not tested. In the present analysis, a group consisting of Pyrosomatidae and Ascidiacea is supported by characters 27, 40, 66 and 89: sexually mature form colonial – colonial forms throughout entire development, internal longitudinal blood vessels and serotonin-lir in endostyle. This implies that coloniality of the sexually mature form evolved in the stem lineage of Ascidiacea plus the thaliacean taxa, and is therefore homologous in phlebobranch ascidians, aplousobranch ascidians, pyrosomes, doliolids and salps but evolved independently in the colonial styelid species within Stolidobranchiata. The metagenetic alternation between a sexual and asexual generation also is present in colonial ascidians. Here, however, the metagenesis is not obvious, because the generations are not only anatomically identical — save the presence of gonads — but usually are present in the same colony. The sexually produced larva, the founding individual of a colony, can be understood as an oozooid, the asexual generation. This founding individual, like the oozooid generation in salps, doliolids and pyrosomes, does not develop gonads but reproduces exclusively by the formation of buds (Berrill, 1935; Deviney, 1934; Lauzon et al., 2002; Nakauchi, 1982). An evolutionary scenario, where a pyrosome-like ancestor settled and evolved into a colonial aplousobranch-like ascidian might be envisioned recalling that a benthic pyrosome was described by Monniot and Monniot in 1966. However, the species description is highly suspicious, as it was based on a single colonial specimen from a dredge tow and it has been argued (Van Soest, 1981) that it might have entered the net on its way to the surface rather than being a benthic species and may actually be classified as *P. atlanticum*.

Position of Appendicularia

The phylogenetic position of Appendicularia has been controversial amongst previous investigators for a long time (Herdman, 1891; Ihle, 1913; Garstang, 1928; Wada, 1998; Stach and Turbeville, 2002, 2005; Zeng et al., 2006). On the one hand, appendicularians show a simple morphology of the branchial basket, direct development, and short generation times that is probably retained from the last common ancestor of tunicates. On the other, the elaborated filter-feeding house and the torsion of the tail indicate that some characters are highly derived (e.g. Ihle, 1913). In 1928 Garstang hypothesized that Appendicularia are neo-tenic doliolids, and suggested that pelagic tunicates are derived from a sessile ascidian-like ancestor. At first, molecular phylogenetic analyses also produced contradictory results regarding the phylogenetic position of Appendicularia. Some earlier molecular studies (Wada, 1998; Swalla et al., 2000) found Appendicularia sister taxon to the rest of Tunicata. Although this hypothesis already had been suggested based on considerations of the evolution of morphological characters (see above), it contradicted ideas of Appendicularia as a taxon evolved through neoteny. In fact, appendicularians had been textbook examples for neoteny, based on the rapid development and it was precisely this bias that led to the christening of the taxon with its alternative name – Larvacea (Herdman, 1891; Garstang, 1928; Lacalli, 2005; Stach et al., 2008; see reviews in: Gee, 1996; Ruppert, 1997a). The fact that appendicularians resembled ascidian larvae and the observation that their intestine followed a U-shaped course seemed to support the

neoteny hypothesis, because U-shaped guts in planktonic organisms were interpreted as characters inherited from a sessile ancestor (Williams, 1996). These characteristics were more easily reconciled with the hypothesis based on a combination of molecular and morphological data that Appendicularia and Aplousobranchiata form sister groups (Stach and Turbeville, 2002). In addition to the aforementioned arguments, this hypothesis was supported by the observation that appendicularians and aplousobranch larvae shared the common derived character of a rotation of the swimming tail through 90 degrees to the left (Stach et al., 2008). Interestingly, this trait found in larval aplousobranch ascidians also is found in perophorid phlebobranch ascidians and had always been interpreted there as a homoplastic trait (Berrill, 1950). The third hypothesis based on molecular data suggested that Appendicularia and Stolidobranchiata form sister groups (Zeng et al., 2006). However, it found no further support in molecular studies and no morphological synapomorphies had been suggested, although the position of the neural gland on the right side of the brain as in many stolidobranch ascidians or the absence of eyes as found in some molgulid ascidians might have been considered as such. All of these studies used 18S rDNA sequences, a molecule that might be limited in its power to resolve tunicate phylogenetic relationships (Wada, 1998; Tsagkogeorga et al., 2010). Recent advances in molecular phylogenetic analyses in respect of taxon sampling as well as number of genes included found unanimous support for a sister-group relationship of Appendicularia to the remaining Tunicata (Delsuc et al., 2018; Kocot et al., 2018); however, taxon sampling in these studies remains limited. Given the caveats discussed above, it was therefore a surprise that the phenotypic data of the present study supported the hypothesis heavily favored in molecular analyses that Appendicularia is sister group to the remaining tunicate taxa. In this hypothesis, appendicularians possess several morphological features that are interpreted as plesiomorphic characters inherited from a free-living, fish-like ancestor. Among these characters is the presence of the notochord in adults, the absence of an atrial cavity, and in general the free-swimming lifestyle. Although the present data support the latest consensus of molecular data in respect of a sister-group relationship of Appendicularia to the remaining Tunicata, apomorphic similarities to different ascidian groups (see above) require additional hypotheses of evolutionary origins and are therefore necessarily interpreted as homoplasies.

Combined analysis of morphological and molecular data

The combined analysis based on morphological and molecular data (aligned 18S rDNA sequences kindly provided by Dr Delsuc, Université de Montpellier) conforms to the phylogeny based only on morphological data in the position of Appendicularia as sister group to the remaining tunicate groups (Fig. 2), whereas relationships of thaliacean taxa differ drastically and are similar to branching patterns derived from analyses of molecular data alone (Tsagkogeorga et al., 2009; Delsuc et al., 2018; Kocot et al., 2018). In the combined analysis herein, a monophyletic Stolidobranchiata is sister taxon to a paraphyletic "Phlebobranchiata", monophyletic Thaliacea and the aplousobranch *Clavelina lepadiformis*. *Clavelina lepadiformis* and Thaliacea form a clade to the exclusion of "Phlebobranchiata". The phlebobranch Perophoridae seem to be closer related to a clade consisting of *C. lepadiformis* and Thaliacea than to other phlebobranch species, rendering "Phlebobranchiata" paraphyletic. Comparing the tunicate phylogeny based on combined morphological and molecular data from the present study with the ones recently published based on phylogenomic methodology (Delsuc et al., 2018; Kocot et al., 2018) reveals many similarities and identical branching of major tunicate taxa. With 32 species as terminal taxa our combined analysis covers a somewhat larger disparity of tunicate taxa compared to the 17 (Delsuc et al., 2018) and 18 (Kocot et al., 2018) tunicate species in previous studies. Nevertheless, there is only minor disagreement between the phylogenomic studies and the result from the combined analysis concerning the phylogenetic positions of Aplousobranchiata, Thaliacea and Phlebobranchiata herein. In the present combined study, the aplousobranch *C. lepadiformis* is sister taxon to Thaliacea similar to the molecular phylogenomic studies that found Aplousobranchiata grouping within paraphyletic "Phlebobranchiata" (Delsuc et al., 2018; some analyses in Kocot et al., 2018). It differs from results under some analysis parameters in the study of Kocot et al. (2018), where Aplousobranchiata was the sister group of a monophyletic Phlebobranchiata. Despite the differences in analysis methods (e.g. parsimony was used as optimizing criterion herein, whereas the phylogenomic studies used model-based optimizing criteria), taxon sampling, and the known elevated and heterogeneous substitution rates (Tsagkogeorga et al., 2010), the studies therefore show general agreement.

Does this observation imply that the morphological data have no or little influence on the outcome of the phylogenetic analysis of the combined data? This indeed seems to be the case in the combined dataset herein, if only the phylogenetic branching pattern is considered. However, it is noteworthy, that, for example, the statistical support of the monophyly of Thaliacea in the equally weighted combined dataset increases considerably compared to the purely molecular analysis from 0.62 to 0.89. Moreover, the contribution of the morphological data to the overall

phylogenetic signal also was of interest: with 2122 positions in the alignment of the 18S rDNA sequences, 2005 nucleotide characters outnumbered the 117 phenotypic characters by roughly 17:1. The paraphyly of Ascidiacea, supported in the molecular partition of the data gave way to a monophyletic Ascidiacea supported by the morphological partition at a weighting scheme of 3:1. Likewise, the monophyly of Thaliacea, supported in the molecular partition of the data gave way to a paraphyletic Thaliacea supported by the morphological partition at a weighting scheme of 3:1. The change in ratios is not as pronounced if only parsimony-informative characters are considered. Here, 545 parsimony-informative molecular characters compared to 97 parsimony-informative phenotypic characters resulted in a ratio of approximately 6:1, whereas the tipping point where a paraphyletic "Ascidiacea" became monophyletic still remained at a weighing scheme of 3:1. In any case, these observations indicate that the morphological data add significantly to the phylogenetic signal in the dataset and per-character is higher in the morphological data compared to the nuclear characters.

Discussion of individual character transformations

Phylogenetic relationships are one main focus of interest and a prerequisite in evolutionary considerations. The tracing of changing morphologies through evolutionary time and the origin of diverse morphologies is another focus in evolutionary research. Even when character transformations are mapped on a sequence-based phylogenetic hypothesis the primary homology hypothesis (sensu Pinna, 1991) is the key component. Here, the contribution of selected morphological characters to the formulation of phylogenetic hypotheses was evaluated. In the following paragraphs the resulting hypotheses of character transformations at nodes of interest are discussed.

Clearly the taxon with the highest support in the present morphological analysis is Tunicata itself. The monophyly is not only supported by a Bremer support index of 6 and statistical support of 96% and 99% (jackknife and bootstrap values), but also by six uncontroverted apomorphic characters under ACCTRAN optimization: tunic (14), heartbeat reversal (21), pyloric gland (62), shape of gastrointestinal tract – U-shaped (63), larval statocyte (81), and brain divided into cortex and neuropil (97). Hermaphroditism (71) is another apomorphic character evolved in the stem lineage of Tunicata; however, it is not uncontroverted, because *O. dioica* and *S. sigillinoides*, are dioecious species. Although several of these characters (14, 21, 62, 63) have been hypothesized before to have evolved in the stem lineage of Tunicata (reviewed in Huus, 1956; Stach, 2008), the character matrix herein suggests additional apomorphic changes not considered before. Moreover, the resulting phylogenetic hypotheses of subordinate tunicate taxa require some additional considerations. The evolution of the ability to secrete cellulose, probably acquired via lateral gene transfer from a bacterium (Nakashima et al., 2004; Sagane et al., 2010), had traditionally been associated with the origin of sessility. With planktonic appendicularians as the sister taxon to the remaining Tunicata (e.g. Seeliger, 1885; see also reviews in Stach and Turbeville, 2002; Giribet, 2018) and, in the present morphological analysis, the planktonic salps and doliolids, and planktonic pyrosomes as consecutively branching taxa, the correlation between the evolution of cellulose secretion and sessility becomes obsolete. However, the ability to secrete an outer, protective tunic containing cellulose may have occurred in the early life-history stages, as a similarly structured larval tunic with an outer electron-dense layer and a more electron-lucid layer invested with fibrous material is present in larval ascidians as well as larval appendicularians (Stach, 2007). Such a larval tunic may protect early ontogenetic stages against pathogens and/or predators, but would eventually require an acceleration of development, because larval stages became unable to feed so long as they are completely enclosed in this protective covering. The character state in adults of the last common ancestor of Tunicata is not entirely obvious, because adult appendicularians feature a highly complicated secretion of the tunic that is based on the complexity and development of the filter-feeding houses (Körner, 1952; Flood and Deibel, 1998). In addition, a duplication of cellulose synthase genes occurred in the stem lineage of appendicularians (Sagane et al., 2010; Hosp et al., 2012). Both facts show that the secretion of the tunic in adult Appendicularia is highly derived. Another character that is not straightforward to understand in light of the phylogenetic position of Appendicularia as sister taxon to the remaining tunicates is the U-shaped gut of appendicularians. As mentioned above, a U-shaped gut is a common feature in sessile bilaterian animals, as can be seen, for example, in such diverse taxa as entoprocts, ectoprocts, sedentary polychaetes and crinoids. However, cephalopods might be recalled as a prominent case where marine invertebrates freely roaming the water column possess a U-shaped intestinal tract. Moreover, because the analyses of the phenotypic data and combined analysis herein, and previous molecular analyses (e.g. Delsuc et al., 2018; Kocot et al., 2018) concur on the position of Appendicularia, this difficulty afflicts molecular and morphological phylogenies alike.

Besides the phylogenetic inter-relationships of higher tunicate taxa, the present analysis of phenotypic characters and combined analyses find support for several

other monophyletic taxa that are traditionally recognized in tunicate taxonomy. For example, the monophyly of Botryllinae is supported by the presence of a larval photolith, a sensory organ that combines a gravity sensor and a light-receptive organ; Molgulidae is characterized by the storage kidney as an apomorphic character, and Didemnidae by their peculiar mode of asexual reproduction via pyloric budding and the rearing of sexually produced larvae within brood chambers in the common tunic. A tabulated summary of uncontroverted apomorphies supporting nodes in the strict consensus of the most-parsimonious cladograms (Fig. 1) is listed in Table 2 together with the information on monophyly of the respective taxa in the analysis of the combined dataset. As an instance of conflict between the results of the analyses of the two different datasets besides the one concerning Ascidiacea and Thaliacea discussed in detail above, the relationship of Molgulidae and pyurid species is notable because the monophyly of these taxa together is supported by two uncontroverted apomorphic character changes, the evolution of branched oral tentacles (9) and of a hepatic gland (60). Both characters show an additional reversal in the stem lineage of Styelidae in the analysis of the combined dataset.

The major difference in the results of the present analysis of purely phenotypic characters and combined dataset (which is equivalent to previously published sequence-based phylogenies) concerns the monophyly of Ascidiacea and the paraphyly of the planktonic "Thaliacea" in the purely morphology based results. This paraphyly of the planktonic "Thaliacea" and the sister-group relationship of Appendicularia to the remaining Tunicata suggests that the early evolutionary history of Tunicata took place in the plankton. As discussed above, this conclusion is in conflict with the interpretation of a U-shaped gut and the tunic as a protective covering as evolutionary consequences of a sessile adult mode of life. This conflict, however, also arises in phylogenetic studies based on sequence data alone (e.g. Zeng and Swalla, 2005; Tsagkogeorga et al., 2009; see review in Giribet, 2018), in which the position of planktonic Appendicularia as sister taxon to the remaining tunicates, also leads to the conclusion that the last common ancestor of Tunicata was free-living throughout its entire life and, consequently, the apomorphies of Tunicata (see Table 2) had been evolved in a free-living, fish-like animal (see, e.g., Swalla and Smith, 2008). Appendicularians adapted to the planktonic environment by exploiting the extracorporal tunic evolving it into the most complex external filtering device in combination with an extraordinarily fast life cycle. Both traits can be seen in correlation to a holoplanktonic life cycle, because mortality rates are higher in the plankton ensuring a fast developmental rate (e.g. Staver and Strathmann, 2002), and food sources can be plentiful but are unpredictable and patchy, leading also to fast developmental rates in planktonic organisms (e.g., Alldredge and Madin, 1982; Nakamura, 1998; Henschke et al., 2016). Thaliaceans are characterized by fast developmental rates as well, but differ from appendicularians in possessing an asexual period during their life cycles that leads to the formation of a colony. Clonal reproduction has been interpreted as an adaptation to the spotty and unpredictable supply with nutrients in the plankton (reviewed, e.g., in Hughes, 1989; Jackson and Coates, 1986) and can be found in diverse groups of animals such as cladoceran crustaceans, hydrozoans or siphonapterans (Boero et al., 1992; Zakson-Aiken et al., 1996; Decaestecker et al., 2009). Sessility, on the other hand, also is often correlated with coloniality, such as in the case of ectoprocts, entoprocts and anthozoans (Schuchert, 1993; Wood, 2015; see also review in Blackstone and Jasker, 2003). In the present phylogenetic hypothesis, the last common ancestor of Ascidiacea is reconstructed as a colonial species. This correlates well with the simple morphology of the branchial basket in Aplousobranchiata. Traditionally, Aplousobranchiata comprise only colonial species and the simplicity of their branchial basket has been interpreted by most authors as primitive within ascidians (Lahille, 1890; Stach, 2009). The evolutionary transition from a planktonic colonial form (as present in Salpida, Doliolida and Pyrosomatida) to a sessile colonial form would remain difficult to understand and requires the parallel evolution of coloniality in Botryllinae within Stolidobranchiata. A repeated evolution of coloniality, however, also has been concluded by mapping of this character on different phylogenetic hypotheses based on molecular data (Wada, 1998; Swalla et al., 2000; Zeng et al., 2006) and likewise on the phylogeny resulting from analysis of the combined dataset. Interestingly, stalked colonial forms such as that found in the aplousobranch genus *Sycozoa* are similarly organized as the colonies of planktonic pyrosomes and the interpretation of a benthic pyrosome species (Monniot and Monniot, 1966; but see Lebrato and Jones, 2009 for an alternative interpretation) becomes pivotal in understanding the evolutionary origin of Thaliacea (see also Stach and Turbeville, 2002, 2005). Currently, although the evolutionary interpretations of the phenotypic analysis and combined analysis herein agree in many respects (see Table 2), the two phylogenies necessitate an opposite interpretation of character polarity concerning the transition from benthic to planktonic in the stem lineage of Thaliacea or vice versa from planktonic to benthic in the stem lineage of Ascidiacea. In the present discussion of the evolutionary interpretations, it is notable that there currently is no support for a conflict-free phylogenetic hypothesis. Maybe this is unavoidable in a taxon that

shows such a degree of disparity (Berrill, 1950; Kott, 1985, 1990, 1992, 2001; Lemaire, 2011; Shenkar and Swalla, 2011) and with such a long evolutionary history (Shu et al., 2001; Chen et al., 2003).

The present study compiled conceptualized phenotypical characters into the biggest data matrix available on tunicate morphology and analyzed it in a consistent cladistic framework, yet it is not suggested that this is the final solution of tunicate phylogeny, but merely a first step to use the potential phylogenetic information present in phenotypic characters to elucidate the inter-relationships of this diverse marine taxon.

Acknowledgements

We are grateful for access to the tunicate collection and to the Leica SPE CLSM granted by Priv.-Doz. Dr Carsten Lüter (Museum für Naturkunde Berlin). Financial support by the Deutsche Forschungsgemeinschaft (DFG) and the Elsa-Neumann-Stipendium des Landes Berlin is gratefully acknowledged. We are thankful to the invaluable help of Woody Lee and Scott Jones from the Smithsonian Marine Station in Fort Pierce, Florida, in securing specimens of *Fritillaria borealis*. We also are indebted to Professors Valerie Paul and Mary Rice for generously providing access to the facilities of the Smithsonian Marine Station.

References

Alldredge, A.L. and Madin, L.P., 1982. Pelagic tunicates: unique herbivores in the marine plankton. Bioscience 32, 655–663.

Ax, P., 2001. Das System der Metazoa: ein Lehrbuch der phylogenetischen Systematik. Spektrum Akademischer Verlag GmbH, Heidelberg.

Barreiro-Iglesias, A., Cornide-Petronio, M.E., Anadón, R. and Rodicio, M.C., 2009. Serotonin and GABA are colocalized in restricted groups of neurons in the larval sea lamprey brain: insights into the early evolution of neurotransmitter colocalization in vertebrates. J. Anat. 215, 435–443.

Baumgarten, H.G., Björklund, A., Lachenmayer, L., Nobin, A. and Rosengren, E., 1973. Evidence for the existence of serotonin-, dopamine-, and noradrenaline-containing neurons in the gut of *Lampetra fluviatilis*. Z. Zellforsch. Mik. Ana. 141, 33–54.

Berrill, N.J., 1935. Studies in tunicate development. Part IV - Asexual reproduction. Philos. Trans. R. Soc. Lond. B 225, 327–379.

Berrill, N.J., 1948. The development, morphology and budding of the ascidian *Diazona*. J. Mar. Biol. Assoc. U.K. 27, 389–399.

Berrill, N.J., 1950. The Tunicata – With an Account of the British Species. The Ray Society, London, UK.

Blackstone, N.W. and Jasker, B.D., 2003. Phylogenetic considerations of clonality, coloniality, and mode of germline development in animals. J. Exp. Zool. B Mol. Dev. Evol. 297B, 35–47.

Boero, F., Bouillon, J. and Piraino, S., 1992. On the origins and evolution of hydromedusan life cycles (Cnidaria, Hydrozoa). In: Dallai, R. (Ed.), Sex Origin and Evolution, Vol. 6, Selected Symposia and Monographs U.Z.I. Mucchi, Modena, Italy, pp. 59–68.

Bone, Q., 1998. The Biology of Pelagic Tunicates. Oxford University Press, Oxford, UK.

Bone, Q., Braconnot, J.-C. and Carré, C., 1997. On the heart and circulation in doliolods (Tunicata: Thaliacea). Sci. Mar., 61, 189–194.

Braun, K. and Stach, T., 2016. Comparative study of serotonin-like immunoreactivity in the branchial basket, digestive tract, and nervous system in tunicates. Zoomorphology 135, 351–366.

Braun, K. and Stach, T., 2017. Structure and ultrastructure of eyes and brains of *Thalia democratica* (Thaliacea, Tunicata, Chordata). J. Morphol. 278, 1421–1437.

Braun, K. and Stach, T. (2018) Distribution and evolution of serotonin-like immunoreactive cells in Thaliacea (Tunicata). Zoomorphology, 137, 565–578.

Braun, K. and Stach, T., 2019. Morphology and evolution of the central nervous system in adult tunicates. J. Zool. Syst. Evol. Res., 57, 323–344.

Brien, P., 1948. Embranchement des Tuniciers. In: Grasse, P.P. (Ed.), Morphologie et reproduction. Traité de Zoologie, Paris, France, pp. 757–866.

Brien, P. and Brien-Gavage, E., 1927. Bourgeonnement de *Clavelina lepadiformis* Müller. Rec. Inst. Zool. Torley-Rousseau 1, 31–81.

Burighel, P., Cloney, R.A., 1997. Urochordata: Ascidiacea. In: Harrison, F.W., Ruppert, E.E. (Eds.), Microscopic Anatomy of Invertebrates. Hemichordata, Chaetognatha, and the Invertebrate Chordates. Willey-Liss, Inc., New York, NY, pp. 221–347.

Burighel, P., Lane, N.J., Fabio, G., Stefano, T., Zaniolo, G., Carnevali, M.D.C. and Manni, L., 2003. Novel, secondary sensory cell organ in ascidians: in search of the ancestor of the vertebrate lateral line. J. Comp. Neurol. 461, 236–249.

Candiani, S., Augello, A., Oliveri, D., Passalacqua, M., Pennati, R., De Bernardi, F. and Pestarino, M., 2001. Immunocytochemical localization of serotonin in embryos, larvae and adults of the lancelet, *Branchiostoma flordiae*. Histochem. J. 33, 413–420.

Chamisso, A.v., 1819. De animalibus quibusdam e classe vermium Linnaeana in circumnavigatione terrae auspicante Comite N. Romanzoff duce Ottone de Kotzebue annis 1815. 1816. 1817. 1818. peracta observatis. Fasciculus primus. De Salpa. Dümmler Verlag, Berlin.

Chen, J.-Y., Huang, D.-Y., Peng, Q.-Q., Chi, H.-M., Wang, X.-Q. and Feng, M., 2003. The first tunicate from the early Cambrian of South China. Proc. Natl Acad. Sci., USA 100, 8314–8318.

Cohen, A.I., 1963. Vertebrate retinal cells and their organization. Biol. Rev. 38, 427–459.

Cohen, B.L., Holmer, L.E. and Lüter, C., 2003. The brachiopod fold: a neglected body plan hypothesis. Palaeontology 46, 59–65.

Collin, R., Fredericq, S., Freshwater, D.W., Gilbert, E., Madrid, M., Maslakova, S., Miglietta, M.P., Rocha, R.M., Rodríguez, E. and Thacker, R.W., 2016. TaxaGloss – a glossary and translation tool for biodiversity studies. Biodivers. Data J. 21, e10732.

Cuvier, G., 1840. Animal Kingdom: Arranged According to its Organization, Forming the Basis for a Natural History of Animals, and Introduction to Comparative Anatomy. Holborn Hill, London.

Decaestecker, E., De Meester, L. and Mergeay, J., 2009. Cyclical parthenogenesis in *Daphnia*: sexual versus asexual reproduction. In: Schön, I., Martens, K., Dijk, P. (Eds.), Lost Sex: The Evolutionary Biology of Parthenogenesis. Springer Netherlands, Dordrecht, pp. 295–316.

Deibel, D. and Paffenhöfer, G.A., 1988. Cinematographic analysis of the feeding mechanism of the pelagic tunicate Doliolum nationalis. Bull. Mar. Sci. 43, 404–412.

Delsuc, F., Brinkmann, H., Chourrout, D. and Philippe, H., 2006. Tunicates and not cephalochordates are the closest living relatives of vertebrates. Nature 439, 965–968.

Delsuc, F., Philippe, H., Tsagkogeorga, G., Simion, P., Tilak, M.-K., Turon, X., López-Legentil, S., Piette, J., Lemaire, P. and Douzery, E.J.P., 2018. A phylogenomic framework and timescale for comparative studies of tunicates. BMC Biol. 16, 39.

Deviney, E.M., 1934. The behavior of isolated pieces of ascidian (*Perophora viridis*) stolon as compared with ordinary budding. J. Elisha Mitchell Sci. Soc. 49, 185–224.
Drasche, R.v., 1884. Über einige neue und weniger gekannte aussereuropäische einfache Ascidien. Denkschr. Kais. Akad. Wiss. 48, 369–387.
Eakin, R.M., 1979. Evolutionary significance of photoreceptors: in retrospect. Am. Zool. 19, 647–653.
Fenaux, R., 1998. Anatomy and functional morphology of the Appendicularia. In: Bone, Q. (Ed.), The Biology of Pelagic Tunicates. Oxford University Press, Oxford, UK, pp. 25–34.
Fitzhugh, K., 2006. The 'requirement of total evidence' and its role in phylogenetic systematics. Biol. Philos. 21, 309–351.
Flood, P.R. and Deibel, D., 1998. The appendicularian house. In: Bone, Q. (Ed.), The Biology of Pelagic Tunicates. Oxford University Press, Oxford, UK, pp. 105–124.
Franz, V., 1927. Morphologie der Akranier. Z. ges. Anat. 27, 464–692.
García-Bellido, D.C., Lee, M.S.Y., Edgecombe, G.D., Jago, J.B., Gehling, J.G. and Paterson, J.R., 2014. A new vetulicolian from Australia and its bearing on the chordate affinities of an enigmatic Cambrian group. BMC Evol. Biol. 14, 214.
Garstang, W., 1928. The morphology of the Tunicata, and its bearings on the phylogeny of the Chordata. Q. J. Microsc. Sci. 72, 51–187.
Gee, H., 1996. Before the Backbone. Chapman & Hall, London, UK.
Gee, H., 2001. On being vetulicolian. Nature 414, 407.
Gill, H.S., Renaud, C.B., Chapleau, F., Mayden, R.L., Potter, I.C. and Douglas, M.E., 2003. Phylogeny of living parasitic lampreys (Petromyzontiformes) based on morphological data. Copeia 2003, 687–703.
Giribet, G., 2018. Phylogenomics resolves the evolutionary chronicle of our squirting closest relatives. BMC Biol. 16, 49.
Godeaux, J., 2003. History and revised classification of the order Cyclomyaria (Tunicata, Thaliacea, Doliolida). Bull. Inst. Roy. Sci. Nat. Belgique 73, 191–222.
Godeaux, J.E.A., Bone, Q., Braconnot, J.C., 1998. Anatomy of Thaliacea. In: Bone, Q. (Ed.), The Biology of Pelagic Tunicates. Oxford University Press, Oxford, UK., pp. 1–24
Goloboff, P.A., Farris, J.S. and Nixon, K.C., 2008. TNT, a free program for phylogenetic analysis. Cladistics 24, 774–786.
Goodrich, E.S., 1909. Vertebrata, Craniata I. Cyclostomes and fishes. In: Lankester, E.R. (Ed.), Treatise on Zoology, Part 9. Adam and Charles Black, London, UK, pp. XVI–518.
Gorbman, A., 1995. Olfactory origins and evolution of the brain-pituitary endocrine system: facts and speculation. Gen. Comp. Endocrinol. 97, 171–178.
Gorbman, A., 1999. Brain-Hatschek's pit relationships in amphioxus species. Acta Zool. 80, 301–305.
Govindarajan, A.F., Bucklin, A. and Madin, L.P., 2011. A molecular phylogeny of the Thaliacea. J. Plankton Res. 33, 843–853.
Grave, C., 1926. *Molgula citrina* (Alder and Hancock). Activities and structure of the free-swimming larva. J. Morphol. 42, 453–471.
Groepler, W., 2016. Die Seescheiden von Helgoland. Westarp Wissenschaften-Verlagsgesellschaft mbH, Hohenwarsleben.
Groepler, W. and Stach, T., 2019. On organ development in larvae of Diplosoma migrans(Menker & Ax, 1976) (Tunicata, Ascidiacea, Didemnidae). Zoomorphology. 138, 493–509. https://doi.org/10.1007/s00435-019-00454-4
Gutierrez, S. and Brown, F.D., 2017. Vascular budding in *Symplegma brakenhielmi* and the evolution of coloniality in styelid ascidians. Dev. Biol. 423, 152–169.
Hartmeyer, R., 1923. Ascidiacea, Part I. The Danish Ingolf-Expedition. H. Hagerup, Copenhagen, pp. 1–370.
Hawkins, C.J., Kott, P., Parry, D.L. and Swinehart, J.H., 1983. Vanadium content and oxidation state related to ascidian phylogeny. Comp. Biochem. Physiol. 76B, 555–558.
Hennig, W., 1982. Phylogenetische Systematik. Verlag Paul Parey, Berlin.
Henschke, N., Everett, J.D., Richardson, A.J. and Suthers, I.M., 2016. Rethinking the role of salps in the ocean. TREE 31, 720–733.
Herdman, W.A., 1891. A revised classification of the Tunicata, with definitions of the orders, suborders, families, subfamilies, and genera, and analytical keys to the species. Zool. J. Linn. Soc. 23, 558–652.
Hirose, E., Nishikawa, T., Saito, Y. and Watanabe, H., 1992. Minute protrusions of ascidian tunic cuticle -some implications for ascidian phylogeny. Zool. Sci. 9, 405–412.
Hirose, E., Aoki, M. and Chiba, K., 1996. Fine structures of tunic cells and distribution of bacteria in the tunic of the luminescent ascidian Clavelina miniata (Ascidiacea, Urochordata). Zool. Sci. 13, 519–523.
Hirose, E., Kimura, S., Itoh, T. and Nishikawa, J., 1999. Tunic morphology and cellulosic components of pyrosomas, doliolids, and salps (Thaliacea, Urochordata). Biol. Bull. 196, 113–120.
Holland, L.Z., 1992. The phylogenetic significance of tunicate sperm morphology. In: Baccetti, B. (Ed.), 6th International Congress on Spermatology. Raven Press, Siena, pp. 961–965.
Holland, N.D. and Holland, L.Z., 1993. Serotonin-containing cells in the nervous system and other tissues during ontogeny of a lancelet, *Branchiostoma floridae*. Acta Zool. 74, 195–204.
Hosp, J., Sagane, Y., Danks, G. and Thompson, E.M., 2012. The evolving proteome of a complex extracellular matrix, the *Oikopleura* house. PLoS ONE 7, e40172.
Hughes, R.N., 1989. Functional Biology of Clonal Animals. Springer Science & Business Media. Retrieved from https://www.springer.com/gp/book/9780412331305.
Huus, J., 1956. Zweite und letzte Unterklasse der Acopa: Ascdiacea = Tethyodeae = Seescheiden. In: Krumbach, T. (Ed.), Handbuch der Zoologie, Fünfter Band, Zweite Hälfte. Walter de Gruyter, Berlin, pp. 545–692.
Ihle, J.E.W., 1913. Die Appendicularien. In: Spengel, J.W. (Ed.), Ergebnisse und Fortschritte der Zoologie, Dritter Band. Verlag von Gustav Fischer, Jena, pp. 463–534.
Ihle, J.E.W., 1956. Dritte und letzte Ordnung der Thaliacea: Desmomyaria. In: Krumbach, T. (Ed.), Handbuch der Zoologie, Fünfter Band, Zweite Hälfte. Walter de Gruyter, Berlin, pp. 401–544.
Ihle, J.E.W., 1971. Die Urogenitalorgane. In: Ihle, J.E.W., van, Kampen, P.N., Nierstrasz, H.F., Versluys, J. (Eds.), Vergleichende Anatomie der Wirbeltiere. Springer, Berlin, pp. 708–787.
Jackson, J.B.C. and Coates, A.G., 1986. Life cycles and evolution of clonal (modular) animals. Philos. Trans. R. Soc. Lond. B 313, 7–22.
Jonasova, K. and Kozmik, Z., 2008. Eye evolution: lens and cornea as an upgrade of animal visual system. Semin. Cell Dev. Biol. 19, 71–81.
Julin, C., 1904. Recherches sur la phylogenese des Tuniciers. Archiascidia neapolitana nov. gen., nov. sp. Mitt. Zool. Stn. Neapel. 16, 489–552.
Kah, O., Lethimonier, C., Somoza, G., Guilgur, L.G., Vaillant, C. and Lareyre, J.J., 2007. GnRH and GnRH receptors in metazoa: a historical, comparative, and evolutive perspective. Gen. Comp. Endocrinol. 153, 346–364.
Karnovsky, M.J., 1965. A formaldehyde-glutaraldehyde fixative of high osmolality for use in electron microscopy. J. Cell Biol. 27, 137A.
Kluge, A.G., 1998. Total evidence or taxonomic congruence: cladistics or consensus classification. Cladistics 14, 151–158.
Kocot, K.M., Tassia, M.G., Halanych, K.M. and Swalla, B.J., 2018. Phylogenomics offers resolution of major tunicate relationships. Mol. Phylogenet. Evol. 121, 166–173.
Körner, W.F., 1952. Untersuchungen über die Gehäusebildung bei Appendicularien (*Oikopleura dioica* Fol). Z. Morph. Ökol. Tiere 41, 1–53.

Kott, P., 1985. The Australian Ascidacea. Part 1, Phlebobranchia and Stolidobranchia. Mem. Queensl. Mus. 23, 1–440.
Kott, P., 1990. The Australian Ascidacea. Part 2, Aplousobranchia (1). Mem. Queensl. Mus. 29, 1–266.
Kott, P., 1992. The Australian Ascidacea. Part 3, Aplousobranchia (2). Mem. Queensl. Mus. 32, 375–620.
Kott, P., 2001. The Australian Ascidacea. Part 4, Aplousobranchia (3), Didemnidae. Mem. Queensl. Mus. 47, 1–410.
Kowalevsky, A., 1866. Entwickelungsgeschichte der einfachen Ascidien. Mem. Acad. Imp. Sci. Sa.-Pétersbourgh VIIe Série, 1-19, 13 plates.
Kriebel, M.E., 1967. Conduction velocity and intracellular action potentials of the tunicate heart. J. Gen. Physiol. 50, 2097–2107.
Lacalli, T.C., 1996. Frontal eye circuitry, rostral sensory pathways and brain organization in amphioxus larvae: evidence from 3D reconstructions. Phil. Trans. R. Soc. Lond. B 351, 243–263.
Lacalli, T.C., 2002. Vetulicolians – are they deuterostomes? chordates? BioEssays 24, 208–211.
Lacalli, T.C., 2005. Protochordate body plan and the evolutionary role of larvae: old controversies resolved? Can. J. Zool. 83, 216–224.
Lacalli, T.C., Holland, L.Z., 1998. The developing dorsal ganglion of the salp *Thalia democratica*, and the nature of the ancestral chordate brain. Phil. Trans. R. Soc. Lond. B 353, 1943–1967.
Lacalli, T.C., Holland, N.D. and West, J.E., 1994. Landmarks in the anterior central nervous system of amphioxus larvae. Phil. Trans. R. Soc. Lond. B 344, 165–185.
Lahille, F., 1890. Recherches sur les tuniciers des côtes de France. Imprimerie Lagarde et Sebille, Tulouse.
Lamb, T.D., Collin, S.P. and Pugh, E.N., 2007. Evolution of the vertebrate eye: opsins, photoreceptors, retina and eye cup. Nat. Rev. Neurosci. 8, 960–976.
Lambert, G. and Lambert, C.C., 1987. Spicule formation in the solitary ascidian, *Herdmania momus*. J. Morphol. 192, 145–159.
Lauzon, R.J., Ishizuka, K.J. and Weissman, I.L., 2002. Cyclical generation and degeneration of organs in a colonial urochordate involves crosstalk between old and new: a model for development and regeneration. Dev. Biol. 249, 333–348.
Lebrato, M. and Jones, D.O.B., 2009. Mass deposition event of *Pyrosoma atlanticum* carcasses off Ivory Coast (West Africa). Limnol. Oceanogr. 54, 1197–1209.
Lemaire, P., 2011. Evolutionary crossroads in developmental biology: the tunicates. Development 138, 2143–2152.
Lemaire, P. and Piette, J., 2015. Tunicates: exploring the sea shores and roaming the open ocean. A tribute to Thomas Huxley. Open Biol. 5, 150053.
Li, Y., Williams, M., Gabbott, S.E., Chen, A., Cong, P. and Hou, X., 2018. The enigmatic metazoan *Yuyuanozoon magnificissimi* from the early Cambrian Chengjiang Biota, Yunnan Province, South China. J. Paleontol., 92, 1081–1091.
Lohmann, H., 1914. Die Appendicularien der Valdivia-Expedition. Verh. Deut. Zool. Gesell. 24, 157–192.
Lohmann, H., 1956. Erste Klasse der Tunicaten. Appendiculariae. In: Krumbach, T. (Ed.), Handbuch der Zoologie. Walter de Gruyter & Co., Berlin, pp. 15–202.
Lützen, J.G., 1967. Sækdyr (Tunicata). Danm. Fauna 75, 267.
Mackie, G.O., 1995. On the visceral nervous system of *Ciona*. J. Mar. Biol. Assoc. U.K. 75, 141–151.
Mackie, G.O., Bone, Q., 1978. Luminescence and associated effector activity in Pyrosoma (Tunicata: Pyrosomida). Phil. Trans. R. Soc. Lond. B 202, 483–495.
Maddison, W.P., Maddison, D.R., 2018. Mesquite: a modular system for evolutionary analysis. Retrieved from http://mesquite project.org
Mallat, J., 1979. Surface morphology and functions of pharyngeal structures in the larval lamprey *Petromyzon marinus*. J. Morphol. 162, 249–274.
Manni, L. and Pennati, R., 2016. Tunicata. In: Schmidt-Rhaesa, A., Harzsch, S., Purschke, G. (Eds.), Structure and Evolution of Invertebrate Nervous Systems. Oxford University Press, Oxford, UK, pp. 699–718.
Manni, L., Zaniolo, G., Cima, F., Burighel, P. and Ballarin, L., 2007. *Botryllus schlosseri*: a model ascidian for the study of asexual reproduction. Dev. Dyn. 236, 335–352.
Millar, R.H., 1954. The breeding and development of the ascidian *Pelonaia corrugata* Forbes and Goodsir. J. Mar. Biol. Assoc. U.K. 33, 681–687.
Millar, R.H., 1966. Ascidiacea. Mem. Nat. Mus. Vic. 27, 357–384.
Millar, R.H., 1970. British Ascidians, Tunicata: Ascidiacea: Keys and Notes for the Identification of the Species. Academic Press, London.
Millar, R.H., 1971. The biology of Ascidians. In: Russell, F.S., Yonge, M. (Eds.), Advances in Marine Biology. Academic Press. London, pp. 1–100.
Monniot, C. and Monniot, F., 1966. A benthic pyrosoma, *Pyrosoma benthica* n. sp. Fr. Acad. Sci. 263, 368–370.
Monniot, C. and Monniot, F., 1972. Clé mondiale des genres d'ascidies. Arch. Zool. Exp. Gener. 113, 311–367.
Monniot, F. and Monniot, C., 2001. Ascidians from the Tropical Western Pacific. Editions Scientifiques du Muséum, Paris, France.
Moreno, T.R. and Rocha, R.M., 2008. Phylogeny of the Aplousobranchia (Tunicata: Ascidiacea). Rev. Bras. Zool. 25, 269–298.
Mukai, H., Koyama, H. and Watanabe, H., 1983. Studies on the reproduction of thee species of *Perophora* (Ascidiacea). Biol. Bull. 164, 251–266.
Nakamura, Y., 1998. Blooms of tunicates *Oikopleura* spp. and *Dolioletta gegenbauri* in the Seto Inland Sea, Japan, during summer. Hydrobiology 385, 183–192.
Nakashima, K., Yamada, L., Satou, Y., Azuma, J.-i. and Satoh, N., 2004. The evolutionary origin of animal cellulose synthase. Dev. Genes. Evol. 214, 81–88.
Nakauchi, M., 1982. Asexual development of ascidians: its biological significance, diversity, and morphogenesis. Am. Zool., 22, 753–763.
Neumann, G., 1956. Zweite Klasse der Tunicata. Acopa = Caducichordata. In: Krumbach, T. (Ed.), Handbuch der Zoologie, Fünfter Band, Zweite Hälfte. Walter de Gruyter, Berlin, pp. 203–400.
Nieuwenhuys, R., 1977. The brain of the lamprey in a comparative perspective. Ann. N. Y. Acad. Sci. 299, 97–145.
Perrier, J.O., 1898. Note sur la classification des Tuniciers. C. R. Acad. Sci. Paris 126, 1758–1762.
Pietschmann, V., 1962. Acrania. In: Kükenthal, W., Krumbach, T. (Eds.), Handbuch der Zoologie. Walter de Gruyter, Berlin, pp. 3–124.
Piette, J. and Lemaire, P., 2015. Thaliaceans, the neglected pelagic relatives of ascidians: a developmental and evolutionary enigma. Q. Rev. Biol. 90, 117–145.
Pinna, M.C.C., 1991. Concepts and tests of homology in the cladistic paradigm. Cladistics 7, 367–394.
Plough, H.H., 1978. Sea Squirts of the Atlantic Continental Shelf from Maine to Texas. Johns Hopkins University Press, Baltimore, MD.
Pourquié, O., 2001. A macho way to make muscles. Nature 409, 679–680.
Richter, S., Loesel, R., Purschke, G., Schmidt-Rhaesa, A., Scholtz, G., Stach, T., Wanninger, A., Brenneis, C., Döring, C., Fritsch, M., Grobe, P., Heuer, C.M., Kaul, S., Møller, O.S., Müller, C.H.G., Rieger, V., Stegner, M.E.J. and Harzsch, S., 2010. Glossary of invertebrate neuroanatomical terms. Front Zool. 7, 29.
Rigon, F., Stach, T., Caicci, F., Gasparini, F., Burighel, P. and Manni, L., 2013. Evolutionary diversification of secondary mechanoreceptor cells in Tunicata. BMC Evol. Biol. 13, 112.
Roch, G.J., Tello, J.A. and Sherwood, N.M., 2014. At the transition from invertebrates to vertebrates, a novel GnRH-Like peptide emerges in amphioxus. Mol. Biol. Evol. 31, 765–778.

Rocha, R.M.d., Zanata, T.B. and Moreno, T.R., 2012. Keys for the identification of families and genera of Atlantic shallow water ascidians. Biota. Neotrop. 12, 269–303.
Romer, A.S. and Parsons, T.S., 1986. The Vertebrate Body. Saunders College Publishing, Philadelphia, PA.
Ruppert, E.E., 1997a. Introduction: microscopic anatomy of the notochord, heterochrony, and chordate evolution. In: Harrison, F.W., Ruppert, E.E. (Eds.), Microscopic Anatomy of Invertebrates. Hemichordata, Chaetognatha, and the Invertebrate Chordates. Willey-Liss, Inc., New York, NY, pp. 1–13.
Ruppert, E.E., 1997b. Cephalochordata (Acrania). In: Harrison, F.W., Ruppert, E.E. (Eds.), Microscopic Anatomy of Invertebrates. Hemichordata, Chaetognatha, and the Invertebrate Chordates. Wiley-Liss Inc., New York, NY, pp. 349–504.
Sagane, Y., Zech, K., Bouquet, J.-M., Schmid, M., Bal, U. and Thompson, E.M., 2010. Functional specialization of cellulose synthase genes of prokaryotic origin in chordate larvaceans. Development 137, 1483–1492.
Sakharov, D.A. and Salimova, N.B., 1980. Serotonin neurons in the peripheral nervous system of the larval lamprey, *Lampetra planeri*. A histochemical, microspectrofluorimetric and ultrastructural study. Zool. Jb. Allg. Zool. 84, 231–239.
Sakharov, D.A. and Salimova, N., 1982. Serotonin-containing cells in the ascidian endostyle. Cell. Mol. Life Sci. 38, 802–803.
Salvini-Plawen, L.V., 1982. On the polyphyletic origin of photoreceptors. In: Westfall, J.A. (Ed.), Visual Cells in Evolution. Raven Press, New York, NY, pp. 137–154.
Schuchert, P., 1993. Phylogenetic analysis of the Cnidaria. J. Zool. Syst. Evol. Res. 31, 161–173.
Seeliger, O., 1885. Die Entwicklungsgeschichte der socialen Ascidien. Jenaische Zeitschrift für Naturwissenschaften 18, 45–120.
Shenkar, N. and Swalla, B.J., 2011. Global diversity of Ascidiacea. PLoS ONE 6, e20657.
Shenkar, N., Koplovitz, G., Dray, L., Gissi, C. and Huchon, D., 2016. Back to solitude: solving the phylogenetic position of the Diazonidae using molecular and developmental characters. Mol. Phylogenet. Evol. 100, 51–56.
Shu, D., Chen, L., Han, J. and Zhang, X., 2001. An early Cambrian tunicate from China. Nature 411, 472–473.
Sköld, H.N., Stach, T., Bishop, J.D., Herbst, E. and Thorndyke, M.C., 2011. Pattern of cell proliferation during budding in the colonial ascidian Diplosoma listerianum. Biol Bull. 221, 126–136.
Slingsby, C., Wistow, G.J. and Clark, A.R., 2013. Evolution of crystallins for a role in the vertebrate eye lens. Protein Sci. 22, 367–380.
Sorrentino, M., Manni, L., Lane, N.J. and Burighel, P., 2000. Evolution of cerebral vesicles and their sensory organs in an ascidian larva. Acta Zool. 81, 243–258.
Stach, T., 1996. On the preoral pit of the larval amphioxus (*Branchiostoma lanceolatum*). Ann. Sci. Nat. Zool. Paris 17, 129–134.
Stach, T., 2005. Comparison of the serotonergic nervous system among Tunicata: implications for its evolution within Chordata. Org. Divers. Evol. 5, 15–24.
Stach, T., 2007. Ontogeny of the appendicularian *Oikopleura dioica* (Tunicata, Chordata) reveals characters similar to ascidian larvae with sessile adults. Zoomorphology 126, 203–214.
Stach, T., 2008. Chordate phylogeny and evolution: a not so simple three-taxon problem. J. Zool. 276, 117–141.
Stach, T., 2009. Anatomy of the trunk mesoderm in tunicates: homology considerations and phylogenetic interpretation. Zoomorphology 128, 97–109.
Stach, T., 2014. Deuterorstome phylogeny – a morphological perspective. In: Wägele, W. (Ed.), Deep Metazoan Phylogeny: The Backbone of the Tree of Life. De Gruyter, Berlin, pp. 425–457.
Stach, T. and Turbeville, J.M., 2002. Phylogeny of Tunicata inferred from molecular and morphological characters. Mol. Phylogenet. Evol. 25, 408–428.
Stach, T. and Turbeville, J.M., 2005. The role of appendicularians in chordate evolution – a phylogenetic analysis of molecular and morphological characters, with remarks on 'neoteny-scenarios'. In: Gorsky, G., Youngbluth, M.J., Deibel, D. (Eds.), Responses of Marine Ecosystems to Global Change. Ecological Impact of Appendicularians. Contemporary Publishing International, Paris, France, pp. 9–26.
Stach, T., Winter, J., Bouquet, J.-M., Chourrout, D. and Schnabel, R., 2008. Embryology of a planktonic tunicate reveals traces of sessility. Proc. Natl Acad. Sci. USA 105, 7229–7234.
Staver, J. M. and Strathmann, R. R., 2002. Evolution of fast development of planktonic embryos to early swimming. Biol Bull. 203, 58–69.
Stokes, M.D. and Holland, N.D., 1995. Embryos and larvae of a lancelet, *Branchiostoma floridae*, from hatching through metamorphosis: growth in the laboratory and external morphology. Acta Zool. 76, 105–120.
Swalla, B.J. and Smith, A.B., 2008. Deciphering deuterostome phylogeny: molecular, morphological and palaeontological perspectives. Phil. Trans. R. Soc. Lond. B 363, 1557–1568.
Swalla, B.J., Cameron, C.B., Corley, L.S. and Garey, J.R., 2000. Urochordates are monophyletic within the deuterostomes. Syst. Biol. 49, 52–64.
Swofford, D.L., 2003. PAUP*. Phylogenetic Analysis Using Parsimony (*and Other Methods). Sinauer Associates, Sunderland, MA.
Terakado, K., 2010. Generation of prolactin-like neurons in the dorsal strand of ascidians. Zool. Sci. 27, 581–588.
Tsagkogeorga, G., Turon, X., Hopcroft, R., Tilak, M., Feldstein, T., Shenkar, N., Loya, Y., Huchon, D., Douzery, E. and Delsuc, F., 2009. An updated 18S rRNA phylogeny of tunicates based on mixture and secondary structure models. BMC Evol. Biol. 9, 187.
Tsagkogeorga, G., Turon, X., Galtier, N., Douzery, E. and Delsuc, F., 2010. Accelerated evolutionary rate of housekeeping genes in tunicates. J. Mol. Evol. 71, 153–167.
Van Name, W.G., 1945. The North and South American ascidians. Bull. Am. Mus. Nat. Hist. 84, 1–475, 431 plates.
Van Soest, R.W.M., 1981. A monograph of the order Pyrosomatida (Tunicata, Thaliacea). J. Plankton Res. 3, 603–631.
Wada, H., 1998. Evolutionary history of free-swimming and sessile lifestyles in urochordates as deduced from 18S rDNA molecular phylogeny. Mol. Biol. Evol. 15, 1189–1194.
Wägele, J.-W., 2001. Grundlagen der Phylogenetischen Systematik. Verlag Dr. Friedrich Pfeil, Munich.
Wicht, H. and Lacalli, T.C., 2005. The nervous system of amphioxus: structure, development, and evolutionary significance. Can. J. Zool. 83, 122–150.
Williams, J.B., 1996. Sessile lifestyle and origin of chordates. N. Z. J. Zool. 23, 111–133.
Wood, T.S., 2015. Chapter 16 - Phyla Ectoprocta and Entoprocta (Bryozoans). In: Thorp, J.H., Rogers, D.C. (Eds.), Thorp and Covich's Freshwater Invertebrates (Fourth Edition). Academic Press, Boston, MA, pp. 327–345.
Zakson-Aiken, M., Gregory, L.M. and Shoop, W.L., 1996. Reproductive strategies of the cat flea (Siphonaptera: Pulicidae): parthenogenesis and autogeny? J. Med. Entomol. 33, 395–397.
Zeng, L. and Swalla, B.J., 2005. Molecular phylogeny of the protochordates: chordate evolution. Can. J. Zool. 83, 24–33.
Zeng, L., Jacobs, M.W. and Swalla, B.J., 2006. Coloniality has evolved once in stolidobranch ascidians. Integr. Comp. Biol. 46, 255–268.

Supporting Information

Additional supporting information may be found online in the Supporting Information section at the end of the article.

Fig. S1. Strict consensus tree of three equally parsimonious trees found in an heuristic analysis conducted in PAUP analyzing 117 morphological characters (113

parsimony-informative) coded for 49 tunicate species and 5 outgroup species with characters reweighed according to the rescaled consistency index found in the main analysis with equally weighed characters. TL = 109.23, CI = 0.65, RI = 0.91.

Fig. S2. Single most parsimonious tree found in an heuristic analysis conducted in PAUP analyzing 117 morphological characters (97 parsimony informative) combined with 18S rDNA-sequence data (2005 nt-positions, 545 parsimony informative) resulting in 2122 characters for 32 tunicates (21 species and 11 OTUs consisting of two species concatenated from the same genus; see Table 3 for names of species used for concatenation and text for further details) and 5 outgroup species. Weighting scheme: morphological characters : molecular sequence positions 2:1 TL = 2639, CI = 0.55, RI = 0.72. Numbers indicate Jackknife values (green), bootstrap percentages (red).

Fig. S3. Single most parsimonious tree found in an heuristic analysis conducted in PAUP analyzing 117 morphological characters (97 parsimony informative) combined with 18S rDNA-sequence data (2005 nt-positions, 545 parsimony informative) resulting in 2122 characters for 32 tunicates (21 species and 11 OTUs consisting of two species concatenated from the same genus; see Table 3 for names of species used for concatenation and text for further details) and 5 outgroup species. Weighting scheme: morphological characters : molecular sequence positions 3:1 TL = 2888, CI = 0.55, RI = 0.72. Numbers indicate Jackknife values (green), bootstrap percentages (red).

Fig. S4. Single most parsimonious tree found in an heuristic analysis conducted in PAUP analyzing 117 morphological characters (97 parsimony informative) combined with 18S rDNA-sequence data (2005 nt-positions, 545 parsimony informative) resulting in 2122 characters for 32 tunicates (21 species and 11 OTUs consisting of two species concatenated from the same genus; see Table 3 for names of species used for concatenation and text for further details) and 5 outgroup species. Weighting scheme: morphological characters : molecular sequence positions 4:1 TL = 3128, CI = 0.55, RI = 0.73. Numbers indicate Jackknife values (green), bootstrap percentages (red).

Fig. S5. Single most parsimonious tree found in an heuristic analysis conducted in PAUP analyzing 117 morphological characters (97 parsimony informative) combined with 18S rDNA-sequence data (2005 nt-positions, 545 parsimony informative) resulting in 2122 characters for 32 tunicates (21 species and 11 OTUs consisting of two species concatenated from the same genus; see Table 3 for names of species used for concatenation and text for further details) and 5 outgroup species. Weighting scheme: morphological characters : molecular sequence positions 5:1 TL = 3367, CI = 0.55, RI = 0.74. Numbers indicate Jackknife values (green), bootstrap percentages (red).

Fig. S6. Single most parsimonious tree found in an heuristic analysis conducted in PAUP analyzing 18S rDNA-sequence data (2005 nt positions, 545 parsimony informative) for 32 tunicates (21 species and 11 OTUs consisting of two species concatenated from the same genus; see Table 3 for names of species used for concatenation and text for further details) and 2 outgroup species. TL = 2390, CI = 0.56, RI = 0.71. Numbers indicate Jackknife values (green), bootstrap percentages (red).

Appendix S1. Nexus file containing data matrix conceptualized for 117 phenotypic characters (113 parsimony-informative) for 49 tunicate species comprising all higher tunicate taxa, and five craniate and cephalochordate outgroup species.

Appendix S2. Nexus file containing data matrix concatenated from the aligned 18S rDNA-sequence data kindly provided by Dr Frédéric Delsuc (Université de Montpellier) and the phenotypic characters in the data matrix F1 (Appendix S1).